1984

Selectivity In Junctional Communication

Michael George Blennerhassett

CANADIAN THESES ON MICROFICHE

I.S.B.N.

THESES CANADIENNES SUR MICROFICHE

National Library of Canada
Collections Development Branch

Canadian Theses on
Microfiche Service

Ottawa, Canada
K1A 0N4

Bibliothèque nationale du Canada
Direction du développement des collections

Service des thèses canadiennes
sur microfiche

NOTICE

The quality of this microfiche is heavily dependent upon the quality of the original thesis submitted for microfilming. Every effort has been made to ensure the highest quality of reproduction possible.

If pages are missing, contact the university which granted the degree.

Some pages may have indistinct print especially if the original pages were typed with a poor typewriter ribbon or if the university sent us a poor photocopy.

Previously copyrighted materials (journal articles, published tests, etc.) are not filmed.

Reproduction in full or in part of this film is governed by the Canadian Copyright Act, R.S.C. 1970, c. C-30. Please read the authorization forms which accompany this thesis.

THIS DISSERTATION
HAS BEEN MICROFILMED
EXACTLY AS RECEIVED

AVIS

La qualité de cette microfiche dépend grandement de la qualité de la thèse soumise au microfilmage. Nous avons tout fait pour assurer une qualité supérieure de reproduction.

S'il manque des pages, veuillez communiquer avec l'université qui a conféré le grade.

La qualité d'impression de certaines pages peut laisser à désirer, surtout si les pages originales ont été dactylographiées à l'aide d'un ruban usé ou si l'université nous a fait parvenir une photocopie de mauvaise qualité.

Les documents qui font déjà l'objet d'un droit d'auteur (articles de revue, examens publiés, etc.) ne sont pas microfilmés.

La reproduction, même partielle, de ce microfilm est soumise à la Loi canadienne sur le droit d'auteur, SRC 1970, c. C-30. Veuillez prendre connaissance des formules d'autorisation qui accompagnent cette thèse.

LA THÈSE A ÉTÉ
MICROFILMÉE TELLE QUE
NOUS L'AVONS REÇUE

SELECTIVITY IN JUNCTIONAL COMMUNICATION

by

Michael George Blennerhassett

Department of Zoology

Submitted in partial fulfillment
of the Requirements for the degree of
Doctor of Philosophy

Faculty of Graduate Studies
The University of Western Ontario
London, Ontario

December, 1984

ABSTRACT

The regulation of gap junction permeability may be important during development, since this could change the nature and rate of movement of molecules passing between cells. Results in developing insect epidermis show that intercellular channels close in a graded fashion, altering the kind of substances passing between cells over time, and that reduced junctional permeability at the intersegmental border establishes spatial patterns of coupling within the epidermis.

The nature of channel closure, which might be graded or all-or-none, determines how junctional permeability changes when the coupling level is varied. The passage of small fluorescent dyes and inorganic ions between cells was examined during gradual uncoupling by Li of epidermis from the beetle Tenebrio molitor. The junctional resistance increases monotonically over 60 minutes, but the intercellular passage of the fluorescent tracers carboxyfluorescein (CF) and lissamine rhodamine B (LRB) is blocked long before electrical coupling is lost. There is discrimination by size, since LRB, with a limiting dimension for channel passage of 14A, is blocked before CF (12A). This

suggests that intermediate levels of coupling are selective, and indicates that the average channel diameter decreases during uncoupling.

The cells in adjacent segments develop largely independently of each other, under the control of separate morphogenetic gradients, but the epidermis is continuous and there is cooperation in cuticle synthesis. Regulation of intercellular communication at the intersegmental boundary may be responsible, since in the bug Oncopeltus fasciatus, LRB, CF and Lucifer yellow move freely between cells within the segment but are impeded from passage to the adjacent segment. A strip of cells at the segment border has reduced junctional permeability, which is modulated independently of that within the segment. Under conditions that block the passage of dye, electrical coupling between segments remains strong, although an increase in junctional resistance of the border cells can be detected. Exposure to the molting hormone 20-hydroxyecdysone removes the barrier to intersegmental dye spread. This suggests that while depressed junctional coupling normally limits segmental interaction, developmental regulation ensures full cooperation at critical times.

ACKNOWLEDGEMENTS

I am grateful to Dr. S. Caveney and the members of my advisory committee, Dr. M. Locke and Dr. M. D. Owen, for guidance.

I thank Dr. G. M. Kidder for the critical reading of this thesis.

TABLE OF CONTENTS

Page

LIST OF FIGURES

LIST OF TABLES

LIST OF APPENDICES

CHAPTER 1

GENERAL INTRODUCTION

1.1 Introduction

When cells form tissues, they can take advantage of interconnections with other cells for the exchange of the smaller cytoplasmic molecules, and so do not remain wholly self-reliant, as independently functioning units. The first evidence of such cell coupling was in cardiac tissue, where Weidmann (1952) showed that a voltage shift in one cell caused a parallel shift in other cells. Subsequently, Furshpan and Potter (1959) showed electrical coupling at a synapse, not involving chemical intermediates. The 'electrotonic synapse' in coupled excitable cells allows transmission of electrical impulses more rapidly than by chemical means, and is found in contractile organs, some interneuronal connections (Bennett and Goodenough, 1978), and in excitable epithelia (Bassot et al., 1978).

The membrane structure responsible for cell coupling is the gap junction, and its first description was in both excitable and non-excitable tissues (Revel and Karnovsky, 1967). The implication of intercellular coupling in nonexcitable cells is less clear than in excitable cells.

It is assumed to serve in homeostasis and the coordination of cell activity, since its abilities include the passage of electrolytes, low molecular weight nutrients, and waste products (see the reviews of Larsen, 1983, and Loewenstein, 1981). The coupled cell, by extending its virtual borders to include its neighbours, has access to their resources.

However, limitation of cell coupling may be necessary for the organisation of structure within multi-cellular structures. Coupling allows cells to cooperate in a similar purpose, but in complex tissues, cells show different patterns of activity over time, and at one time, there may be functionally distinct subpopulations, so that coupling must be limited to maintain the biochemical differences in cytoplasmic make-up. An active role for the limitation of coupling has grander implication: this may partition tissues into physiologically distinct regions, or in an embryonic tissue, into morphogenetically different domains.

I have defined selectivity in junctional communication as the purposeful modulation of intercellular coupling that prevents the passage of a molecular size class, or that permits the passage of a previously restricted class. Temporal selectivity results from the variation of coupling level over time, and spatial selectivity from different levels of coupling within an area of cells. In either case, this could be achieved though a change in channel number or by the modulation of the permeability of a given population of channels.

Variation in gap junction number would not permit or prevent the passage of particular molecules, unless there is change between the extremes of presence and absence of junctions, but it will affect the quantity or rate of passage.

In general, gap junctions can be found between cells of distinct origins that are contiguous in vivo, as in germ and somatic cells in mammals (Gilula et al., 1978) and insects (Szollosi and Marcaillou, 1980), or that have been manipulated into contact as in the case of most vertebrate cell types (Hunter and Pitts, 1981; and reviewed in Larsen, 1981). However, heterocellular coupling does not occur between fibroblasts and epithelial cells (Fentiman et al., 1976).

In insects, Caveney and Berdan (1982) found examples of spatial selectivity, where diversification of cells in the epidermis was accompanied by loss of coupling with the general epidermis. For example, columnar cells in the transporting epithelium of the cockroach rectum are coupled amongst themselves, but not to the population of sheath cells that separate them from the general epidermis; the sheath cells are themselves coupled but not to either one of the adjacent cell groups. In such cases, the selectivity could stem from conflicting patterns of activity, where the biochemical make-up of a cell's cytoplasm is so characteristically different that coupling with a neighbouring cell of different type would impede its function.

Selectivity in coupling in cells with a constant number of junctions requires modulation of the coupling level. Full uncoupling is an example of this: when uncoupled after damage a cell does not act as a drain on the channel-permeant substances of the coupled tissue. Such extreme examples illustrate the principle, but the same regulatory mechanisms can produce intermediate coupling levels in intact tissues.

1.2 Literature Review

Regulation of junctional coupling can occur in two ways, by change in the number of gap junctions, or by modulation of the permeability of an existing population of channels. These may occur together, but the intact tissues in which ultrastructural analysis can show altered gap junction number are frequently not amenable to quantitative physiological investigation as well.

1.2.1 Modulation of gap junction number

When change in the number of gap junctions is detected by electron microscopy, the coupling level is assumed to have changed as well. The action of hormones in a number of tissues has been associated with a change in gap junction number. Gap junctions increased in thyroid-stimulated frog ependyma (Decker, 1976) and in frog ooctye/follicle cell junctions exposed to chorionic gonadotropin (CG) (Browne and

Wiley, 1979). Follicle stimulating hormone (FSH) caused loss of coupling at mammalian oocyte/cumulus cell junctions (Moor et al., 1980), while both CG, in interstitial cells of the rat ovary (Burghardt and Anderson, 1979) and oestrogen, in granulosa (Merk et al., 1972) increased gap junction number. Oestrogen stimulated both an increase in gap junction number in myometrium (Garfield et al., 1980) and an increased rate of intercellular diffusion (Cole et al., 1983).

Other extracellular agents can increase gap junction number, as in the case of glucose stimulation of insulin production from pancreatic B-cells (Meda et al., 1979) and K channel blockers applied to smooth muscle (Kannan and Daniel, 1978).

In some cases, gap junctions develop as an apparent need for them arises, or disappear when no longer required. In the insect ovary, gap junctions couple follicle cells and the oocyte (and by indirectly linking successive oocytes, may regulate their development) but disappear when vitellogenesis is complete (reviewed in Caveney and Berdan, 1982). De novo formation of junctions occurs when haemocytes, a dispersed circulating population of cells in the insect haemocoel, come together to encapsulate foreign material (Baerwald, 1975).

The second messenger cAMP, itself able to pass between cells (Lawrence et al., 1978), seems able to induce

increased protein synthesis that leads to increased gap junction number and raised intercellular permeability (Flagg-Newton et al., 1981). Supporting this, cAMP caused a junction-deficient cell line to become communication competent (Azarnia et al., 1981). Radu et al. (1981) showed that catecholamine and prostaglandin, which act via cAMP, increased gap junction number and intercellular permeability in two cell lines and that the effect on coupling could be mimicked by exogenous cAMP. In insect cells, however, the action of cAMP is unclear (Caveney, 1978, 1978; Hax et al., 1974).

In tissues where gap junction number is modulated, increase probably occurs by the insertion into the membrane of single particles which then aggregate, since plaques develop with reduction in the number of dispersed particles rather than by insertion of complete structures (Lane and Swales, 1980; Yancey et al., 1979; Yee and Revel, 1978). When gap junction number decreases, particles either disperse into surrounding membrane (Lane and Swales, 1980; Yancey et al., 1979), or intact junctional membrane is taken into the cytoplasm of one cell as an 'annular gap junction' (Larsen, 1983).

1.2.2 Structure of the gap junction

Electron and X-ray diffraction analysis of isolated gap junctions have provided the best picture so far of the

structure of the channel. These preparations are crystalline, hexagonal arrays of connexons (the gap junctional unit, or particle) in two opposing sheets of membrane, with abutting connexons linked to each other. Unwin and Zampighi (1980) used electron diffraction analysis to show that there are 6 subunits to a connexon. Subsequently, Unwin and Ennis (1983; 1984) used the higher resolution of X-ray analysis to form a 3-dimensional map of the channel, and to show that Ca^{++} caused change in its structure.

The channel forming protein has an average diameter of 64Å in the plane of the membrane and is 70Å perpendicular to it. Slightly tapered, the bulkier portion is within the membrane, with more protrusion (15-20Å) outside the membrane than within the cytoplasm (<10Å). Six subunits are tilted about a radial axis at the extracellular end, to enclose the central channel. Calcium causes these to decrease cooperatively the angle of the tilt and, by moving towards each other at the cytoplasmic face, decrease the channel diameter by 18Å. This physical evidence of gating cannot alone explain uncoupling, since a portion of the channel bore remains open. However, X-ray analysis by Makowski et al. (1983; 1984) showed a distinct funnel shape to the entrance of the channel, decreasing rapidly from an initial 50Å diameter to 20Å at a level approximately 15Å below the membrane surface. This suggests that the transition which narrows the cytoplasmic channel bore may be causing complete closure at a point deeper inside.

1.2.3 Control of junctional coupling

The experimental work to be presented uses an insect system, and so this review emphasizes the physiology of junctional coupling in insects. While arthropod and vertebrate gap junctions have characteristically different ultrastructural appearances, vertebrate junctional coupling is also examined because some aspects are more fully studied there, and may have a common application.

1.2.3a Regulation of Coupling in Arthropod Cells

(i) Modulation by Intracellular Ions

Loewenstein (1966) proposed that the permeability of junctional channels was regulated by the cytoplasmic concentration of Ca^{++}. After Rose and Loewenstein (1976) demonstrated that elevation of free Ca only in the perijunctional cytoplasm could cause decreased junctional conductance, the Ca ion was considered the agent primarily responsible for control of junctional coupling in arthropod cells. This view has been re-evaluated following the demonstration in vertebrate cells of the far more potent action of H^+(Spray et al., 1981). Since an interrelationship between the Ca and H levels in the cell does exist - increased Ca_i causes a fall in pH_i in cardiac muscle (Vaughan-Jones et al., 1983) and in snail neuron (Meech and Thomas, 1977) - independence of action must also be tested.

In the intact salivary gland, Rose and Rick (1978)

showed that intracellular injection of Ca, buffered to intracellular pH levels, caused uncoupling when [Ca] was >10 μM, but without change in pH_i. Conversely, injection of a low [Ca], but acidic solution lowered pH_i to 6.8 from 7.5 without uncoupling. Therefore, increased Ca alone can cause uncoupling. Indeed, pH_i may increase during uncoupling: by withdrawal of exposure to propionate-containing medium, pH_i was increased from 7.5 to 8.7. However, the electrical coupling was not related to the pH_i change, but to a rise in $[Ca]_i$ that ensued (Rose and Rick, 1978).

Rose and Rick (1978) employed three different methods to decrease pH_i directly, but these either did not cause uncoupling, or resulted in uncoupling via elevated $[Ca]_i$. They concluded that cytoplasmic acidification does not directly decrease junctional conductance. However, Obaid et al. (1983) stated that H independently uncoupled cell pairs from Chironomus salivary gland when weak acids in the medium caused pH_i to drop from 7.4 to 6.5, but the necessary description of Ca_i is lacking. Also, in the same experiment Rose and Rick (1978) had found only a small decrease in pH_i that corresponded poorly with uncoupling.

The Chironomus salivary gland shows that Ca can act independently of H in modulating coupling, and that a decrease in pH_i is insufficient to cause uncoupling. When cytoplasmic acidification leads to uncoupling, it is probable that increased $[Ca]_i$ is derived from intracellular

sources, since intracellular injection of H could cause this effect in Ca-free medium (Rose and Rick, 1978). Mitochondria may be responsible for this, since they exchange H for Ca (Chance, 1965) and isolated rat liver mitochondria release Ca when the surrounding medium is acidified (Akerman, 1978).

It remains to be shown that change in pH_i can alone change junctional conductance. In modulation of conductance by ions, the available evidence suggests that Ca serves as the prime regulator of channel patency.

(ii) Membrane Potential Control of Conductance

In 1971, Socolar and Politoff reported that depolarizing current uncoupled cell junctions in the salivary gland of Chironomus. This was elaborated by Obaid et al. (1983), who determined that junctional conductance depends upon the membrane potential (E) - the 'inside/out' potential - of the cell. For isopotential cell pairs, more negative E increased the junctional conductance, while more positive E reduced it and could fully uncouple the cells. In cell pairs that were voltage clamped to different potentials, the less negative E set an upper limit to conductance, so that the difference (the transjunctional voltage, found important in vertebrate junctional regulation) did not determine the conductance. Sufficiently positive E in the one cell could always cause uncoupling.

The membrane potential control of coupling is an

entirely separate control from that exerted by Ca (or possibly H). Potential changes that caused transmembrane ion fluxes, or affected ion uptake or release from the cytosol, could have controlled pCa, but these, along with pCa, were ruled out (Obaid et al., 1983).

The converse situation, that Ca and H may be acting via the membrane potential mechanism, must be considered, because increase of intracellular levels is accompanied by cell depolarization (Rose and Rick, 1978). Obaid et al. (1983) showed ion control of conductance to occur independently of voltage control, by elevation of these ions in voltage-clamped preparations: uncoupling still resulted.

The effect of one can even act counter to the other; during elevation of $[Ca]_i$, depressed junctional conductance can be restored by changing E to more negative values; however, when junctional conductance has been abolished by raised $[Ca]_i$, no restoration of conductance is seen with even extremely negative E (Obaid et al., 1983).

The two independent factors of Ca and E may act on the same structure, a "gate" integral to the channel. This gate has its permeability determined by the sum of the actions upon it of Ca and E, either to open or close. Control of junctional conductance by E was best described by a function involving two separate, E-dependent relationships, and interpreted to mean that there are two gates in series per channel (Obaid et al., 1983). A cell of a coupled

tissue could then take independent action by closing the one gate in each hemichannel that it contributed to the junctional membrane.

1.2.3b Regulation of coupling in vertebrates

(i) Modulation By Intracellular Ions

Ca and H are present in the cytoplasm in roughly equal concentrations of 0.1 μM (Rink et al., 1980). Their roles in coupling regulation have been established through the use of the large blastomeres of fish and amphibian embryos. Ca decreased junctional conductance independently of pH in coupled blastomere pairs of the teleost Fundulus (Spray et al., 1982). H uncouples embryonic cells of Fundulus and the amphibian Ambystoma (Spray et al., 1981) and in Fundulus, H acts independently of Ca or other cytoplasmic intermediates (Spray et al., 1982).

However, comparison of the relative concentration changes necessary to decrease junctional conductance showed that H became effective at a concentration 3 - 4 orders of magnitude less than that for Ca (Spray et al., 1982) implying that junctional conductance was sensitive to changes in pH_i that were near the normal resting level, while pCa is normally far below the levels required to affect junctional conductance. Spray et al. (1981; 1982) showed that the action of pH on junctional conductance conformed to a Hill plot, with a Hill coefficient of 4 - 5, which implies that H

interacts with 4 to 5 cooperative, titratable binding sites in or near the hemichannel, and presumably to neutralize negatively charged groups there. The less effective Ca ion has a Hill coefficient of 2 to 3, or half that for H. These agents may use a common binding site, one which has a much greater affinity for H ions.

This suggests that junctional conductance in vertebrates is normally regulated by H, and that Ca acts only in the pathological circumstances of cell disruption or death. However, the rapid sequestering of ions within the cell causes difficulty in predicting their levels, and in the intact cell system, pH might be more strongly buffered than pCa. This, or localized ion level changes in perijunctional cytoplasm, could allow significant Ca elevation.

Coupling regulation in differentiated cell types could become quite different from that in blastomeres. Specialization of excitable cardiac cells has involved loss of sensitivity to pH_i changes (Reber and Weingart, 1982), but retention of Ca sensitivity (de Mello, 1975). Therefore, the extent of application of evidence from embryonic cells is not yet clear.

(ii) Transjunctional Voltage Control

The junctional conductance decreases in proportion to the transjunctional voltage, a potential applied across the junctional membrane, in blastomeres of the amphibians

Ambystoma, Xenopus and Rana (Spray et al., 1979; Harris et al., 1981) and of the teleost Fundulus (White et al., 1982; Spray et al., 1984). Transjunctional voltage does not cause complete uncoupling, no matter how large the potential, and the residual conductance is fairly substantial, being 20% of the maximum in Fundulus (Spray et al., 1984) and 4% in Ambystoma (Harris et al., 1983).

Coupling between rat heart myocytes was unaffected by transjunctional voltage (White et al., 1983), and again suggests that the properties of junctional coupling may change with differentiation to specialized cellular function.

The response of a single channel to transjunctional voltage appears to have all-or-none characteristics, because the first order changes in conductance that were caused by voltage are best explained in terms of transition between open and closed states (Spray et al., 1984). While there may be a voltage insensitive channel type, it is also possible that there is rapid transition between fully open and nearly fully closed states.

1.2.4 Models of channel closure

Physiological regulation of coupling occurs by change in the intracellular ion level and electrical potential in both vertebrates and invertebrates. This likely involves intermediate coupling levels as well as complete or patho-

logical uncoupling - at least such intermediate levels can be demonstrated in vitro. What is the nature of permeability in such intermediate states?

Channel gating, the control of patency by physical change in the channel structure, may be different between vertebrates and invertebrates. The channel itself seems to be different, since Schwarzmann et al. (1981) showed the insect channel to have a maximum channel diameter between 20 and 30Å, larger than the vertebrate channel at less than 16Å. A further structural difference is shown in regulation of conductance, since ion level and potential act separately on two independent gates in the vertebrate channel, while acting together on a single invertebrate (insect) gate.

There are two simple models of channel closure that describe changes in channel structure when junctional conductance is depressed. (I) During uncoupling, individual open channels pass through a number of increasingly restrictive states (with narrower bores) before closing completely. In its simplest form of graded channel closure (GCC), this model assumes that all channels are the same, and that response to an uncoupling stimulus is uniform among all channels. (II) In all-or-none (AON) closure, the individual channels of a population can be either fully open or closed, and the equilibrium shifts towards the closed state during uncoupling. Either a non-uniform channel response, with some closing before others, or careful

control of the closing stimulus near the junctional membrane is necessary in order to produce intermediate coupling levels.

Rose et al. (1977) concluded that graded channel closure occurred in cells of the midge salivary gland, since the passage of larger tracer molecules between cells was the first impeded during uncoupling - it would be expected that all sizes would suffer equal, increasing impedance if closure had occurred by the all-or-none model. Despite a considerable literature on intercellular communication, no other reports can discriminate between channel closure models. However, workers on the vertebrate junction tend arbitrarily to select AON closure (for example, Spray et al., 1984; Kimmel et al., 1984).

This is an important problem in cell and developmental biology, for we perceive a different effect from the subtle regulation of coupling level depending on the model of channel closure selected. AON closure simply reduces the quantity of all substances passing between cells, while GCC changes the quality or nature of the intercellular 'traffic', as the decreasing channel bore discriminates by size among the molecules originally able to pass between the cells.

1.2.5 The experimental system

In general, the methods that detect modulation of

coupling are limited in application to cells that form 2-dimensional structures, such as a pair or chain of cells. The insect epidermis is one tissue that forms a 3-dimensional structure but is suitable for quantitative measurements of cell coupling. The basically tubular exoskeleton or cuticle is the product of a monolayer of epidermal cells. Dissection of a piece of integument (the cells plus the corresponding cuticle) provides an effectively 2-dimensional field of cells supported by translucent cuticle. This simple structural arrangement, with the position of each epidermal cell indicated by the nature of the cuticle above it, has allowed the demonstration of some fundamental properties of developmental biology. Prominently, it has shown that a cell in the segment knows its location relative to the margins by sensing a gradient of positional information, repeating in each segment along the body and discontinuous at the segment borders.

In the continuous sheet of epidermis, the segment borders are cryptic barriers to several cell interactions. They mark the extent of serial semi-autonomous units of epidermis, that develop according to their position in the animal, but can cooperate in cuticle manufacture and in the developmental events of the molt, which affect the entire organism. Cells at these borders may have altered channel number or permeability producing spatial selectivity, since adjacent segments are electrically coupled (Caveney, 1974;

Warner and Lawrence, 1973) but may not share larger molecules (Warner and Lawrence, 1982).

1.3 Thesis Objectives

The two principal techniques for investigation of intercellular coupling are intracellular current injection and the microinjection of fluorescent tracers. These allow the quantification of electrical coupling, which can then be examined for change, while the second technique allows a qualitative test for the passage of small molecules between cells. These techniques were applied to the insect epidermis to find answers to the following questions, the first concerning temporal selectivity, and the second spatial selectivity, namely:

1. Can the permeability of gap junctions be regulated to give rise to temporal selectivity? That is, does the mechanism of channel closure result in intermediate levels of permeability that are seen as discrimination against some of the molecules that were earlier able to pass?

2. Can regional patterns in junctional communication be detected that correlate with known developmental events? Specifically, is there selectivity in intercellular communication in the epidermis at the boundary between developmental compartments?

If so, can a simple reduction in the number of communicating channels account for this, or does the regulation of junctional coupling cause discrimination among the molecules able to pass between compartments?

CHAPTER 2

TEMPORAL SELECTIVITY IN JUNCTIONAL COMMUNICATION

2.1 Introduction

Temporal selectivity requires that variation in the permeability of intercellular channels alters the nature of the molecules that pass among cells. A change in coupling due to a shift in the proportion of open to closed channels will not block any particular molecule from passage, but a graded change in the individual channel bore will affect its selectivity.

One way to distinguish between graded and AON channel closure is to correlate junctional permeability to inorganic and to organic ions at different levels of coupling. In the epidermis of the larval beetle Tenebrio molitor, electrical coupling can be quantified and correlated with the ability of small fluorescent dyes to pass between cells as junctional coupling is reduced. If coupling regulation occurred by AON closure, then the intercellular passage of the dyes, would decrease in proportion to the decrease of electrical coupling. However, if channel closure is by GCC, tracer molecules would be blocked from passage during uncoupling in order of decreasing size, i.e., occlusion of

each tracer would be expected to occur at a different level of the decreasing electrical coupling. This chapter shows that in insect epidermis, intercellular channels appear to close in graded fashion, which suggests that intermediate coupling levels are truly selective.

2.2 Materials and Methods

2.2.1 Beetle Culture

Larvae of the yellow mealworm Tenebrio molitor (L.) were reared on a whole wheat flour-bran-yeast mixture maintained at 27°C in a 12 hr light/dark cycle. Last instar larvae were collected immediately after ecdysis (weight > 0.1 g). These were used within 4 hours of collection as newly molted animals, or were kept a further 5 or 6 days in 50 mm Petri dishes under the same conditions. These were used as intermolt larvae, being roughly in the middle of the stadium and yet to start the sequence of events leading to pupation.

2.2.2 Dissection and Tissue Culture

Tenebrio larvae, either newly molted (0-4 hr) or intermolt, were anaesthetized prior to dissection by immersion in 70% methanol for 3 minutes. This treatment is reversible and does not affect subsequent development. The abdominal sternites (ventral integument) from segments II through VII

were dissected free of the animal into tissue culture medium (see below). The fat body and adhering muscles were removed and the sternites, now consisting of a single layer of epidermal cells attached to cuticle, were transferred to fresh medium.

The culture medium used was a standard vertebrate culture medium modified to approximate the ionic and osmotic conditions of beetle blood. It consisted of HB597 (Connaught, Toronto) with 10% foetal calf serum (Gibco), and added KC1 (30mM), $MgCl_2$ (20mM), and sucrose or trehalose (50mM). The medium was buffered with 20 mM PIPES (Sigma), adjusted to pH 6.8 with 1N NaOH.

One of the dissected preparations was selected for immediate use and transferred into a 35 mm Petri dish with inset glass cover slip, containing 2 ml of either medium or experimental saline. The other preparations were placed in Petri dishes and kept in an incubator (Hotpack) at 27 °C in air with 2% CO_2.

The saline solutions were taken from Popowich (1975), and their compositions are shown in Table 1. The control saline was a simple solution of salts, organic acids and sugar, while the experimental saline had Li substituted for Na, but was otherwise the same. Both were buffered with 10 mM PIPES, adjusted to pH 6.8 with 1N NaOH and KOH respectively, and had foetal calf serum added to 10%.

TABLE I: Composition of control and experimental salines (after Popowich, 1975).

Saline	Li Saline (mM)	Control (mM)
NaCl	--	80
KCl	40	40
LiCl	80	--
$CaCl_2$	1	1
$MgCl_2$	1	1
Malic acid	2.7	2.7
Glutamic acid	2.7	2.7
Sucrose	98	98
PIPES	10	10
Phenol Red	trace	trace
to pH 7.0,	KOH	NaOH

2.2.3 Electrophysiology

Tissue preparations were placed into 35 mm Petri dishes containing medium and held flat against the inset glass coverslip by bent fragments of razor blade touching the edge of the preparation. They were observed with a Zeiss IM35 inverted microscope with 40x phase contrast objective. Room temperature was maintained at 25-27 °C.

Glass microelectrodes were made from microcapillary tubing (Quikfil, W-P Instruments No. 1B100F) with a vertical microelectrode puller (Narashige, Japan). After backfilling with 3M KCl, the electrodes had tip resistances of 20-40 MΩ in medium. They were mounted on DeFonbrune pneumatic micromanipulators (Beaudouin, Paris) and connected by chlorided silver wires to electrometers with input impedance of 10^{11} Ω (W-P Instruments, Model M-707). The preparation was grounded through a KCl/agar electrode immersed in the bathing medium. Two independent microelectrodes were used, one to pass current into a cell, and the other to record electrotonic potentials (the change in membrane potential due to injected current passing across a passive cell membrane) at various interelectrode distances in the cell sheet.

Electrotonic potentials were generated by passing hyperpolarizing pulses of current (6×10^{-8} amp; 200 msec) down either electrode from a stimulus isolating unit (W-P instruments #305-R). Electrotonic potentials, as well as the electrode resistances and membrane potentials, were recorded on a Brush 2200 two channel recorder.

The theory describing electrotonic spread in cell monolayers has been developed by several authors, principally Eisenberg and Johnson (1970) and subsequently Shiba (1971) and Siegenbeek van Heukelom (1972). The model used here consists of an infinite planar sheet of cytoplasm bounded on both sides by membrane, and the electrotonic spread of current is predicted by a relationship based on a Bessel function:

$$V(\ell) = I_o \cdot \frac{R_i}{2\pi t} \cdot K_o(\ell/\lambda) \qquad (1)$$

where $V(\ell)$ is the electrotonic potential (volts) recorded at distance ℓ (cm) from the point of current injection into the sheet; I_o the injected current (amp) at $\ell = 0$; R_i is the resistivity of the core material (Ω cm) and t the sheet thickness (cm). K_o is a zero-order Bessel function of the second kind with imaginary argument (Jahnke and Emde, 1960). Equation (1) holds true provided that $\ell > t$, a condition satisfied here. The space constant in the model is defined as:

$$\lambda = \sqrt{\frac{R_m \cdot t}{2 \cdot r_i}} \qquad (2)$$

where R_m is the specific resistance of the membrane bounding the cytoplasm (Ωcm^2). For quantification of experimental data, equation (1) was rewritten as

$$V(\ell) = A \cdot \frac{2}{\pi} \cdot K_o(x) \qquad (3)$$

where $A = I_o\ r_i/4$ and is constant for each experimental determination, $x = \ell/\lambda$ and $r_i = R_i/t$. Values for A (and hence r_i) were obtained by fitting a theoretical curve to each set of experimental data. In this analysis, interelectrode distances are much less than the space constant and so x in the tabulated function $2/\pi\ .K_o(x)$ ranged between 0.02 and 0.3.. $r_i(\Omega)$ is the effective resistance to current within the cytoplasm of the model and so is inversely proportional to the ability of current to pass among cells.

The spatial decay of potential described by the Bessel function has three identifiable phases: initially, more rapid than exponential over short distances (less than a cell diameter, where current spread is actually 3-dimensional), approximately exponential for 'intermediate' distances and slower than exponential for large distances. The interelectrode distances used in experimental measurements ranged between 40 and 440 μm, and fit the exponential phase of voltage decay. Therefore, in a semi-logarithmic plot of voltage against $\log_{10}$ distance, a straight line can be placed through experimental values of electrotonic potential. Here, r_i is directly proportional to the slope of the spatial decay and was obtained in practise by the following method: from the line fitted by eye through the data points, the value of [V(10 μm) - V (100μm)] was determined and divided by 2.04×10^{-6} (amp). This scaling

factor is simply an adjustment for the input current to give the r_i that the more rigorous treatment above has determined. Once found, this number can be used repeatedly and on data sets from other preparations.

Each measurement of the electrotonic voltage at a given interelectrode distance required that both the polarizing and recording electrodes obtain and hold the full membrane potential. Current pulsing, which aids the penetration of the electrode through the cell membrame, was continued until the electrotonic potentials seen on the chart recorder had reached a stable maximum before re-positioning the electrode at a different distance. These potentials were measured by examining the chart recording at 7x magnification with a Wild stereoscope. Routinely, between 6 and 10 data points were used for each determination of r_i. However, when r_i was changing rapidly, fewer points were used to determine each line - usually 5 or 6, but not less than 4.

The space constant (λ) was also determined empirically, using the slope and position of the line of electrotonic decay. The ratio of the slope to the electrotonic potential at a fixed interelectrode distance, [V(10 μm) - V(100 μm]/ V(100 μm), was related to the true using a standard curve. This was previously determined by Popowich (1975) from trial-and-error fit of data points to the actual value of λ.

2.2.4 Fluorescence Microscopy

Two fluorescent dyes were selected for use as intracellular tracers due to extremely low membrane permeability. These were 6-carboxy fluorescein (MW 376; Eastman Kodak) and lissamine Rhodamine B (MW 559; Polysciences) (Appendix I). The molecular dimensions were measured from CPK space-filling models, and for carboxyfluorescein (CF) were 12 x 12 x 8 Å and for lissamine Rhodamine B (LRB), 18 x 14 x 11 Å. These molecules can pass through a channel of diameter equal to, or greater than, their second largest dimension. This channel limiting dimension is underlined in each case.

Fluorescence was observed on a Zeiss IM35 inverted microscope with epifluorescence optics. CF and LRB were excited by light from a mercury vapor lamp (HBO 50W) using the following Zeiss interference-filter sets: excitation filters, BP485 (CF) and BP546 (LRB); barrier filters BP520 (CF) and LP580 (LRB); with dichroic mirrors: FT510 (CF), and FT580 (LRB). The colours of fluorescing CF and LRB are quite different, with CF appearing yellow-green and LRB orange-red. There is little overlap in their excitation and emission spectra, and so by simply exchanging the filter sets, mounted on a sliding fitting, each tracer could be viewed selectively when both were present in the tissue.

Tracers were dissolved in distilled water and brought to pH 7.0 with 1N NaOH. CF was used at 10 and 20 mM, and

LRB at 20 mM. The solutions were filtered before use (0.22 μm, Millipore) to minimize electrode clogging. For simultaneous injection of dyes, CF and LRB were combined in a ratio of 1:4, usually 10 mM CF and 40 mM LRB, that gave roughly equal intensities when injected into control epidermal preparations. (While derived empirically, this ratio also reflects the different quantum efficencies of fluorescence of the two molecules; Nairn, 1976). Filled electrodes were stored for less than 2 days, in contact with dye solution in small plastic microscope slide boxes (E.F. Fullam). Stock dye solutions were stored in a refrigerator in foil-wrapped containers.

For dye injection, glass microelectrodes were made to specifications that minimized the electrical resistance when filled with KCl (5-10 MΩ), while preserving much of the sharpness of the sub-micron tip. This greatly reduced electrode blocking during iontophoresis, otherwise common with LRB solutions. After backfilling with dye solution by capillary action, dye electrodes had resistance of 100-200 MΩ.

For iontophoresis into cells, dye was expelled from the electrodes by hyperpolarizing (negative) current pulses at 5×10^{-9} amp for 200 msec. Occasionally, a single pulse of higher current (6×10^{-8} amp) was useful in obtaining the full membrane potential as the electrode was inserted into a cell. This gives more rapid dye delivery, but increases the chance of electrode clogging.

2.3 Results

The sternite of the larval mealworm is typical of arthropod integument, and has cellular and acellular components. A monolayer of epidermal cells is attached apically to the translucent cuticle which it secretes, and basally, to a poorly developed basal lamina. There are secretory cells and nerves, but epithelial cells are by far the most numerous: in the last larval instar, nearly 50,000 cells in the sternite, each 10 μm in diameter, are packed in a hexagonal array to form a rectangle roughly 230 cells long by 200 wide. Among the 20,000 cells of the sternite preparation (Fig. 1), electrical coupling is extensive and isotropic (Caveney, 1974).

The detection of electrical coupling in the epidermis and its quantification has been described in detail previously (Caveney, 1974; Caveney and Blennerhassett, 1980). An electrode inserted into an epidermal cell records a negative potential, uniform (+/- 2 mV) among cells in the sheet. In a typical chart recording (Fig. 2), current pulsed into one cell causes an electrode in another cell to record a matching deflection of the membrane potential, the electrotonic potential, that becomes smaller as the distance between the polarizing and the recording electrode is increased.

The intercellular resistance (r_i) of the epidermal sheet in medium is fairly constant at $2.4 \pm 0.7 \times 10^5 \Omega$ in

Figure 1

A preparation excised from the animal and viewed in phase contrast shows a monolayer of thousands of epidermal cells, supported on a translucent cuticle.

A. Individual nuclei are seen as small white spots. At the posterior of each segment, there is a zone of thin pliable cuticle, seen to the left as a bright area with little cell detail. Two large bristles (mechanoreceptors) are in the midregion of the border between these zones, and branching nerves extend to these and other smaller bristles in the epidermis, seen as the larger, irregularly spaced bright spots. Clamps hold down the preparation at the edges (out of view), but some curvature remains, throwing part of the field out of focus and changing the appearance of the cells to the right. Scale bar, 50 μm.

B. At the higher magnification used for electrophysiology, nuclei are well resolved, and in most areas, phase-bright regions between them suggest the presence of cell membranes. Ripples in the cuticle cause uneven brightness of the field, also seen in A. Two glass microelectrodes (e) come down to the plane of the cells, but the sub-micron tips are not resolved. Scale bar, 20 μm.

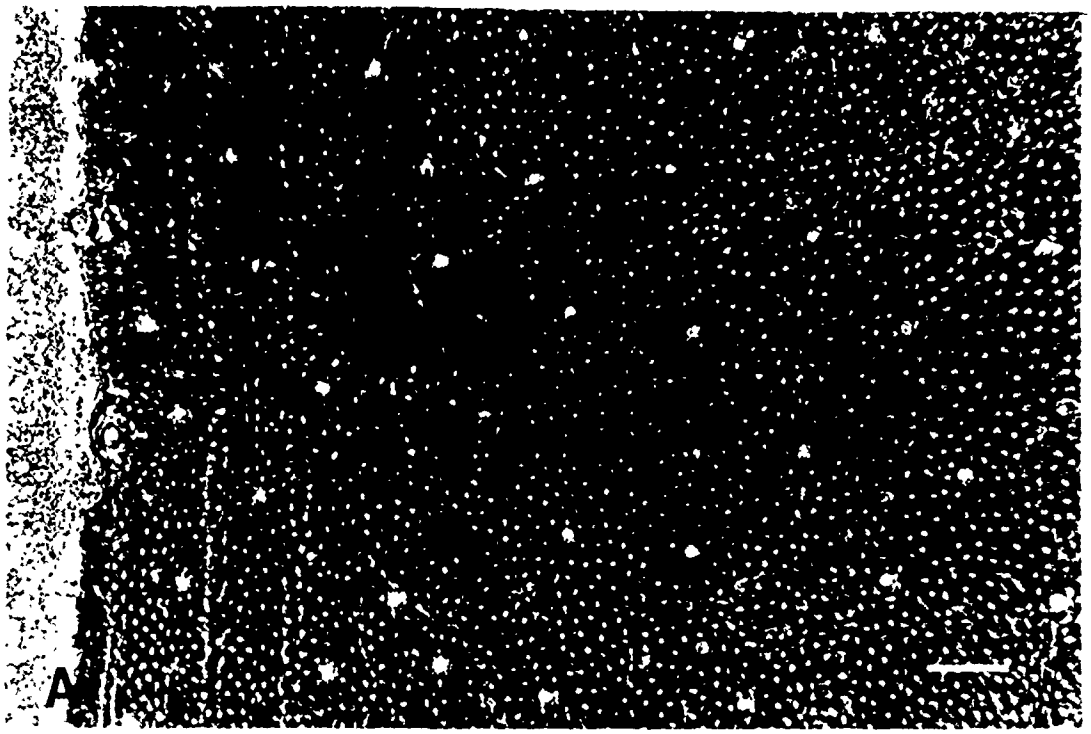
A

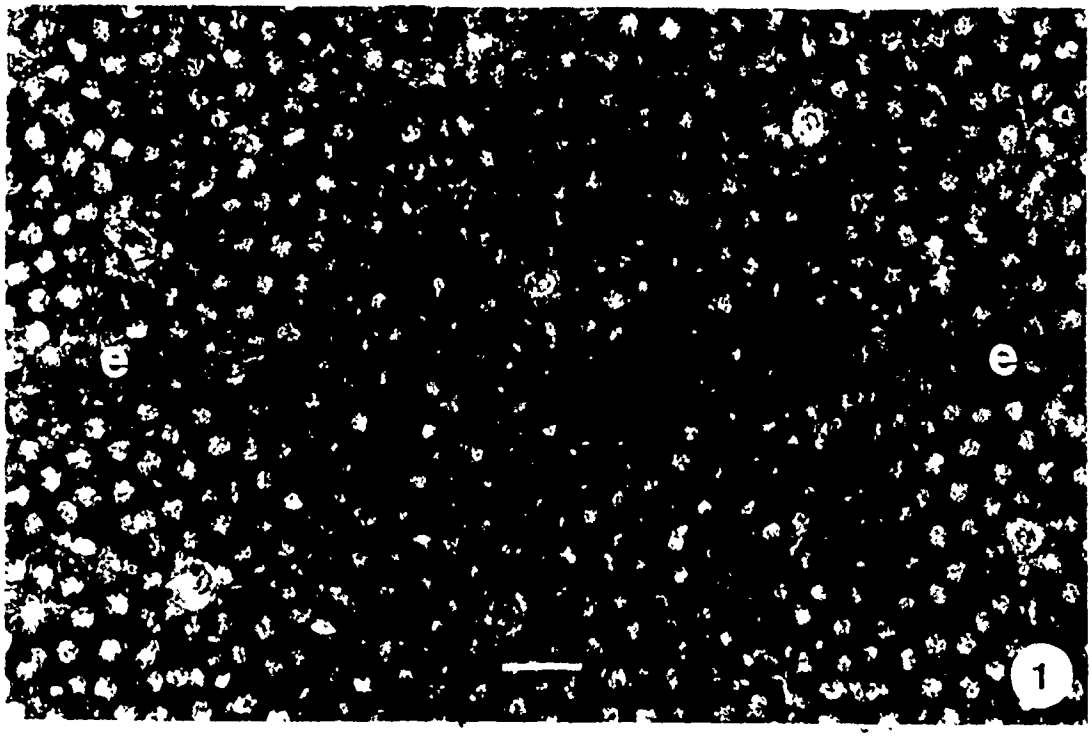
e
e
1

Figure 2

A chart recording shows that current pulsed through a microelectrode into a cell in a coupled cell sheet can be detected many cells distant by an electrode in another cell. The voltage deflections increase as the interelectrode distance is decreased, and the relationship between the electrotonic voltage and the distance is a measure of intercellular coupling.

Current is pulsed into an electrode whose tip is in the medium (lower left, negative-going deflections). There are no corresponding deflections in the trace from the right electrode. ($\sim$1 mV of inter-channel 'cross-talk' is seen regardless of electrode position). The left electrode was placed into a cell, recording the membrane potential (41mV). Current was then pulsed into the other electrode, and it was placed into a cell 440 um* from the recording electrode. In that tracing, the deflection corresponding to the pulsing is the electrotonic potential. The left baseline was manually adjusted (*). As the polarizing electrode was placed in cells that were closer to the recording electrode, the electrotonic voltage increased, becoming approximately twice as large at 44 um. After 1.5 minutes, the left baseline was changed (*) and the electrode removed from the cell.

Scale bars: vertical bar 10 sec; horizontal bar 10 mV.

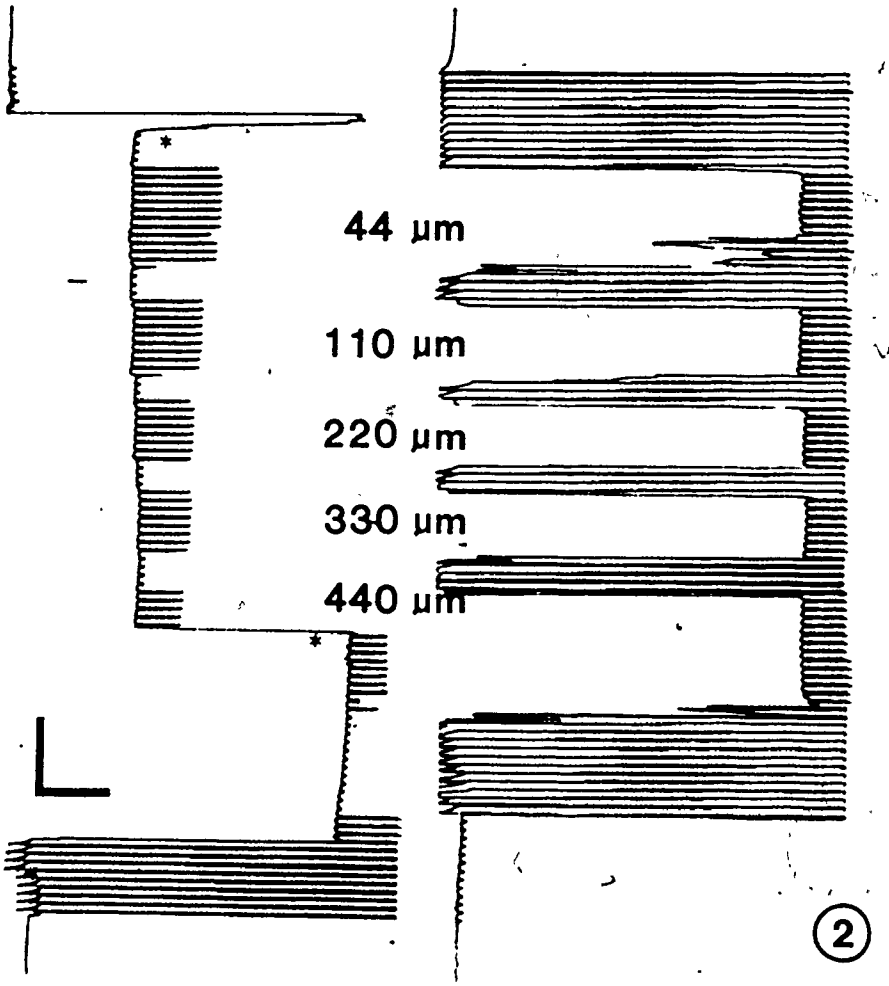

(2)

preparations freshly dissected from newly molted animals. To change the level of coupling, the extracellular Na was replaced with Li in an experimental saline. Fig. 3 shows this can raise the initial r_i value of 2.3 x $10^5\Omega$ to 12.5 x $10^5\Omega$ at 30 minutes - the lower degree of coupling indicated by the more rapid spatial decay of voltage. The control saline, with Na present, had only slight effect upon r_i: initially 2.6 x $10^5\Omega$, it rose slightly by 17 minutes to 4.3 x $10^5\Omega$, then returned to 2.6 x $10^5\Omega$ at 100 minutes, and was 3.9 x $10^5\Omega$ at 200 minutes.

Li substitution was selected for its ability to cause gradual uncoupling, over a period adequate for repeated measurements of coupling parameters. This is discussed in the next section.

2.3.1 Electrical Uncoupling of Newly Molted Epidermis

The sheet resistance of an epidermal preparation was measured at successive time intervals after exposure to Li saline. Electrical coupling remained stable for approximately 15 minutes, but then passed through a number of states of increasingly rapid electrotonic decay (Fig. 4): electrotonic potentials at specific distances became larger, but their rate of decrease over distance was even more rapid, increasing the steepness of the slope and therefore r_i. Membrane potentials became unstable to sustained electrode penetration, and after 51 minutes in Li saline, electrical

Figure 3

A plot of the electrotonic voltage against the logarithm of the interelectrode distance shows a linear relationship. The slope is proportional to the intercellular resistance (r_i), and the height of the line, to the non-junctional membrane resistance (see Methods). Measurements were made in newly molted epidermis in medium (open circles), and in the same preparation after exposure to Li saline (closed circles). The spatial decay of voltage becomes more rapid in Li saline, indicating that intercellular coupling has decreased. The r_i of the epidermis in medium was $2.3 \times 10^5 \Omega$ and in Li saline was $12.5 \times 10^5 \Omega$.

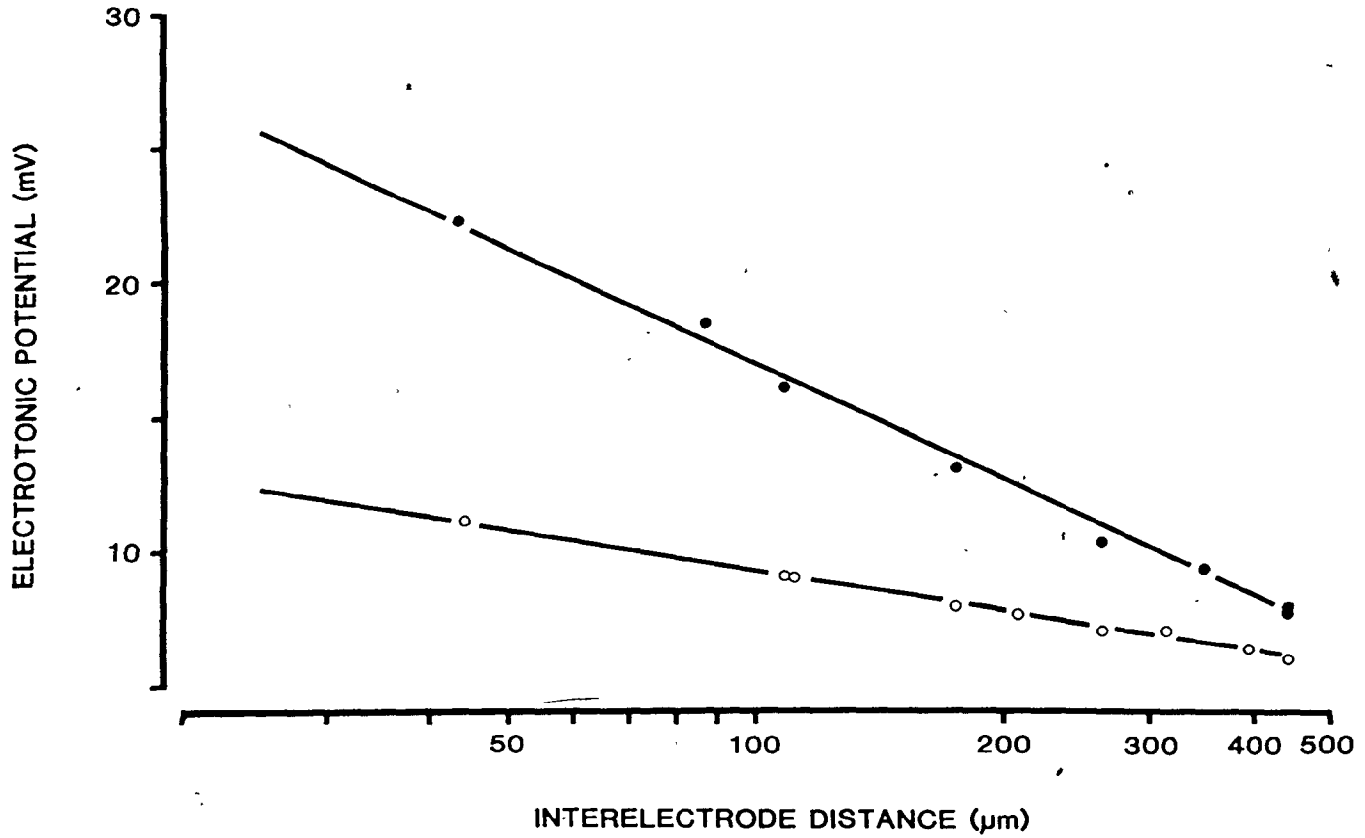
30
20
10
ELECTROTONIC POTENTIAL (mV)
50
100
200
300
400
500
INTERELECTRODE DISTANCE (μm)

③

Figure 4

Successive measurements show that a preparation exposed to Li saline passes through a series of states of decreasing electrical coupling. There was an initial period of little change, where the r_i was $2.3 \times 10^5\ \Omega$ in medium and at 10 minutes (O) and 13 minutes (not shown) in Li saline. The r_i had increased to $2.7 \times 10^5\ \Omega$ by 20 minutes (■), and to $3.5 \times 10^5\ \Omega$ at 28 minutes (+), a relatively slight change on this graph. Subsequently, change was more obvious, with r_i more than twice the control by 33 minutes at $5.9 \times 10^5\ \Omega$ (△), $8.6 \times 10^5\ \Omega$ at 41 minutes (□), $10.3 \times 10^5\ \Omega$ at 45 minutes (●) and $12.5 \times 10^5\ \Omega$ at 51 minutes (▲). Electrical coupling was detected but could not be quantified for a few minutes after this, and then the cells became fully uncoupled.

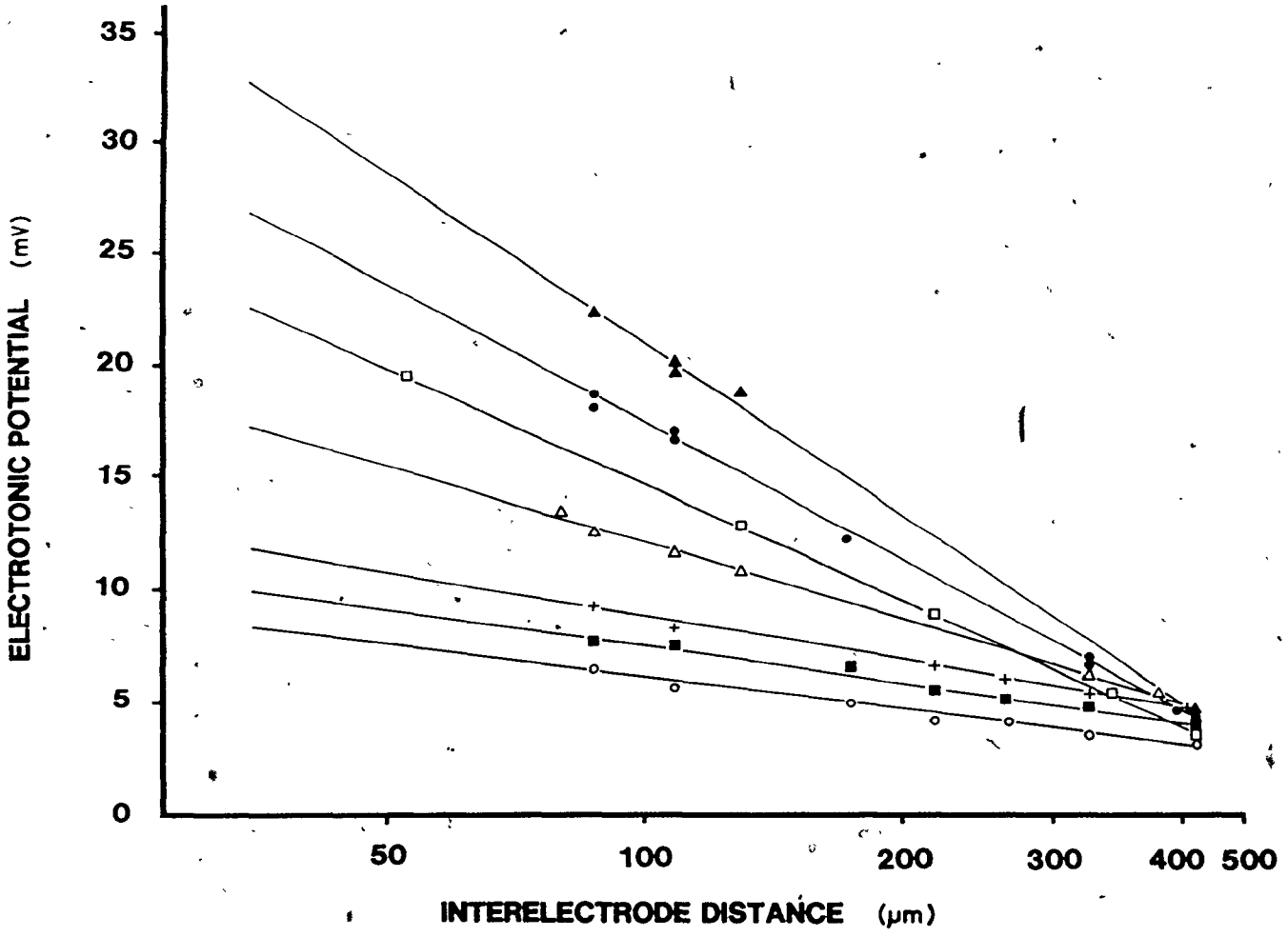
35
30
25
20
15
10
5
0
ELECTROTONIC POTENTIAL (mV)
50
100
200
300
400
500
INTERELECTRODE DISTANCE (μm)

4

039

coupling could not be accurately measured, though present. However, by 55 minutes, electrotonic potentials could not be detected qualitatively at any interelectrode distance, and the preparation was fully uncoupled.

During current injection, considerable amount of Cl and water enter the cell with each pulse. In a coupled cell seen in phase contrast, this is seen as a local change in the refractive index (a bright 'puff') that then quickly disappears at the end of the pulse. However, when current was injected after the cell membrane potential had fallen, and the cell had become uncoupled, this caused rapid swelling, and even rupture. In cells exposed to Li saline, this effect was only seen upon current injection after electrical coupling could not be detected - after 55 minutes in this preparation - and is an independent proof that the cells were uncoupled.

The increase with time of r_i during exposure to Li saline (Fig. 5) was smooth and continuous. Sheet resistance doubled by 30 minutes and was more than 4 times the initial value by 45 minutes. In the preparation in this Figure and all newly molted preparations, r_i always increased monotonically, never dropping to a level lower than the previous measurement. The time course of uncoupling was similar among preparations taken from one animal, and also among those taken from different animals. r_i values were pooled according to the time of measurement, and a line represen-

Figure 5

The intercellular resistance of the epidermis in Li saline increases monotonically after an initial lag period. Twelve consecutive measurements of r_i (left axis; open circles) from one preparation, of which 7 are shown in Figure 4, followed electrical coupling during its decrease over at least a 6 fold range: r_i started at $2.3 \times 10^5 \Omega$ in medium (at 0 time) and increased to $12.5 \times 10^5 \Omega$ at 51 minutes in Li saline. Since r_i increased gradually and monotonically during uncoupling, ionic coupling among cells is capable of continuous modulation over a wide range.

During this period, the membrane potential (closed circles with standard deviation bars; right axis) changed independently of cell coupling. It dropped quickly from 32 mV to 17 mV as r_i began to increase, and was stable during the period of maximum change in r_i. A decrease in membrane potential began after r_i had reached a maximum and could no longer be measured.

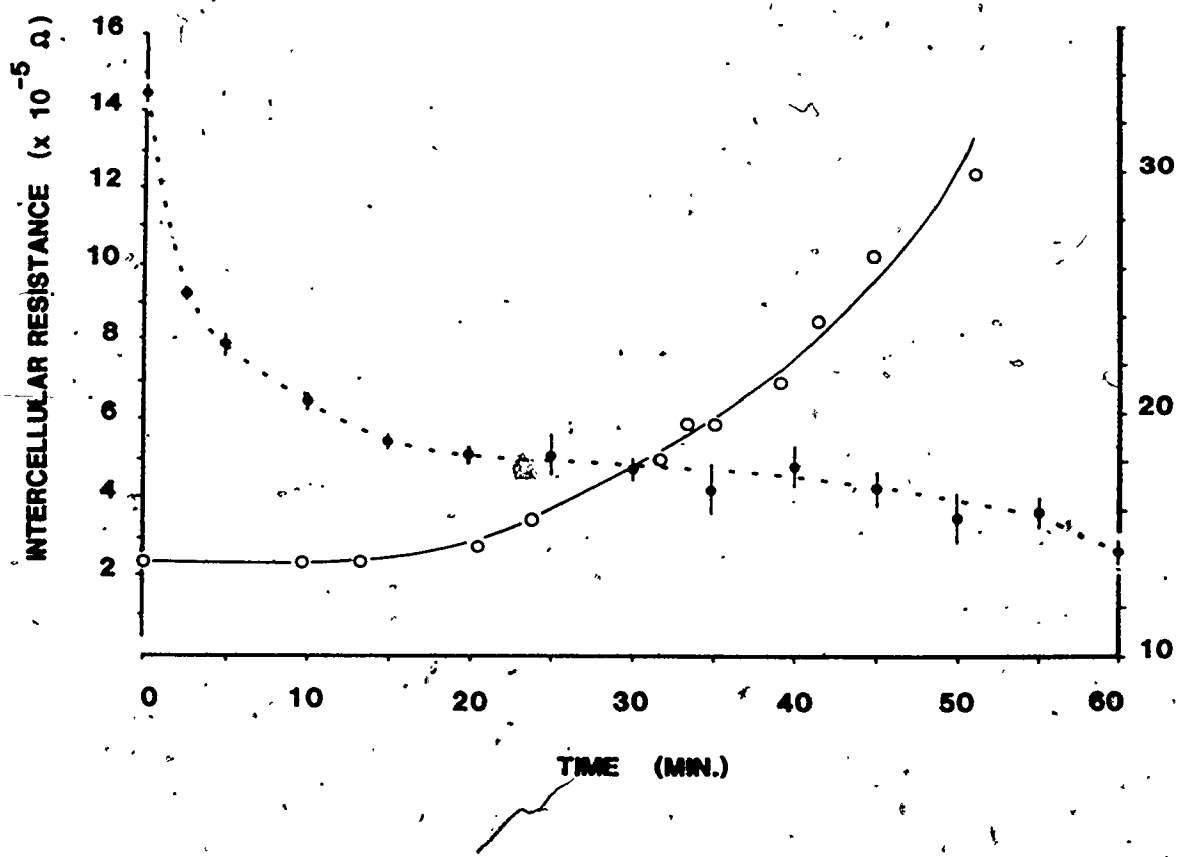
INTERCELLULAR RESISTANCE (x 10^{-5} Ω)
16
14
12
10
8
6
4
2
0
10
20
30
40
50
60
TIME (MIN.)
30
20
10
MEMBRANE POTENTIAL (mV)

(5)

042

ting the typical uncoupling behaviour of newly molted epidermis in Li saline was plotted by eye through the averaged values (Fig. 6). The characteristics seen in the uncoupling curve of the single preparation of Fig. 5 are further emphasized: after an initial period of little change, intercellular resistance increased smoothly over an 8-fold (2.4 to 19.8 x $10^5\Omega$) range of average values, and extreme individual values had a 16-fold range, from 1.7 to 27 x $10^5\Omega$.

Clearly, the junctional membrane can vary widely in its resistance to the passage of current-carrying ions. Considered alone, these results do not explain how individual channels change, but allow the conclusion that their pooled conductance can be modulated continuously. This can produce intermediate conductance states between the maximum (control) and the minimum (closed) states.

2.3.2 Dye uncoupling of newly molted epidermis

2.3.2a Tracer movement in control epidermis

The intercellular movement of both CF and LRB in control tissue was rapid, and easily perceptible by eye. Fluorescence was visible 5-6 orders of cells from the injected cell within a minute.

The appearance of the dye 'spreads' (the range of fluorescence of intracellular dye) was different for the two tracers: CF tended to localize in certain areas of the

Figure 6

The rate of electrical uncoupling in Li saline was uniform among preparations from different animals. Values of r_i were pooled from preparations in medium (C) and at 5 minutes intervals in Li saline. A standard curve was made by fitting a line by eye through the average values (closed circles with standard deviation bars).

Arrows indicate the times (with standard deviation bars) at which the fluorescent dyes Lissamine Rhodamine B (LRB) and carboxyfluorescein (CF) become blocked from intercellular passage. These results are presented in Section 3.3.3.

⑥

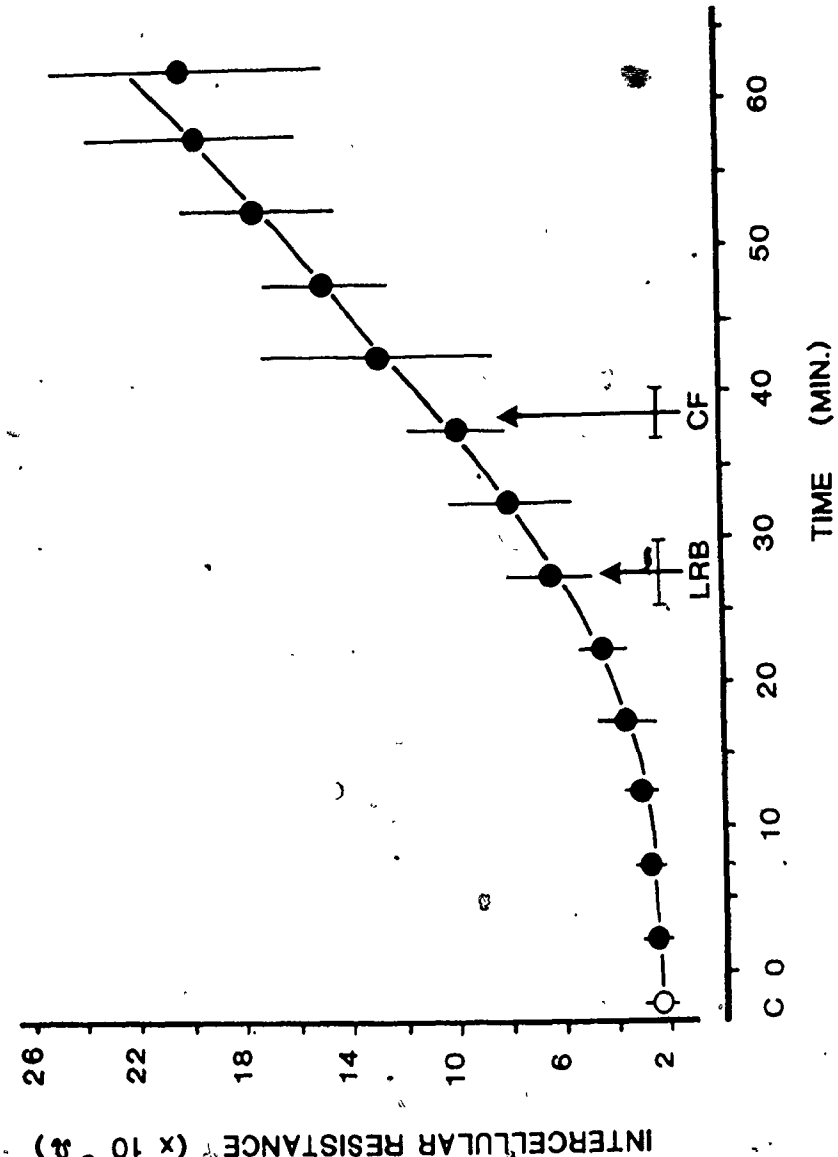
INTERCELLULAR RESISTANCE (x 10⁻⁵ Ω)
26
22
18
14
10
6
2
C
0
10
20
30
40
50
60
TIME (MIN.)
CF
LRB

cytoplasm as it passed through the cells, whereas LRB did not, and so had a more even appearance (Fig. 7). Steps of decreasing LRB fluorescence intensity were visible, corresponding to cell margins. This was not seen with CF except under experimental conditions.

While the dye was injected into the source cell by iontophoresis, its cell-to-cell movement was not dependent upon current pulses. Dye continued to spread after the pulsing was stopped, or the electrode removed, and ultimately the dye diffused away entirely. This ruled out any significant electrophoretic effect extending beyond the source cell. Further, when dye was injected into an uncoupled cell, and providing pulsing was stopped before the cell burst, no dye was forced into adjacent cells. Thus, a nearly-uncoupled cell filled with dye could be re-examined for the gradual passage of dye to adjacent cells, without the contributing factors of initially voltage driven dye passage, or subsequent spread through voltage damaged, leaky membranes.

During the course of dye spread in control epidermis, the fluorescence of the source cell quickly reached a constant level as the rate of dye injected matched the rate of loss to the adjacent cells. Commonly, the prolonged delivery of dye would result in the source cell becoming uncoupled, due to the disruptive effect of iontophoresis. In this case, the fluorescence of the surrounding cells

Figure 7

When CF and LRB are iontophoresed into the epidermis at the same concentration (25 mM), CF appears to pass among the cells more quickly: at an equivalent time of injection, CF has spread 4-5 cell orders away from the source in A, while LRB has spread only 2-3 cell orders in C. Scale bar, 20 μm.

A. Viewed by epifluorescence, an electrode injects CF into an epidermal cell. The exposure was 4 sec during the end of 28 s of injection (E, 30 mV). The spread of CF has a mottled appearance, which seems to be due to its partial exclusion from certain areas of the cell, but does not involve the nucleus. It is difficult to detect steps in the intensity at cell margins, unlike the spread of LRB in C.

B. A phase contrast view of the cell field in A. The electrode was removed before there was any change in the membrane potential and the source cell (+) has a normal appearance under phase contrast (compare with D).

C. The spread of LRB photographed at 28 s of injection (4 s exposure) is not as extensive as that of CF at an equivalent time to A above. LRB has passed to 2-3 cell orders, identified by the steps in intensity at their margins. The fluorescence within the cells is even, with no mottling, although the cells are part of the

same preparation used in A.

D. A phase contrast view of C. The source cell (+) lost its membrane potential of 32 mV during injection and is typically swollen and phase-bright.

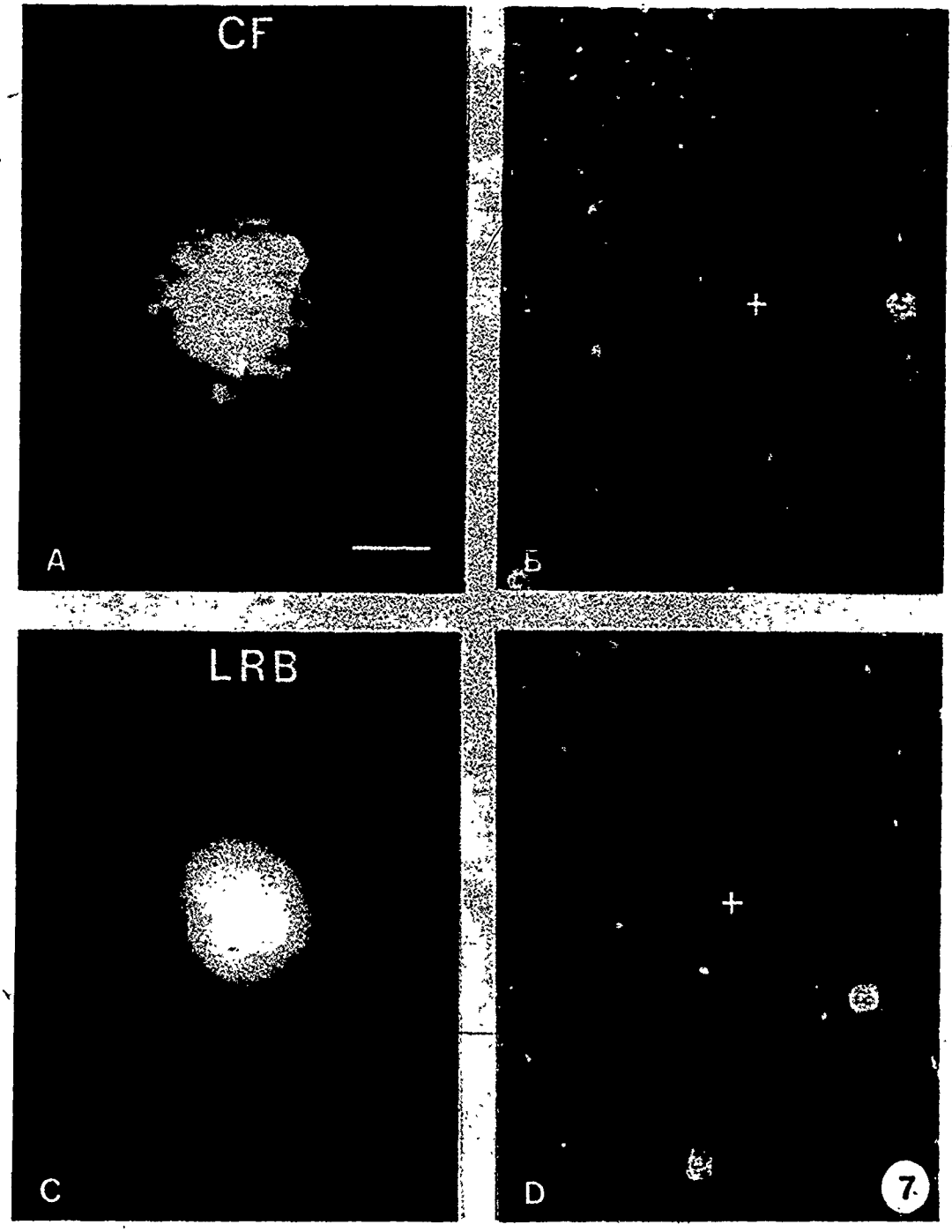
CF
A
Б
LRB
C
D
7

would decrease rapidly, implying that no further dye was entering them. This always occurred when the membrane potential was lost. Sometimes, however, dye uncoupling would precede any change in the membrane potential.

The passage of tracer from an injected cell to its neighbours could only be determined if the fluorescence seen is indeed an indicator of the presence of tracer. The narrow depth of field of the 40x objective used causes out-of-focus areas of the injected cell to superimpose upon the focussed image, and there may also be scattering of the light emitted within the cell. Demonstrating the extent of this non-specific fluorescence, the dye-filled but uncoupled cells in Fig. 8D, and 9 (G, H, K) show that the sharply focussed edge of the cell was accompanied by 'flare' extending less than 1/2 a cell width. In practice, the effect of flare was minimized by focussing through the cell, and so uncoupled cells could be easily distinguished from marginally coupled ones.

2.3.2b Tracer movement during uncoupling

During initial exposure of the preparation to Li saline, the appearance of the tracer spreads was similar to that seen in control preparations. With further time in Li saline, the extent of dye spread from successive injections became steadily reduced, and finally was restricted to the injected cell. Fig. 8 illustrates this sequence.

Figure 8

Li saline causes a progressive reduction in the extent of CF spread at equivalent periods of injection. For 10-15 minutes after epidermis was exposed to Li saline, the appearance of the spread of CF was similar to that in medium: at 8 minutes (A), CF passed into 3-4 cell orders in 25 s of injection. Dye spread more slowly at 22 minutes (B), with pronounced steps in the intensity of fluoresence at the margins of the 2-3 cell orders entered by 22 s of injection. By 28 minuts (C), CF passed only to adjacent cells by 23 s. At 38 minutes, the cells were dye uncoupled: no spread was seen at 10 s of injection (D), and there was no spread to adjacent cells, or reduction of intensity of the source during intermittent observation for the next 3 minutes. Small cell extensions filled with dye stand out against the background. Flare blurs part of the image of the cell, but its limited extent causes no difficulty in distinguishing the uncoupled cell from the first order spread in C. In the phase contrast view (E), an arrow indicates the injected cell.

For A-D, the negatives were exposed for 8 s, and printed identically. Scale bar, 20 μm.

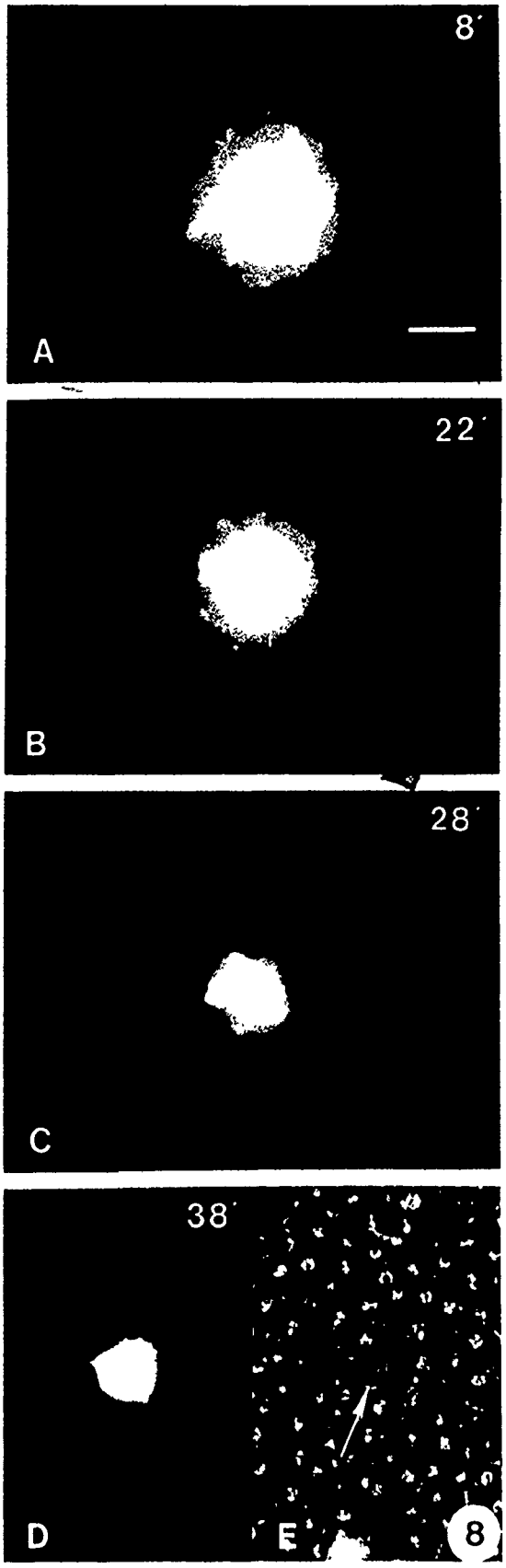
8'
A
22'
B
28'
C
38'
D
E
8

With exposure of the epidermis to Li saline, the smooth appearance of spreading CF fluorescence changed, and intensity steps developed at successive cell margins. Both CF and LRB tended to build to increasingly high levels of fluorescence in the source cell, and in each cell order, before passing to the more distant cells. This intensity profile became ever steeper, decreasing the extent of spread possible during similar injection periods. Later dye spreads were less extensive because the membrane potential tended to depolarize sooner after electrode penetration during this state of decreasing dye permeability.

With time, the extent of spread of each dye was reduced so greatly that adjacent (first order) cells were slow to receive dye during the approximately 20s period of injection. If the source cell had uncoupled, the fluorescence of the adjacent cells would decrease and fluorescence in the second order cells would become perceptible. If, instead, the electrode was carefully removed before the membrane potential was lost, the fluorescence of the source cell usually decreased over the following few minutes, and increased within the adjacent cells.

The final stage was complete dye uncoupling: after penetration by the dye electrode, a cell immediately became intensely fluorescent with the first current pulse, and its outlines were delineated so clearly that its finger-like extensions (cell 'feet') were seen. When injection was

stopped at this stage, observation over at least the next three minutes showed little change in fluorescence intensity of that cell, and no development of fluorescence within the adjacent cells.

The phase contrast appearance of the cells was generally unchanged through the experiment - occasionally, vacuolation (the development of small phase-bright spheres in the cells) occurred after transfer of the preparation to Li saline, but this disappeared after 15 - 20 minutes.

2.3.2c Co-injection of fluorescent tracers

When LRB and CF were injected separately into control epidermis (at equal concentrations of 25 mM in the electrode), CF spread more rapidly through the epidermis than LRB - in Fig. 7, CF was visible 50 µm from the source by 30s of pulsing, while LRB was not detectable beyond 30 µm. This suggested that the difference in size between the tracer molecules had an appreciable affect on their intercellular movement, which might become more evident when coupling was reduced.

By combining LRB and CF at the concentration ratio of 4:1 in the electrode, simultaneous injection into a cell resulted in dye spread with initially equal extent (not shown, but see Fig. 9 A,B). The greater concentration of LRB caused its spread over the first 3 to 4 orders of cells (20-30s of injection) to appear similar to CF, with the

Figure 9

When LRB and CF are co-injected into epidermis during the gradual uncoupling caused by Li saline, LRB is blocked from passing before CF. LRB and CF were combined so that co-injection into epidermis in medium showed equal extents of spread at up to 40 s of injection. Filters allowed selective viewing, and CF was photographed before LRB, with the same exposures.

At 6 min in Li saline, the extents of spread were still the same at 40 s of injection. Note the different appearances of the dyes spreading through the same cells. The mottled appearance in B may obscure the steps in intensity at cell margins, which are apparent in A.

A differential effect on dye passage was evident after 15 minutes, and at 25 min, CF spread into 3 cell orders in 25 s of injection (D), while LRB is visible in 2 cell orders (C). In one injection at 28 min, CF passed into 2 cell orders in 22 s (F), but LRB passed only into adjacent cells at 28 s (E).

The epidermis was uncoupled to LRB by 30 min: CF passed beyond the adjacent cells in 17 s of injection (H) but LRB was restricted to the injected cell at 24 s (G). By 35 min, the spread of CF was reduced sufficiently that only adjacent cells received dye in 20 s of injection (J). LRB failed to spread (I). Note that

in (I), cell feet stand out against a dark background, although there is some scattering of light, while in (J), they blend into the fluorescence of dye starting to fill the adjacent cells. At 40 min, CF failed to spread by 25 s when injected alone.

The membrane potentials were between 15 and 17 mV for A-H, 12 mV for I-J and 10 mV in K. The exposure times were the same for both dyes, between 4 and 8 s, and each pair of negatives was printed in the same way. Scale bar, 20 μm.

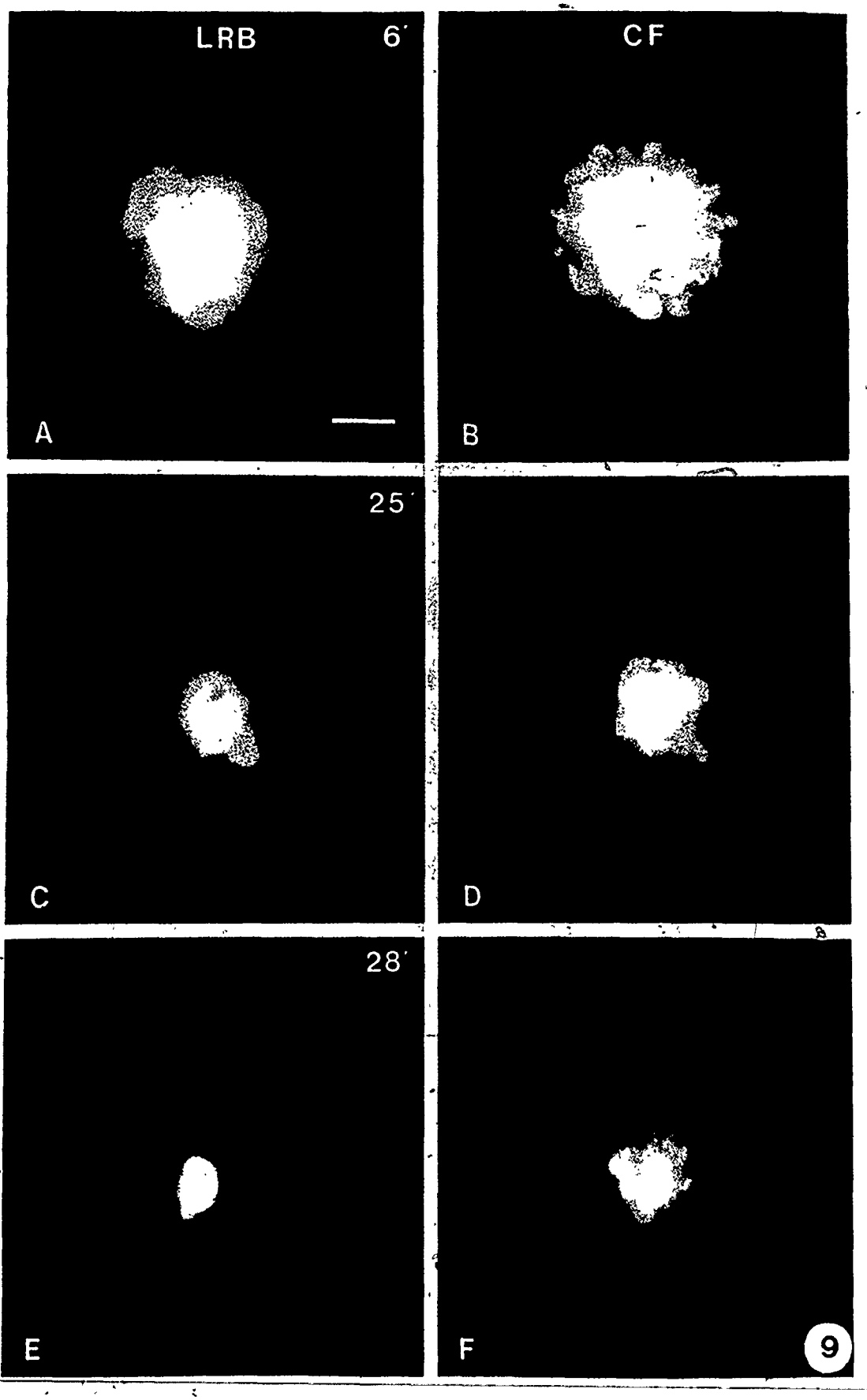
LRB
6'
A
CF
B
25'
C
D
28'
E
F
9

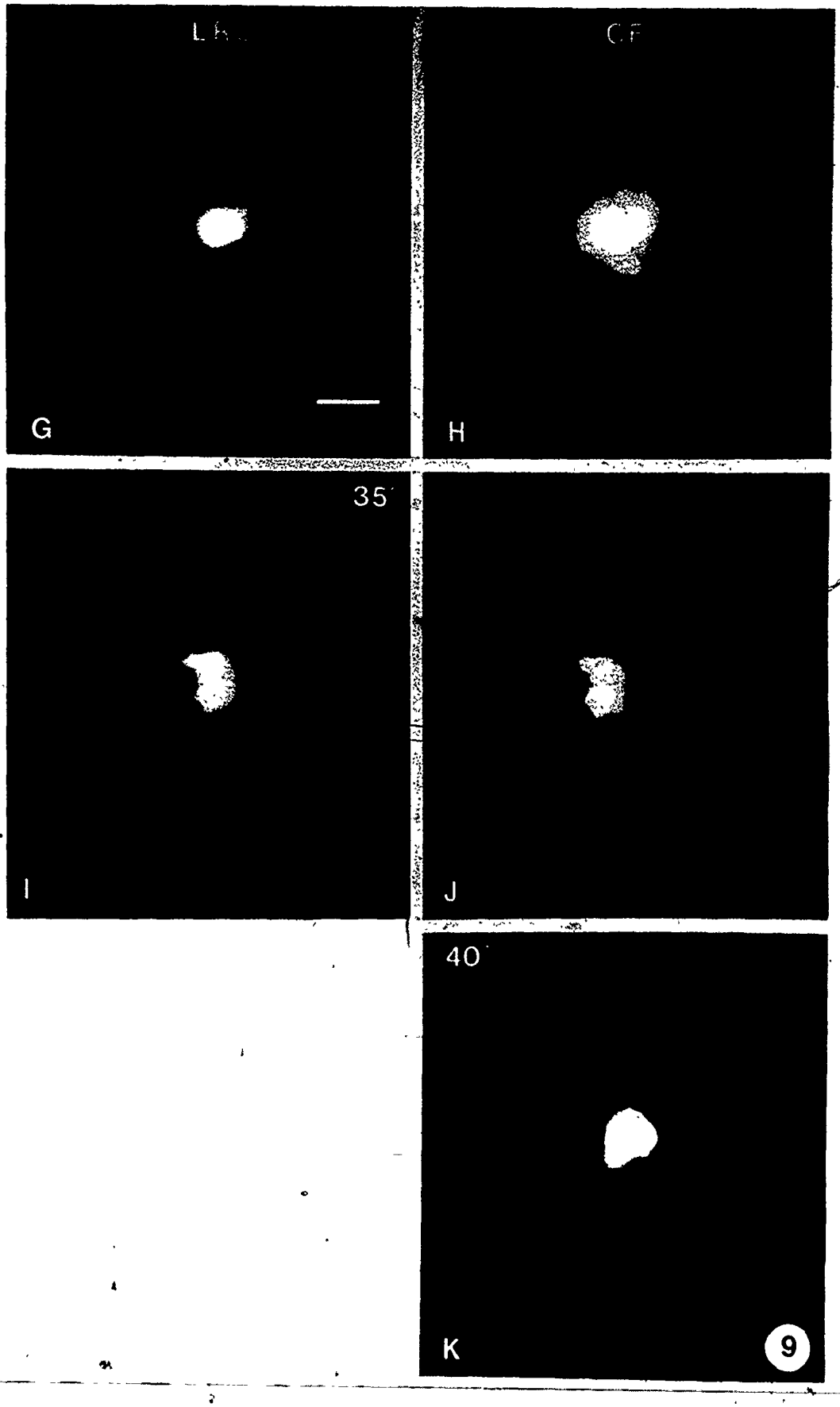
LR
CF
G
H
35'
I
J
40'
K
9

difference in speed of passage becoming apparent during spread through subsequent orders. These dyes were then co-injected into epidermis exposed to Li saline to study the effect of gradual uncoupling on the movement of tracers of different molecular size.

The initial minutes of exposure of the epidermis to Li saline caused no changes in the relative spread of co-injected tracers at 20-30s of injection (Fig. 9A,B). After approximately 1.5 minutes, however, LRB became retarded in its spread, while CF was apparently unchanged (Fig. 9C,D). By 25-30 minutes, LRB spread became limited to adjacent cells, at the same time as CF was passing to third and fourth order cells (Fig. 9E,F). The rate of CF spread appeared little changed, although extensive spread could not be observed, since injectin of LRB into a cell that could only allow slow passage from it hastened membrane potential loss and complete uncoupling, possibly due to osmotic stress.

When cells became uncoupled to LRB passage, CF continued to pass between cells: an injected cell presented the standard appearance of a LRB-uncoupled cell, with sharply defined edges and cell feet visible against non-fluorescent adjacent cells, while CF fluorescence showed that spread had occurred to adjacent cells, and was passing to subsequent cell orders (Fig. 9G,J). Significantly, for the first time cells changed their appearance by swelling

during co-injection, reinforcing the suspicion that tracer was being retained. Full uncoupling induced by electrode penetration, seen by membrane potential loss, resulted in the spread of neither tracer.

After the onset of LRB-uncoupling, co-injected cells uncoupled more rapidly, and the shorter injection periods resulted in limited spread of CF. When CF alone was injected at this time, its extent of spread was reduced*, and followed the usual course of further retardation and uncoupling (Fig. 9K).

In another preparation, the times for LRB and CF to spread to adjacent cell orders after co-injection were measured, and are presented here to show the change in these rates. At 22 minutes in Li saline, LRB filled first and second cell orders at 14 seconds of injection, but at 24 minutes, took 33 seconds, and at 26.5 minutes, took 36 seconds. CF spread was apparently unchanged at 24 minutes, passing freely from the source cell with each current pulse. However, at 28 minutes, CF took 9 seconds to enter adjacent cells, with noticably slower spread. LRB was able to enter only adjacent cells after 25 seconds of pulsing. Cells were subsequently LRB-uncoupled, but at 35.5 minutes, CF passed to adjacent cells within 17 seconds, further reduced in rate.

---

*suggesting that the decreased CF passage was not directly due to decreased LRB passage.

On average, epidermal cells became uncoupled to LRB passage by 27.5 +/- 4.4 (S.D.) minutes of exposure to Li saline (11 preparations from 8 animals). The average time of CF uncoupling (either co-injected with LRB or injected alone) was 38.4 +/- 3.4 (S.D.) minutes after the start of Li saline treatment, measured in 7 preparations from 5 animals.

2.3.3 Correlation of dye and electrical coupling in newly molted epidermis

2.3.3 (a) Results combined from separate preparations

Comparison of electrical coupling with dye permeability changes during Li uncoupling shows that dye coupling was lost before electrical coupling: LRB uncoupling actually occurred less than halfway through the time course of electrical uncoupling (Fig. 6).

Both dye permeability and intercellular resistance remained unchanged during the first 10 minutes in Li saline. The subsequent onset of a perceptible decrease in dye coupling did not coincide with the start of decrease of electrical coupling. Rather, the rate of LRB movement was reduced about 10 minutes after r_i began to increase. CF coupling showed change later still, shortly before the point of LRB-uncoupling.

In Fig. 6, insertion of the average times of dye uncoupling onto the time course of electrical uncoupling shows that the r_i value typically present at the onset of

LRB-uncoupling was 6.5 x $10^5\Omega$ (range; 5.4 - 6.9), while the r_i at CF uncoupling was 10.4 x $10^5\Omega$ (range; 9.7 - 11.4).

Electrical coupling was detectable for approximately 60 minutes after exposure to Li saline, 20 minutes beyond the average time of uncoupling of CF, the smaller organic molecule. Thus, the intercellular resistance in the epidermis increased 2.7 times before LRB was occluded, or 4.3 times before occluding CF, while capable of increasing by at least 10 fold before ionic coupling was no longer detectable.

2.3.3 (b) Results obtained from individual preparations

The preceding results are based on one coupling parameter, either ionic or dye coupling, being followed in each preparation. To support those conclusions further, both dye and electrical coupling were measured in single newly molted preparations during exposure to Li saline. Thus, variation among preparations in the rate of channel closure, showing up as variation in the time of dye uncoupling, or rate of change of r_i, was reduced. In practice, r_i could be determined only close to, and not at, the time of dye uncoupling.

Ionic or dye coupling were measured alternately during the decrease of intercellular coupling. One dye was generally used per preparation. Thus, a set of increasing r_i values measured before the cells became uncoupled to passage of that dye could be compared to another set of

values measured after the cells became uncoupled. The highest r_i before, and the lowest r_i after, dye uncoupling defined a 'window', or range of r_i's, within which uncoupling actually occurred. Table II shows those values, with each number representing one limit in the change in r_i about the time of either LRB or CF-uncoupling. The level of r_i found soon after LRB movement was blocked permitted CF to pass after that particular measurement.

There is variation in the r_i values that define the size of the window, for the following reasons: the exchange of electrodes and their repositioning after an electrical spread, and completion of a dye injection required at least 1-2 minutes (providing that the electrodes were found adequate). The reverse exchange and production of a series of electrotonic potentials took slightly longer (5-10 minutes). This limits the temporal resolution of the technique*. However, each such measurement carries simultaneous knowledge of the state of dye coupling in that same preparation, and so, to the limits of the technique, accurately forms parts of the window spanning the time of

---

* The r_i could not be calculated during the experiment because uncoupling proceeded too rapidly, and a rough estimate of r_i by eye determined when to switch electrodes. The inaccuracy caused each trial to be to an extent, 'hit-or-miss'.

uncoupling. The window was narrowed by selecting from all 6 preparations the highest r_i value before LRB-uncoupling and the lowest after it. This showed that newly molted epidermal cells became LRB-uncoupled at an r_i between 6.4 and 6.9 x $10^5\Omega$ (Table II), confirming the value of 6.5 x $10^5\Omega$ determined previously (Fig. 6). The r_i of 6.5 x $10^5\Omega$ at the time of LRB cut-off was used for future comparisons with CF.

CF was blocked from intercellular transfer between r_i = 9.5 and 15.3 x $10^5\Omega$, a wider range than for the LRB determination due to the time taken for definite establishment of absence of CF coupling at a time when r_i is changing rapidly (Fig. 6). Nonetheless, the previous value of 10.5 x $10^5\Omega$ at CF uncoupling was confirmed, falling within these two limits.

2.3.4 Junctional coupling in Intermolt Epidermis

The epidermal cells of the intermolt larva, at 5 or 6 days post molt, are in the least active metabolic phase of the molt cycle, and the molting hormone 20-hydroxyecdysterone is at its lowest level (Delachambre et al., 1980). This major developmental hormone, shown to increase junctional conductance (Caveney and Blennerhassett, 1980), is still high in newly molted epidermis (Delbecque et al., 1978), as the manufacture and secretion of new cuticle is completed. Relative to the newly molted epidermis (cell

TABLE II: Correlation of r_i with dye occlusion in newly molted epidermis.

Highest r_i at which LRB and CF passed ($\times 10^5\ \Omega$)	r_i after LRB stopped but at which CF passed* ($\times 10^5\ \Omega$)	r_i after CF stopped* ($\times 10^5\ \Omega$)
6.4	6.9	15.3
	7.6	16.0
	7.8	
	9.1	
	9.5	

* Each number is derived from a different preparation.

height 20 μm), the intermolt epidermis is thinner (10 +/- μm), and ultrastructurally, the cells contain three times less gap junctional area (Caveney and Podgorski, 1975). Intermolt epidermis represents a distinctly different stage in the development of the epidermis, characterized by the difference in hormone level, cell volume, metabolic state, and junctional area. Consequently, the junctional permeability to ions and dyes was compared with that in newly molted tissue.

2.3.4 (a) Electrical Uncoupling of Intermolt Epidermis

Epidermis from intermolt larvae has a control r_i of 4.1 +/- 0.5 x $10^5\Omega$, two-fold higher than newly molted epidermis. As before, exposure to Li saline caused the r_i to increase over time: Fig. 10 shows that the r_i of one preparation placed in Li saline remained initially fairly constant, and then increased at an accelerating rate. Compared to newly molted epidermis, the lag period was longer, since r_i was unchanged by 13 minutes, and then increased gradually over the next 30 minutes to a level twice the control. It then increased very rapidly, with the tissue becoming fully uncoupled 15 minutes later. The highest recorded r_i for this preparation was 33 x $10^5\Omega$, which is an 8-fold increase over the control. This is similar to the increase in r_i before uncoupling that was found in newly molted epidermis.

Figure 10

Li saline causes gradual electrical uncoupling of intermolt epidermis, but the time course is different from newly molted epidermis, and variable between preparations. Here, r_i (left axis; open circles) increased slightly at 20 minutes, stabilized and then rose sharply at 40 minutes. An initial lag phase was also seen in newly molted epidermis (Figure 5) but its duration in intermolt tissue is variable, and the final increase in R_i is more rapid. The maximum r_i recorded was $31 \times 10^5\ \Omega$, which is approximately 7 times the value in medium of $4.2 \times 10^5\ \Omega$. This is close to the 8 times increase seen in newly molted tissue. The membrane potential (right axis; closed circles with standard deviation bars) dropped quickly by nearly 50% during the period of initial stability of r_i, and declined gradually as the tissue uncoupled at an increasing rate.

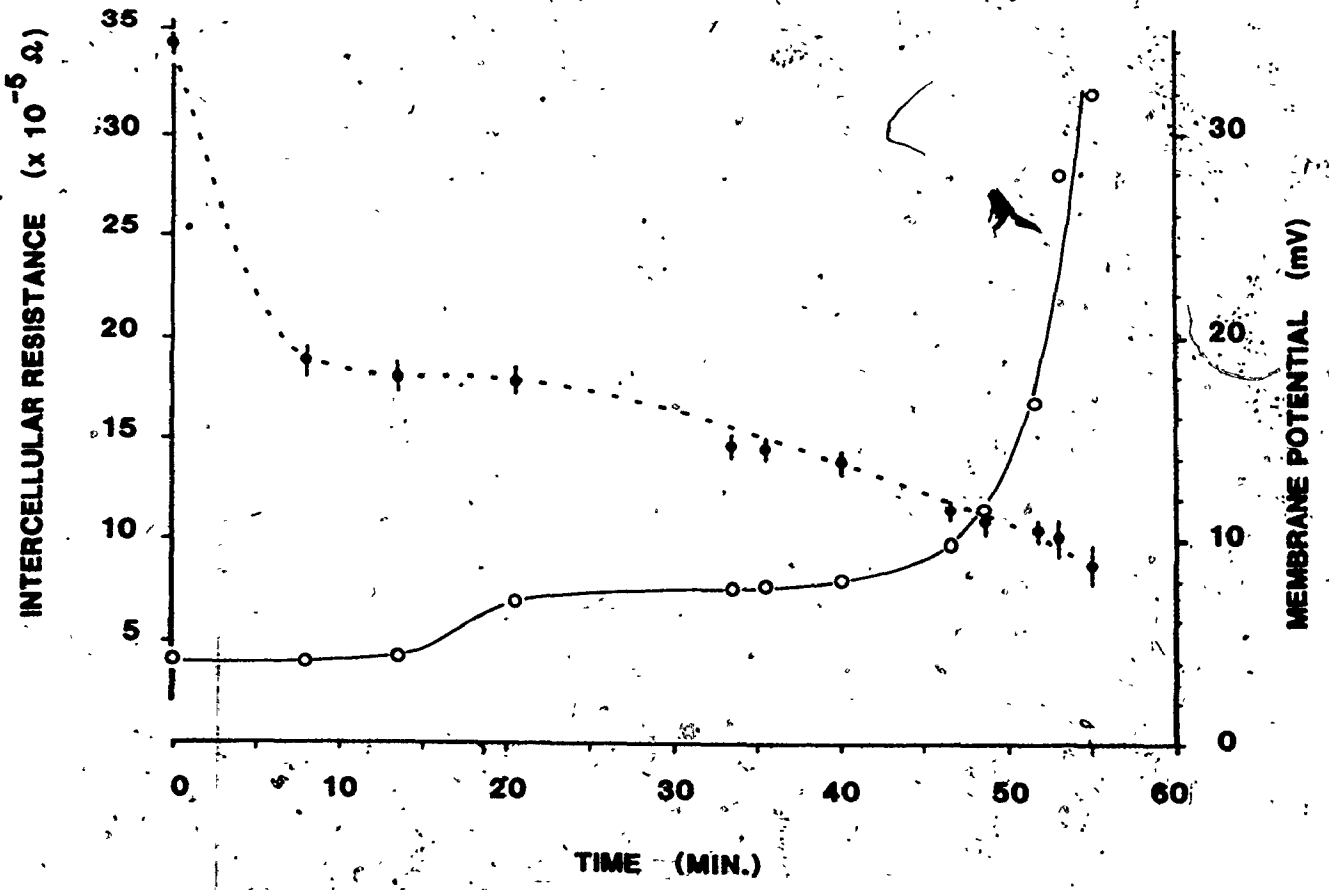
INTERCELLULAR RESISTANCE (x 10^{-5} Ω)
35
30
25
20
15
10
5
0
10
20
30
40
50
60
TIME (MIN.)
MEMBRANE POTENTIAL (mV)
30
20
10
0

(10)

Preparations from different animals showed variation in uncoupling, principally in the duration of the lag phase before rapid r_i increase. In a few trials, there was an initial decrease in r_i, which dropped as low as $1.6 \times 10^5 \Omega$ before starting to increase gradually.

2.3.4 (b) Correlation of dye and electrical coupling

The characteristics of dye spread in intermolt epidermis were similar to those of newly molted epidermis. In control preparations, co-injected LRB and CF appeared initially to spread equally rapidly, with greater CF spread subsequently becoming evident. Exposure to Li saline had no immediate effect upon dye coupling, with the reduction of LRB spread first appearing at 15-20 minutes. LRB uncoupling followed, but at a time when the spread of CF (that is, the extent of spread at a given time after injection) had just started to decline. CF spread decreased further, until finally its movement was blocked.

Variation in the time course of electrical uncoupling made it difficult to construct a mean curve of uncoupling for all preparations examined. Instead, a pair of preparations from one animal was used to establish separately the course of electrical uncoupling and the time(s) of dye uncoupling. The r_i at the time of dye occlusion was then determined for each pair, and the values from all pairs were averaged. For intermolt epidermis, the r_i at LRB occlusion

was found to be 7.5 +/- 2.4 x 10^5 Ω (13 pairs, 11 animals) and at CF occlusion, 21.1 +/- 2.8 x 10^5Ω (5 pairs, 4 animals).

Presumably, variation in uncoupling behaviour within a pair of preparations was responsible for some of the range of values. This limits the accuracy in correlating the onset of dye uncoupling with a specific r_i value.

To overcome this, electrical and dye coupling were therefore examined in a single preparation as before. The r_i values found before LRB uncoupling, those values after LRB uncoupling but during CF coupling, and those after CF uncoupling are shown in Table III. The highest value found before LRB uncoupling was 8.5 x 10^5Ω, but in another preparation, r_i = 8.5 x 10^5 Ω was again measured immediately after the onset of LRB uncoupling. The range from the next limiting values (between 8.1 and 9.1 x 10^5 Ω) was narrow and centered about 8.5 x 10^5Ω. This suggests that within the resolution of measurement of r_i, LRB occlusion occurred at an r_i of 8.5 (range, +/- 0.5) x 10^5Ω.

Due to the technical difficulty, only two values of r_i were determined during the period of rapid change after CF occlusion. These, and the corresponding minimum r_i value prior to CF uncoupling show that the r_i at CF uncoupling was between 18.6 and 23.8 x 10^5Ω.

The previous values of r_i at dye uncoupling based on the assumption of equivalent behaviour among preparations

TABLE III: Correlation of r_i with dye occlusion in intermolt epidermis.

r_i at which LRB and CF passed* ($\times 10^5\ \Omega$)	r_i after LRB stopped but at which CF passed* ($\times 10^5\ \Omega$)	r_i after CF stopped* ($\times 10^5\ \Omega$)
4.5	+8.5	#23.8
6.0	9.1	33.2
6.4	9.3	
7.1	12.5	
7.4	14.9	
8.1	15.3	
8.5+	16.3	
	18.6#	

* Each number is derived from a different preparation.

+,# These numbers form the 'window' of r_i values for the occlusion of LRB (+) or CF (#).

corresponded well with the range determined from single preparations: the average r_i value of 7.5 +/- 2.4 (S.D.) x $10^5 \Omega$ at LRB cut-off fell close to the stronger value of 8.5 x $10^5 \Omega$. The average r_i at CF cut-off (Method I) fell at the centre of the defined range (Method II), i.e., the r_i (+/- range) was 21.1 +/- 1.3 x $10^5 \Omega$.

The increase in r_i necessary to block tracer passage was related to molecular size, roughly doubling (2.1x) to block the LRB molecule (14Å) but increasing by 5.1x to block CF (12Å). Electrical coupling persisted after occlusion of the smaller tracer, with the r_i at cut-off being approximately 60% of the maximum measured. Thus, ionic movement may still be present long after dye movement is blocked.

2.3.5 Membrane potential and intercellular resistance

The membrane potential (E) can regulate cell coupling in midge cell pairs (Obaid et al., 1983). Since E of newly molted epidermal cells decreased in Li saline, the relationship of E and r_i was examined. Fig. 5 shows the typical change in E during Li uncoupling: E quickly dropped by 50%, from 33 mV in medium to 18 mV in Li saline at 15 minutes, but showed only slight further decrease to 14 mV by 60 minutes. The r_i did not show a parallel change, being relatively constant over the first 15 minutes and increasing rapidly thereafter.

The membrane potential of intermolt larvae changed similarly. In one preparation (Fig. 10), E initially fell sharply from 34 mV to 18 mV, while r_i was constant. E then dropped gradually to 9 mV, showing no relationship with r_i, which passed through the lag phase and increased rapidly.

Therefore, change in the average membrane potential of the preparation did not affect the intercellular resistance.

For quantification of electrical coupling, an electrode must measure the full E of a cell in order to record accurately an electrotonic potential, since a poor seal around the microelectrode will allow current loss to ground. Eventually, the E will drop as the cell dies. However, when the E of a cell fell even slightly, preparatory to its complete loss, the electrical coupling of that cell decreased immediately as well. This suggested that the electrical coupling of a cell to its neighbours could be controlled by its relative polarization. The relationship of E with cell coupling was studied by passing current between two cells some distance apart, and examining the change in electrotonic potential (V) that occurred when E of the injected cell finally declined.

Chart recordings of this experiment in newly molted preparations are shown in Fig. 11. In Fig. 11A, the decrease of E was sigmoidal, and matched by decrease in V. The more irregular decrease of E in Fig. 11B also had an

Figure 11

A drop in the membrane potential of a cell causes a proportional decrease in the electrical coupling of the cell with the rest of the epidermis. An electrode in a cell records the membrane potential and the electrotonic potentials (upper trace, A and B) generated by current pulsed into a cell by another electrode (lower trace, A and B). The magnitude of the electrotonic potential is constant while the membrane potential is stable, but depolarization causes an immediate drop in the electrotonic potential, whether it occurs gradually (A), or more abruptly (B).

Arrows mark the time of removal of the electrode from the injected cell. Scale bars: horizontal, 5 s; vertical 10 mV.

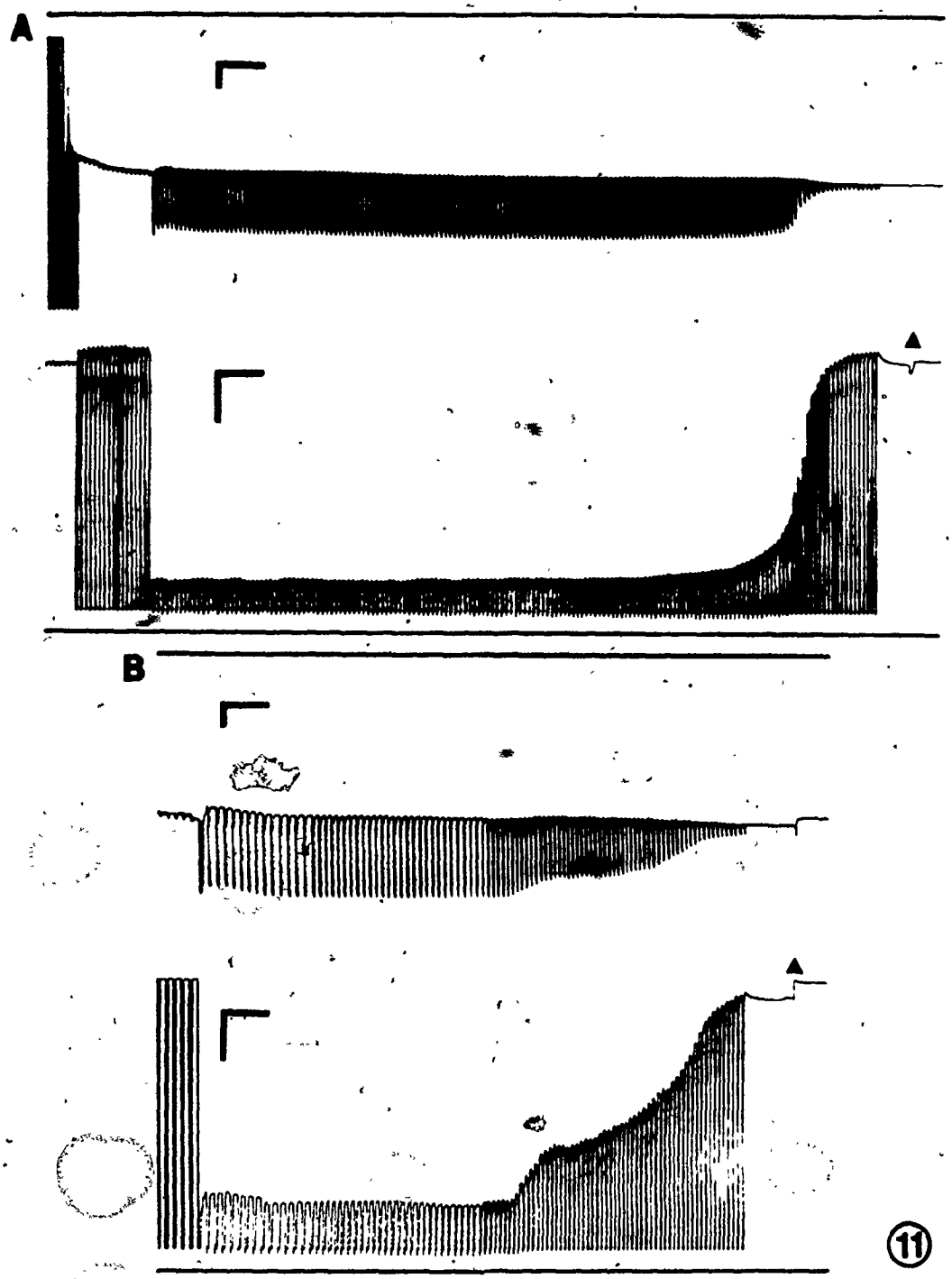

(11)

exactly parallel decrease in V. This relationship was remarkably precise: in Fig. 11B, E initially decreased by only 0.2 mV (<0.6% of the maximum) between successive pulses, but a decrease in V still resulted.

The electrotonic and membrane potentials were measured from chart recordings of cell uncoupling, normalized by dividing by the maximum values, and plotted against each other. A typical result is shown in Fig. 12, where E is exactly proportional to V throughout its range. V declined as soon as E fell, and was reduced to zero when E was fully lost.

The relationship of E to electrical coupling was also examined in the epidermis of the bug Oncopeltus fasciatus, using the abdominal tergite from IV nymphs (for culture methods and preparation details, see Chapter III). Here also, decreased cell membrane potential during current injection caused a proportional reduction in V, with a linear relationship between E and V (Fig. 12B).

A possible trivial explanation for these results is that the cell membrane becomes 'leaky' (constitutes a lower electrical resistance) when the E drops. More current then passes to ground through the cell membrane, and less to an electrode elsewhere in the sheet. This was ruled out in the following way. Simple electrical theory predicts that the decreased membrane resistance in a leaky source cell would cause a second electrode in that cell to record a decreased

Figure 12

When the membrane potential of an epidermal cell begins to depolarize, the degree of electrical coupling with its neighbours decreases in an exactly proportional relationship. From records such as those in Figure 11, the membrane potential (E) was measured during depolarization of the injected cell, and plotted against the corresponding electrotonic potential (V) measured in another cell. These were each normalized by dividing by the initial value (E_o, equal to the tissue average, and V_{max}). In epidermis from Tenebrio (A) and Oncopeltus (B), these points fell along a line drawn between (0,0) and (1,1), showing that decrease in the inside/out potential results in a proportional drop in the junctional conductance of a cell.

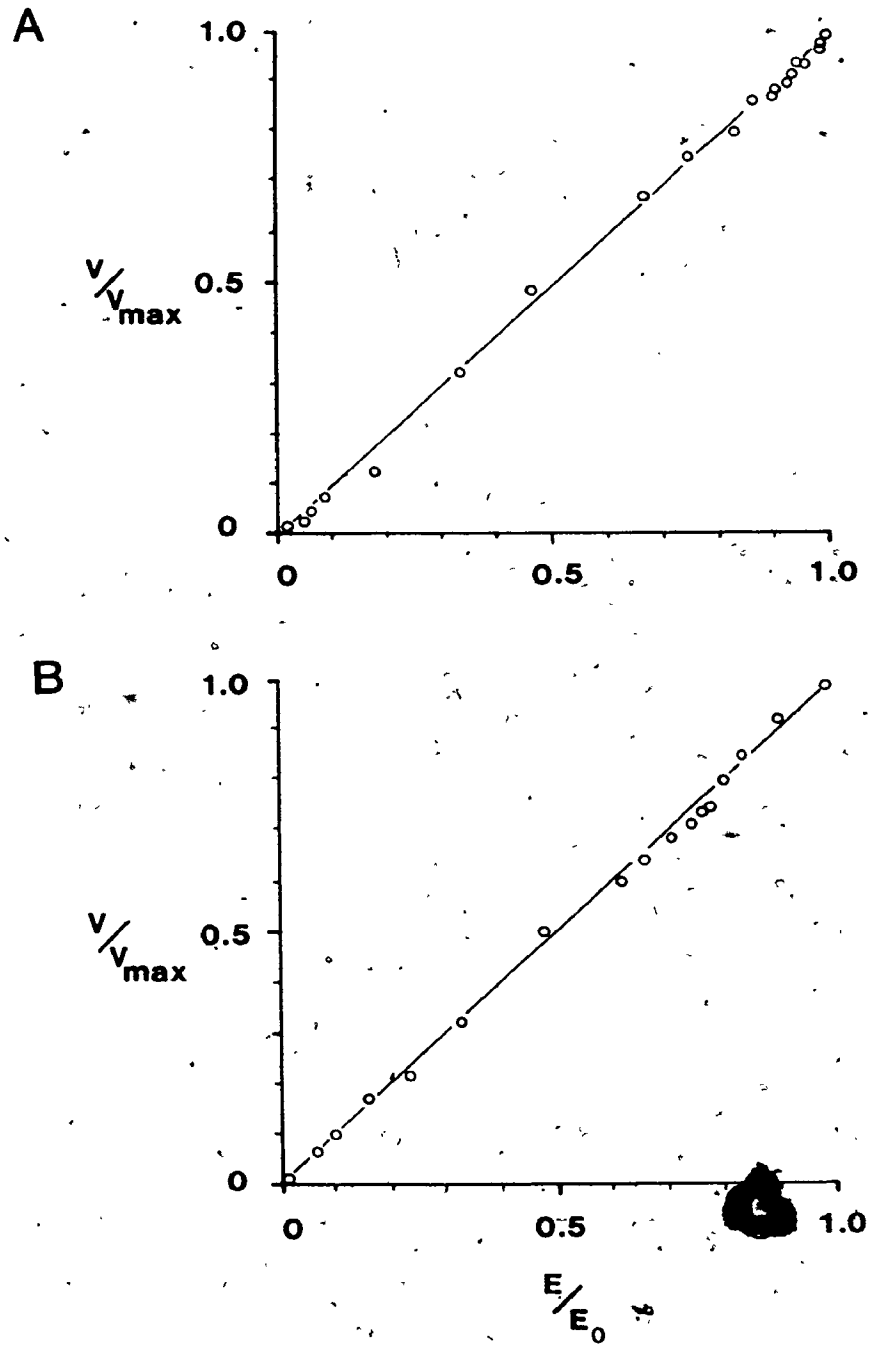
A
Tenebrio
1.0
0.5
0
V/Vmax
0
0.5
1.0
B
Oncopeltus
1.0
0.5
0
V/Vmax
0
0.5
1.0
E/E0

12

voltage, but that the increased membrane resistance of an uncoupling cell would cause increased voltage.

In bug epidermis, it was possible to place two electrodes in one cell. This showed that a decrease in E caused an immediate increase in the intercellular voltage (Fig. 13A). Therefore, a decrease in E increases the membrane resistance directly, presumably by closing the junctional channels. This effect is not an artefact of current leakage, either through the membrane, or through the seal around the electrode.

This may be a different type of coupling control from the one that regulates r_1, since r_1 and E were independent. In addition, the permeability to dye seems able to change despite a constant E, since sometimes the source cell in a dye injection would clearly dye-uncouple before E had changed. This was always followed by depolarization, within the next 10-15 seconds.

Electrical measurements should also be able to show that a cell can become uncoupled despite a constant E. This was never seen in experiments with Tenebrio, but Fig. 13B shows this result from an experiment in Oncopeltus. With both electrodes in one cell, the voltage recorded by the second electrode was initially stable and then increased steadily as before (indicative of uncoupling), but with a constant E. Here, control of coupling is presumably by intracellular ionic level, rather than the apparently more

Figure 13

The membrane potential can control the junctional conductance of a cell directly, but uncoupling can also occur independently of the membrane potential.

A. Two electrodes placed in an epidermal cell of Oncopeltus show that the electrotonic potential (lower trace) is constant during pulsing while the membrane potential is unchanged (upper trace). The electrotonic potential within the cell begins to increase as the cell starts to depolarize, showing that the cell membrane has increased its resistance to current flow, i.e., that the junctional resistance has increased.

B. Rarely, two electrodes in a coupled cell can show that the electrotonic potential within the cell increases (lower trace) while the membrane potential is unchanged (upper trace), demonstrating that uncoupling can also occur independently of cell polarization. This was seen earlier in Figures 5 and 10, where the electrical uncoupling of epidermis proceeded independently of the membrane potential. Here, curved marks indicate the deletion of 4 minutes of the recording, where no change occurred. Note the scale change in the lower trace as the electrotonic potential increases.

In A and B, arrowheads indicate the removal of the electrodes. Scale bars: horizontal, 5 s; vertical, 10 mV.

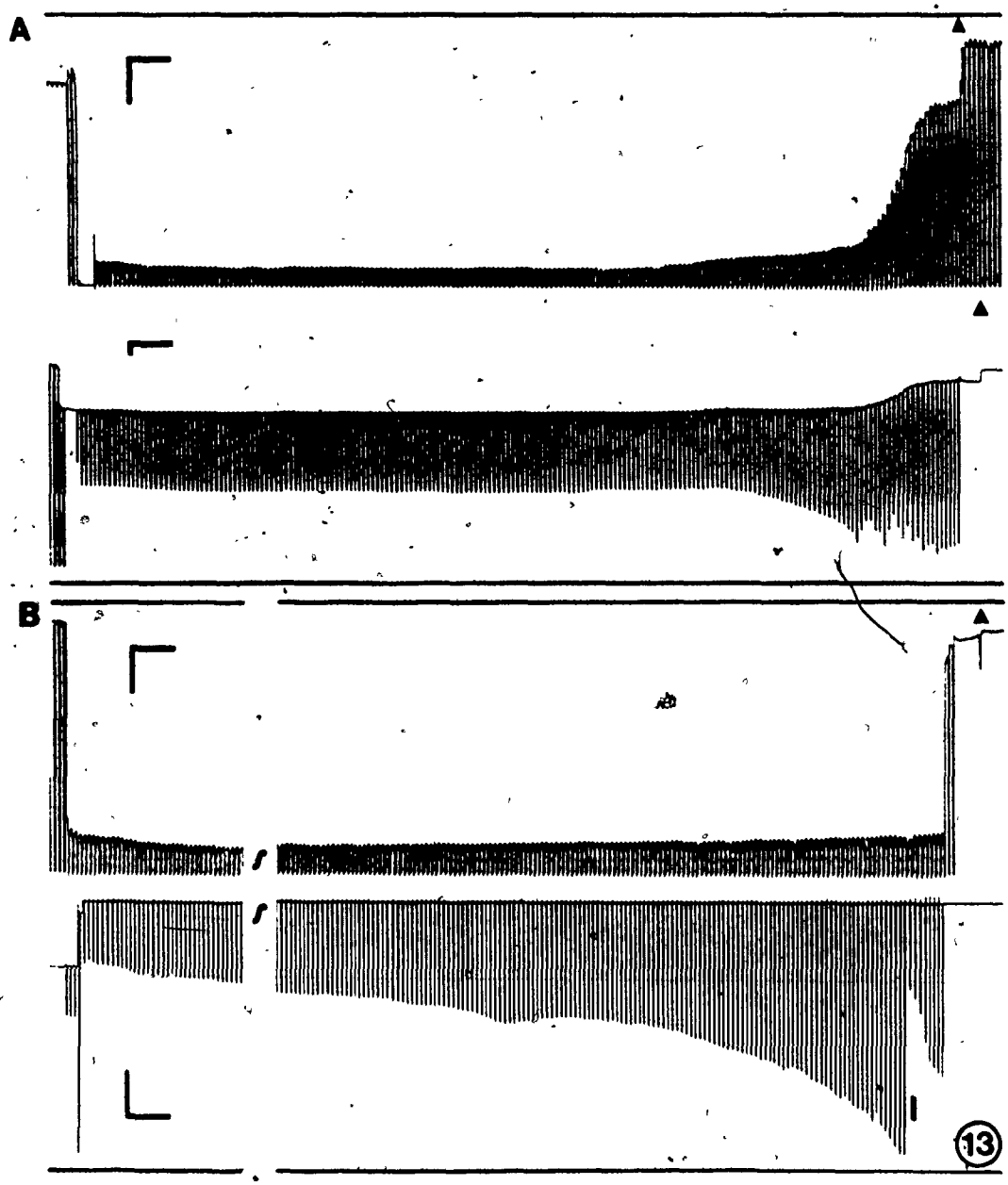
A
B
13

sensitive control by membrane potential.

2.3.6 The space constant and nonjunctional membrane resistance

The resistance of the nonjunctional membrane (R_m) determines the proportion of an injected intracellular current that will pass through the apical and basal membranes, rather than through junctional channels into the next cells. r_i measures the resistance of the channels and is independent of R_m, but in 'leaky' cells, where R_m is low and a larger amount of current is lost to ground, the magnitude of the electrotonic potentials can be reduced below detectable levels.

The space constant (λ), determined from R_m and r_i as defined previously, is the distance over which voltage falls to a standard fraction (1/e) of the initial value. The average λ was found at successive time intervals during the uncoupling of 9 newly molted preparations from 8 animals and is shown in Fig. 14. The average λ of control preparations was 1900 μm, which increased to 4000 μm at 5 minutes, and decreased thereafter. The large initial variation between preparations disappeared by 20 minutes, when decreased below the control level. λ approached a minimum value of 500 μm as r_i continued to decrease, and increased slightly after 50 minutes to 1000 μm.

Measured in one intermolt preparation, λ changed

2

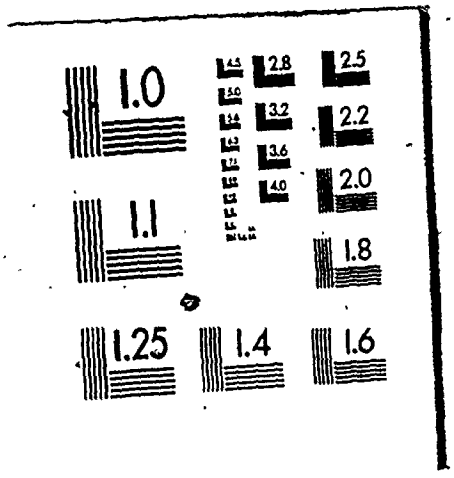

Figure 14

The space constant of newly molted preparations in Li saline decreased, but not sufficiently to prevent the quantification of electrical coupling. For 10 preparations, the space constant was found in medium (C), and at 5 minute intervals in Li saline. The average values in Li saline (bars; standard deviation) decreased, as well as the considerable initial variation, when r_i increased above the control level at 15-20 minutes (data incorporated in Figure 6).

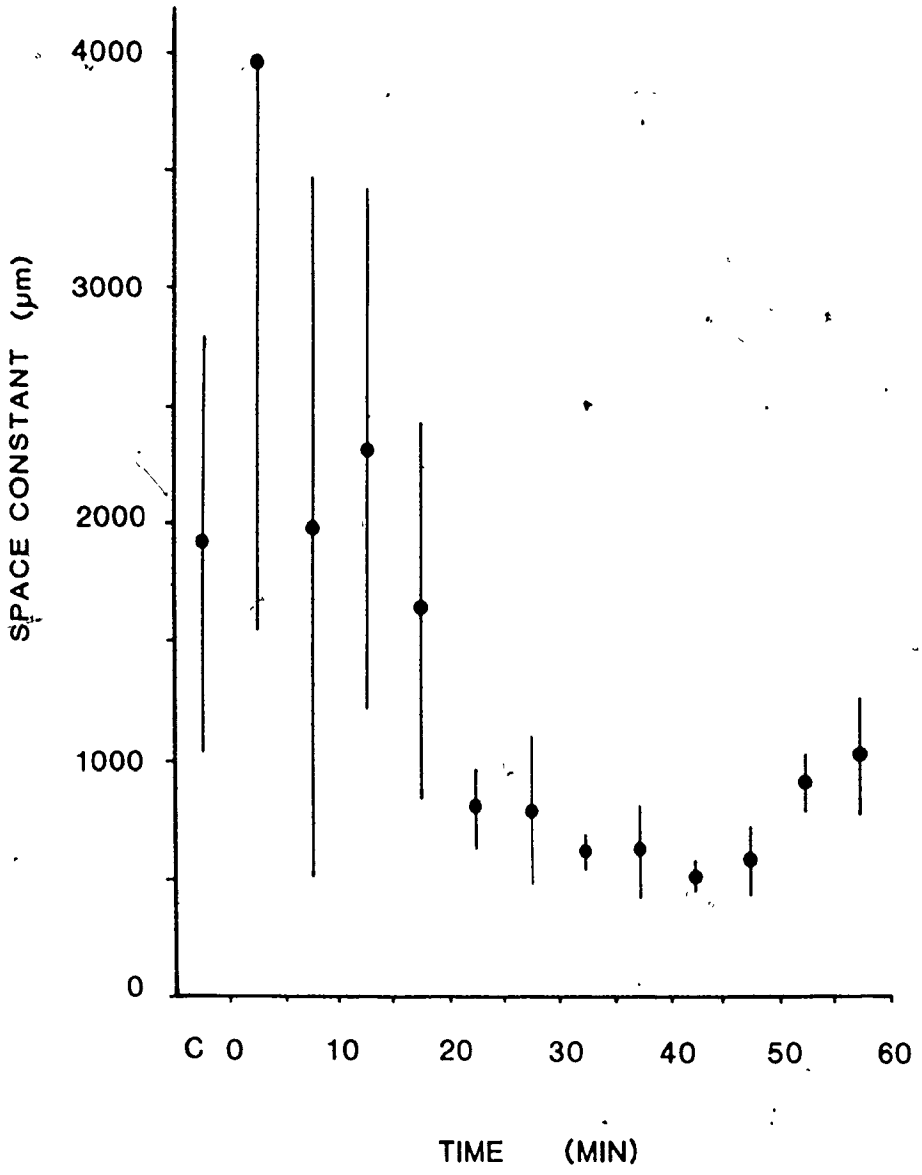
4000
3000
2000
1000
0
SPACE CONSTANT (μm)
C 0
10
20
30
40
50
60
TIME (MIN)

(14)

similarly. The initial value of 1620 um decreased to slightly less than 500 μm as r_i rose from 4.4 to 16.8 x 10^5 Ω.

R_m can be calculated, but is inaccurate in the absence of data on membrane folding. Neglecting this as a constant error, R_m was found during the uncoupling of a newly molted and an intermolt preparation. In newly molted epidermis, R_m was between 3-16 x 10^3 Ωcm^2 and roughly constant. Intermolt R_m values were initially higher, at 62-64 x 10^3 Ωcm^2, but as r_i increased above the control level, R_M decreased to coincide with the values for newly molted tissue.

This establishes that the nonjunctional membrane did not become increasingly leaky during exposure to Li saline, which might have prevented accurate quantification of coupling. Ranging between 10^3 and 10^4 Ωcm^2, R_m was always much greater than the specific resistance of junctional membrane (10^{-1} Ωcm^2; Caveney and Bennerhassett, 1980). While λ decreased as junctional resistance increased, it was not less than the field width of 440 μm, even at maximum r_i.

2.4 Discussion

This work correlates junctional resistance and permeability during decrease in cell coupling, and shows that they are linked together in the changes that defined Li-induced uncoupling. The tight relationship between electrical resistance and dye permeability, where an r_j of a specific value characterizes the blockage of passage of each dye, suggests that the degrees of both electrical and molecular coupling are determined by the same set of intercellular channels, i.e., that dye and electrical coupling use the same channels. Since Brink (1983) showed that dye molecules are hydrated when they pass through junctional channels, presumably the channels are themselves hydrophilic. Such channels in a lipid membrane must offer a low resistance route to current passage as well, so that dye and electrical coupling will use the same channel. But, is there an additional route of electrical coupling, that might allow electrical coupling to persist when dye coupling is lost?

Tight junctions are suspected of such a role in one case with electrical coupling but no identifiable gap junctions (Larson and Sheridan, 1982). In the literature, electrical coupling is always found to be present where metabolic or dye coupling occurs (Finbow, 1983), but it is not always true that electrically coupled cells are dye coupled (as in Santos-Sacchi and Dallos, 1983). Small

amounts of dye passing between cells may not be easily detected (for example, Bennett et al., 1972; and reevaluated, 1978), and this might be due either to small numbers of (open) channels (whose physical presence would be hard to detect as well), or to a partial restriction of the channel bore that prevents dye coupling. This interpretation accommodates such results, and being more simple, is preferable to proposing additional pathways of intercellular coupling.

The problems of scale prevent an easy bridge between the physical and the physiological aspects of junctional coupling. The Ca-induced change in connexon structure shown by Unwin and Ennis (1984) is analogous to channel gating, and may be the strongest evidence that the gap junction is the ultrastructural correlate of the intercellular channel. Even without certainty of this relationship, the properties of intercellular coupling indirectly demonstrate the nature of the channels.

2.4.1 Channel Closure in Tenebrio Epidermis is Graded.

The model of channel closure should be the simplest one that fits the observed changes in intercellular passage of fluorescent dyes and electrical current during coupling. The major findings were:

1. Electrical coupling decreased smoothly over a wide range before becoming undetectable.

2. The larger dye molecule was blocked from intercellular passage before the smaller one.

3. Dye occlusion occurred at a characteristic value of electrical coupling. The smaller molecule was blocked at a higher sheet resistance and both were blocked before electrical coupling was lost.

While both graded and AON channel closure accommodate the continuous modulation of conductance alone, discrimination against molecular passage by size during uncoupling is a property of the GCC model. Experimentally, the uncoupling of LRB and CF was separated into distinct events in two ways. First, the times of dye-uncoupling, whether determined separately or by co-injection, showed that LRB was blocked from passage before CF: direct observation showed that CF continued to pass from a cell that no longer permitted the passage of LRB. Second, the electrical resistance increased during the period between blockage of the two dyes; that is, the r_i after LRB uncoupling was less than r_i values found before CF uncoupling.

Because electrical coupling persists after the loss of dye coupling, it seems definite that AON closure is ruled out. The manner of channel closure implies at least three different states, where both, one or neither dye pass. Since CF and LRB occlusion were distinct events, and could be tied to the monotonically increasing electrical resistance, it seems that there is a gradual decrease in

channel diameter. Therefore, when cells in the epidermis uncouple in response to Li, the intercellular channels close in a graded fashion.

Variation or error in the times of dye uncoupling might have resulted from different sensitivities of detection of dye passage, or from different degrees of molecular charge or hydration. For equal amounts of dye, LRB shows less intensity of fluorescence so that in reduced dye passage, LRB might seem to stop before the more easily detected CF, although this was compensated by the different concentrations of dye in the electrode. However, dye uncoupled cells promptly swell upon injection, apparently from dye build-up and the resulting influx of water. This distinguished the presence of low levels of dye passage from its absence, since poorly coupled cells did not swell appreciably, and dye appeared in adjacent cells within a minute.

Apart from size, other molecular properties that affect tracer passage are electrical charge and hydration. Discrimination against the passage of negatively charged molecules does occur in mammalian cells, but has not been detected in insect cells (Flagg-Newton and Loewenstein, 1979). Both LRB and CF have a net negative charge, but LRB is less charged than CF (Loewenstein, 1981). Therefore, any charge discrimination that may exist would be expected to cause the CF cut-off to occur at a similar conductance level as that of LRB -- rather than artefactually separate the events.

Hydration of each tracer will cause the effective diameter to be larger than indicated by the space-filling model and disproportionate increase of the smaller molecule might make the tracers equal in effective diameter. The increase in diameter, or any relative difference is not known, but should be slight: the binding of water increases the diameter of Na, a well hydrated ion, by 1.75Å (Alberty, 1979), so that the maximum increase in diameter of a molecule with a fully exposed charge should be half of that or less than 1Å. Further, the hydration of negatively charged molecules such as these tracers is less extensive than that of positively charged ones (Brink and Dewey, 1980). Since there is a 2Å difference between the limiting dimensions of the tracers, and no marked charge difference, hydration should not affect the conclusions.

In the one other analysis of channel closure, Rose et al. (1977) showed graded change in channel permeability in Chironomus salivary gland*. Using a different tissue, the method of channel closure was the same as shown here in epidermis and so might occur in all insect junctions. However, some quality of the channels may be different between insect orders, since homopteran cell lines did not couple with a lepidopteran cell line (Epstein and Gilula,

*However, Zimmerman and Rose (1983) appear to contradict this in an abstract that has not appeared as a published article.

1977). This may be explained by the finding that in vertebrates, the biochemical nature of gap junctions may be specific to the tissue of origin (Gros et al., 1983).

However, these results cannot be extended to vertebrates, since insect and vertebrate gap junctions are structurally and physiologically distinct (Peracchia, 1980; Spray et al., 1984). While cells from vertebrate tissues can form heterotypic junctions when co-cultured (Lawrence et al., 1978), vertebrate cells do not couple with insect cells in vitro (Epstein and Gilula, 1977). In fact, Larsen (1983) suggests that analogous rather than homologous development of gap junctions may have occurred in these two cases.

Despite this evidence for graded closure, there is nevertheless a pronounced bias towards AON closure in considering results that are open to either interpretation. For example, Margiotta and Walcott (1983) conceded the possibility of either mechanism when analysing coupling in crayfish, but state:

> "..we considered only a gating scheme where the channels exist in either open or closed state.".

Similarly, in considering vertebrate and invertebrate coupling, Spray et al. (1984)

> "..assume that channel gating is an all-or-none phenomenon..".

Finally, from the same group that originally demonstrated graded closure, and using isolated cell pairs from the same

tissue, Obaid et al. (1983) now state, without additional evidence, that

> "..the conductance of a cell junction...depends on the number of open channels..".

This prejudice determined the course of quantitative analysis in these three cases and its perpetuation in the absence of concrete evidence will colour our view of cell coupling.

2.4.2 Temporal Selectivity in Tenebrio Epidermis may Alter the Nature of the Intercellular Traffic.

Of the two simple models, only graded channel closure is truly selective. Therefore, it was important to find which of these two were involved in temporal variation of coupling, and to determine whether there was selectivity among the molecules passing between cells, or variation in all their rates of passage.

The significance of the two ways of channel closure is illustrated in the effect of an intermediate level on the following example of cell coupling:

> Two mutant cell types are unable to grow in culture because each is deficient in a different enzyme responsible for nucleotide synthesis, but can do so if cultured together because of mutual nucleotide exchange (Pitts, 1971). The rate of nucleotide exchange was established as $>10^6$ molecules per cell pair per second (Pitts and Finbow, 1977).

A reduction in channel diameter of just over 50% (assuming a diameter of 20Å) would stop the nucleotide

exchange, and hence cell division, although still allowing exchange of the purines, pyrimidines and sugar*, and other smaller molecules. However, an equivalent reduction in coupling by the AON model -- closing 50% of the channels -- would not stop the passage of any component of the metabolic cooperation. Both nucleotide exchange and cell division could continue at reduced rates.

In channel closure by AON, complete uncoupling would be necessary to block the passage of any one molecule. Nevertheless, coupling reduction could have as significant an effect as selectivity -- for example, reduction of passage of a signal molecule might drop its concentration below threshold in the target cell.

AON closure is functionally equivalent to modulation of channel number, which is present in many tissues. By this mechanism, the time for insertion of new channels by translation of mRNA is only 3 to 4 hours (Dahl et al., 1981), and only minutes are required for addition of functional channels (from 3 to 30 minutes in various systems; Loewenstein, 1981). A major reduction in junction number can occur in 4-6 hours in rat liver (Yee and Revel, 1978) and appears separate from the natural turnover, since the half life of gap junctions averages 19 hours in liver (Yancey et al.,

*The limiting dimension for channel passage of AMP is 10Å, and of UMP is 13Å; but is 5Å for ribose phosphate; the limiting dimension of the purines and pyrimidines ranges between 6 and 8Å (from Lehninger, 1975).

1981). Therefore, modulation of channel number could produce intermediate levels of coupling quite rapidly, and AON closure would appear to be redundant. While GCC allows variation of the quality as well as the quantity of the molecules exchanged among cells, the reason for doing so during coupling regulation is unclear.

Cells that uncouple completely are an example of temporal selectivity in coupling, since experimentally induced uncoupling of the cell sheet reveals a graded change in junctional permeability. In the pathological uncoupling of a cell from its neighbours, perhaps selective uncoupling quickly prevents the loss of the larger molecules, which represent the greater energy investment of the cell, while prolonging the passage of small ions and water for support of homeostasis.

2.4.2 (a) Temporal selectivity in development of the epidermis.

Essentially, the changes in r_j caused by Li-saline were just the synchronous uncoupling of individual cells, forced upon the tissue by the uncoupling treatment. However, those changes also appear to occur *in vivo*, since in *Tenebrio* r_j changes in a programmed manner during the course of the last larval instar (Caveney, 1976; 1978).

Results presented here have shown that coupling in intermolt epidermis is typically set below the maximum level

possible, with the control r_i capable of being experimentally lowered about threefold by Li. This means that the junctional membrane of intermolt cells is not maximally conductive, interpreted here to mean that the passage of the largest (otherwise) permeable molecules may be prevented.

Assuming GCC, a rough estimate of the difference in channel diameter between control and maximally open states can be made by correlating r_i with channel diameter and extrapolating to the appropriate r_i values. This assumes that pathway resistance is inversely proportional to the total channel area and, with constant numbers of open channels, to the average channel diameter (d):

$$r_i \propto \text{channel area}^{-1} = (\pi/4.d^2)^{-1} \quad (1)$$

Strictly, r_i is the sum of both cytoplasmic (r_c) and junctional resistance (r_j). Assuming the former to remain constant, r_j is a function of channel area. Expressed as resistivity, or specific resistance, these terms become independent of physical dimensions: the cytoplasmic resistivity (R_c) is 64 Ωcm in epidermis (Caveney and Blennerhassett, 1980) and the junctional resistivity (R_j) is:

$$R_j \propto R_i - R_c \quad (2)$$

(Caveney and Blennerhassett, 1980), so that:

$$(R_i - R_c) \propto d^{-2} \quad (3)$$

Applying the logarithm gives the linear relationship:

$$\log (R_i - R_c) \propto \log(d) \quad (4)$$

At the r_i associated with dye occlusion, the effective channel diameter is taken to be the limiting dimension of that dye. By extrapolating, the predicted channel diameter at normal levels of coupling is 16Å, but increases to 20Å when r_i drops to its minimum. The same calculation for the channels is newly molted tissue suggests that their diameter is 20Å at an average r_i of 4. Although there is little variation in newly molted tissue, at the extreme low value of 1.7×10^5 Ω, the effective maximum channel diameter would be 22Å.

It must be emphasized that these values are very approximate. To determine the maximum channel diameter with this method, at least one other larger fluorescent molecule would have to be used; first to prove the linear relationship, and then for extrapolation. It is satisfying, however, that the maximum channel diameters are similar in epidermis of both conditions, and that they fall near to the range of 20-30Å demonstrated in Chironomus by Schwarzmann et al. (1981) for non-polar tracers: a radical difference in predicted channel diameter would cast suspicion upon the assumptions that were based on graded channel closure.

This demonstrates in theory how cells can regulate their junctions to affect the size of molecules capable of passing among them. Experimentally, the exposure to molting hormone in vitro results in the cells becoming maximally coupled (Caveney, 1978); as seen here, there can be

temporary maximum coupling during the intitial response to Li saline. The existence in the segment of intermediate levels of coupling, which graded channel closure implies are selective, suggests that this is one way in which coordination or direction of cell activity might occur in insect development.

Epidermal cells are apparently fully coupled around the time of ecdysis, during maximum metabolic activity at high blood 20-HE titre. The need for tight coordination may be the reason for elevated coupling, but it appears that events at this time may require the passage of molecules unable to do so at other times. For example, the passage of a signal of low molecular weight might trigger a widespread, synchronous response, or a static concentration gradient might establish a segmental gradient.

Clearly, it is as easy to postulate a role for selectivity in coupling as it was for coupling in general after its discovery (see for instance, Furshpan and Potter, 1968). However, the molecules involved and the cell interactions remain ambiguous.

2.4.3 Membrane Polarization Controls Junctional Conductance

In epidermis, the membrane potential and non-junctional membrane resistance could vary independently of the degree of coupling, since both dropped rapidly to new values in Li-saline without affect on either r_i or junctional

permeability. In Tenebrio epidermis, Popowich and Caveney (1977) found that the membrane potential had a strong dependence on the extracellular $[K^+]$, with increased K causing depolarization and decreased R_M, also without change in r_i. The overall ion balance in Li saline, rather than $[K^+]$ between solutions was less than 5mM.

A drop in E of individual cells in the epidermis appeared to cause uncoupling from their neighbours. The simultaneous onset of depolarization and decrease of coupling might have been coincidental with general changes in ion level, such as increased Ca_i, but for their close relationship during subsequent change in E. Alternatively, cell polarization might determine Ca_i, but Obaid et al. (1983) have shown in salivary gland cell pairs that E controls cell coupling directly, and that it is independent of ion control. Since the junctional resistance increased within an injected epidermal cell when the membrane potential fell, E appears to control cell coupling here as well. Obaid et al. (1983) did not show whether E allowing maximum conductance (E_{max}) was the same as the resting E of cells under those culture conditions; however, E_{max} was within the wide range of resting membrane potentials found before voltage clamping.

Explained that way, the role of E in cell coupling in the epidermis seems to be that for one cell, E less than the tissue average will uncouple it from the rest, but for a

tissue, change in E just resets the reference mark.

The substitution of Li for Na caused uncoupling independently of the membrane potential, and so represents the second and potential-independent form of coupling control. Previously, Popowich and Caveney (1976) and Rose and Loewenstein (1971) had reported that Li decreased junctional permeability in Tenebrio and Chironomus respectively, and suggested that its action was to increase intracellular Ca.

The specific intracellular action of Li is unknown, but presumably causes increased Ca_i either directly or indirectly. Of the variety of treatments that cause cell uncoupling, most are assumed to act through the agents known to regulate coupling directly, while others are general denaturing agents, interfering with membrane or protein structure (for a review of the pharmacology of gap junctions, see Spray et al., 1984). Li may directly increase Ca_i, since this is suggested from its action on another cell system: in toad skin, intracellular Li increased the paracellular permeability, apparently opening the tight junctions through increased Ca_i (Aboulafia et al., 1983; Cereijido et al., 1981). Li action could also be indirect, since it inhibits enzymes responsible for carbohydrate metabolism (Mellerup and Rafaelsen, 1975), and so energy dependent processes generally will be antagonized. Similarly, uncoupling in Tenebrio epidermis was caused by

anticalmodulin drugs acting on Ca_i, and by iodoacetate, a nonspecific inhibitor of glycolysis (Lees-Miller and Caveney, 1982). Therefore Li may act directly on the intracellular Ca level, or indirectly through the active processes that maintain it.

2.4.3 (a) Dual controls of coupling may be distinguished by their speed of action.

The existence of two separate systems for regulating intercellular coupling appears redundant. Both E and Ca can uncouple a damaged cell from a tissue, although only the latter can vary the level of coupling in the tissue (at least in epidermis). However, speed of action may distinguish which control is effective in those circumstances where both seem to apply. Obaid et al. (1983) have shown that potential gating is extremely fast, with a time constant of tenths of a second (similar to that for transjunctional voltage sensitivity in vertebrates; Harris et al., 1982). In crayfish rectifying synapse, change between high and low conductance states required only milliseconds, shown by changing the polarity of an applied constant current (Margiotta and Walcott, 1983). Rapid change in E also occurred in Tenebrio epidermal cells, and could cause uncoupling in less than a second, but experimental results were selected for gradual change that permitted measurement, and ruled out the possibility that the electrode tip

had slipped through the cell membrane into grounded extracellular space.

Uncoupling by Ca control would require a Ca imbalance from a net influx or the release of stored ions. Evaluation of the relative roles of Ca and E under different circumstances would require considerable research in itself, but it seems possible that in some events provoking an uncoupling response -- probably cell damage, perhaps failure of homeostasis -- E gating may isolate a cell before Ca_i will have risen to a level adequate to do so.

CHAPTER 3

SPATIAL SELECTIVITY IN JUNCTIONAL COMMUNICATION

3.1 Introduction

Interactions among cells in a developing organism must control proliferation, differentiation and the activity of the resulting tissue. The insect segment is evidence of all of these interactions. Segmentation, the subdivision of the body plan into a number of similar units, is a fundamental strategy of body organization in multicellular animals. Annelids, anthropods and vertebrates all exhibit at some time of their development a metameric body pattern.

However, the cellular basis can be quite different. In the leech (Annelida), segmentation is first seen as a repeating pattern of mesoblast cell clusters, with each cluster being a clone derived from a single embryonic cell; the pattern within the leech segment then develops through a series of highly stereotyped cell divisions (Zackson, 1982). Therefore, cell lineage is the most important determining factor in segmentation of this animal.

In the insect, however, segmentation starts with a relatively large number of unrelated founder cells, about 50 in *Oncopeltus* (Wright and Lawrence, 1981a) and between 90 and 130 cells in *Drosophila* (Lawrence, 1981). This is shown

by clonal analysis, which marks a single founder cell within the early embryo and so identifies its descendants. This indicates that after a period of 20-30 hours of development, groups of cells become restriced to a single segment. While the shapes of the clonal patches are random within the segment, they are constrained by the intersegmental boundary and never cross over it. This defines the segment as a developmental compartment. Thus, only after compartmentation is lineage involved in segmentation.

Segments form specific parts of the body according to their relative position within the embryo. They are autonomous in this respect, so that the cuticular structure is unique to the segment, for example position-specific structures like antennae, wings or legs, or less obvious differences of form as in the segments of the abdomen.

Within the insect segment, an epidermal morphogenetic gradient controls cuticle patterning (Locke, 1959; Lawrence, 1973; Caveney, 1973) and appears to be a gradient of positional information that conveys information to the cells about their relative location. The axial gradient repeats in each segment so that cells in equivalent positions in different segments perceive the same information. Despite the epidermal continuity, cells on either side of the segment border react independently to their respective, extreme gradient values. The physical basis of the gradient, suggested to be a diffusible molecule or morpho-

gen, must somehow be limited in influence at the segment border. The special properties of the intersegmental zone limit cell position as well as interaction, since cells never cross over after the segment border is laid down.

Thus, the segments are examples of groups of identical cells with similar rules of development that follow different pathways. This suggests the absence of intercellular communication across the segment border, but is incompatible with obvious cooperation in cuticle manufacture of the entire body, and synchrony of action during the molt cycle.

In this chapter, intercellular coupling at the segment border is examined, to see whether spatial selectivity can explain the limitations on cell interaction between segments. Developmental regulation of junctional communication at the segment border may determine which permeant molecules may pass between segments, and when they may do so. In this way, the paradox of segmental autonomy and functional integration in making cuticle may be resolved.

3.2 Materials and Methods

3.2.1 Animal Culture

A culture of Oncopeltus fasciatus (Dallas), the large milkweed bug, was reared in plastic dishes on a diet of milkweed seed and water, with a day/night cycle of 14/10 hours and matching temperature cycle of 27°C/21°C. The cuticle of this bug is either black due to melanin deposits or coloured red by pigments carried in the epidermal cells. The strain used here was the mutant one cb;wb with reduced pigmentation (described in Lawrence, 1970). The 5 juvenile stages (nymphs), have white abdominal cuticle, and after dissection, cells of the epidermis can be easily seen with the phase contrast microscope. In the wild type, light is blocked from passing through the cells by the dense refractile pigment granules.

Stage IV nymphs were selected for experimentation, since earlier instars were too small, and the cuticle of the V instar is rippled and folded, especially at the intersegmental zone. Stage IV nymphs were identified by appearance, which is characteristic of each juvenile stage in this hemi-metabolous insect.

Several cohorts of newly ecdysed IV nymphs were followed to establish the duration of the instar. The average IV stadium was 4.5 days, the same as that reported for the wild type insect under similar conditions by Feir

(1974). Intermolt animals were considered to be a stage greater than 24 hr. post ecdysis but prior to apolysis, which usually occurred on the fourth day. These were readily identified by both weight and appearance, since the average weight increased nearly 4 times during the stadium with progressive expansion of the abdomen (Fig. 15).

3.2.2 Dissection and Tissue Culture

Insects were anaesthetized by immersion in 70% methanol, and removed immediately once immobilization occurred after 10-20 sec. This was usually reversible, with subsequent normal development.

A piece of integument containing 3 segment borders was dissected from the dorsal abdominal wall and placed in culture medium in a 35 mm Petri dish. The most posterior of the segment borders ran past a scent gland, one of two in the midline marked by spots of black cuticle. Tissue suspended from the gland opening was freed and discarded, since the contents appeared to kill epidermal cells in the vicinity if allowed to remain over longer culture periods.

The piece of integument was shaped to reduce the curvature by trimming the anterior and posterior margins close to the segment borders, and removing excess lateral cuticle. It was then transferred to another Petri dish with inset coverslip and razor blade clamps. The lateral edges of the preparation were placed under the clamps to counteract the

Figure 15

IV stage nymphs of the milkweed bug Oncopeltus fasciatus can be staged by appearance, which changes considerably between 12 hours after ecdysis (A) and 3.5 days (B). The major difference is the distension of the abdomen with feeding, which corresponds to a 5 fold weight increase (C; bars, standard deviation) during the approximately 4 day stadium.

M, average time of ecdysis to V stage (range, 100-120 hours). Scale bar, 2 mm.

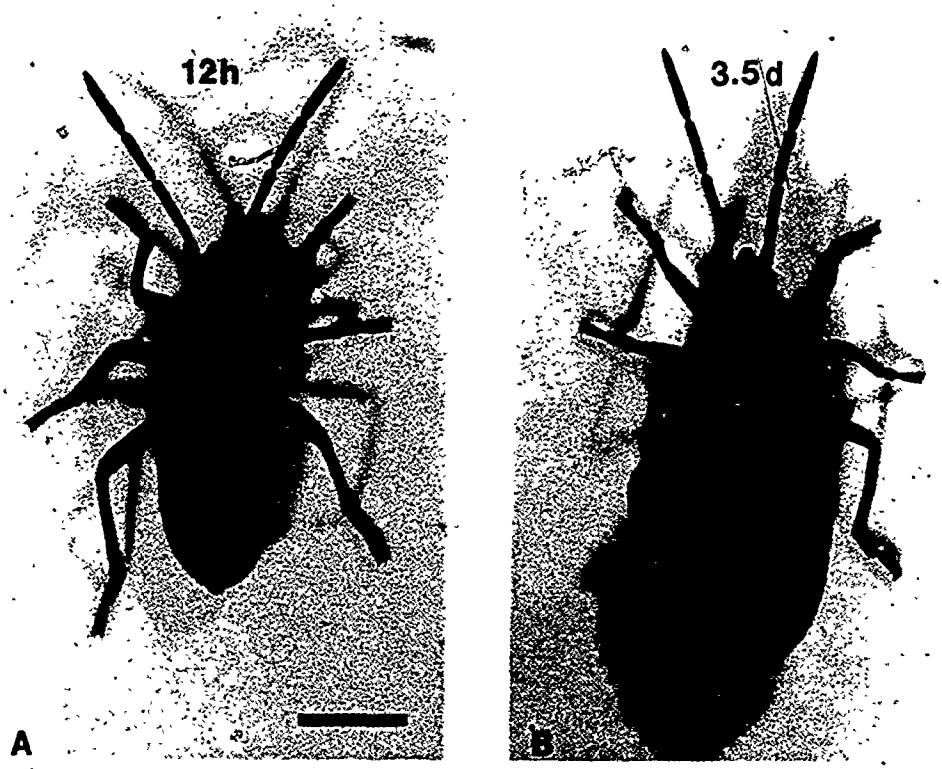
12h
3.5d
A
B

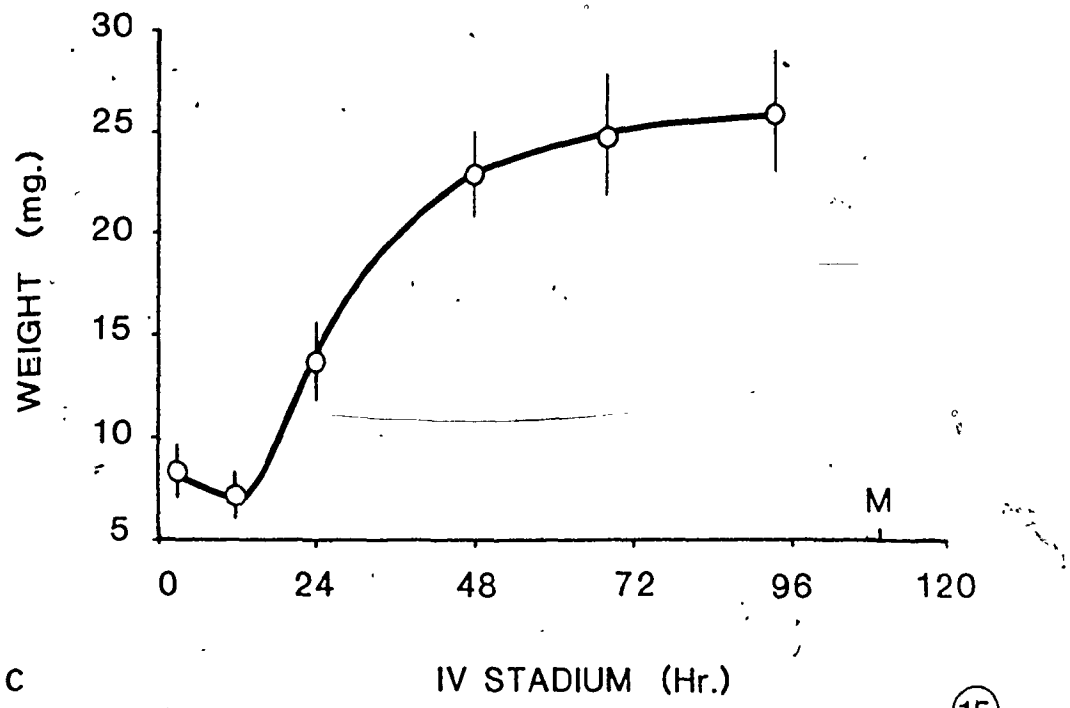
30
25
20
15
10
5
WEIGHT (mg.)
M
0
24
48
72
96
120
IV STADIUM (Hr.)

C

(15)

principal curvature. This allowed most of the preparation to lie in the same focal plane under the microscope. For dye injection, such preparations were sometimes dissected further into narrow strips, each containing a single segment border. Clamping these as before removed much of the local curvature of the segment border and gave a flatter preparation, but at the cost of reduced cell number.

Epidermal preparations were either used immediately after dissection, at an ambient temperature of 25-27°C, or were kept briefly in an incubator (Hotpack) at 27°C in air with 2% CO_2.

Four different culture media were used. Medium 1 was TC199 (Gibco) containing 10 mM PIPES (Sigma), Medium 2 was a leafhopper medium (Mitsuhashi, 1965) and Medium 3 was a Drosophila medium lacking amino acids (Shields and Sang, 1970). Medium 4 was modified Grace's lepidopteran medium (Gibco) supplemented with 15 mM PIPES according to Smith and Nijhout (1983). All media were adjusted to pH 6.8 with 1N NaOH, and contained 10% foetal calf serum.

An osmometer (Advanced Scientific Inc.) was used to determine the osmolarity of 2 ml samples of these culture media. A nanolitre-drop osmometer (Clifton Technical Physics) was used to measure the osmolarity of haemolymph from IV nymphs.

3.2.3 Electrophysiology and dye injection

The techniques of electrophysiology and iontophoresis of intracellular tracers were described previously, in Section 2.2.3. The fluorescent dye Lucifer yellow (MW 457; Polysciences) was used in addition to 6-carboxy fluorescein (CF) and lissamine rhodamine B (LRB) (Appendix I). The dimensions of a CPK space-filling model of Lucifer Yellow (LY) were 14.5 x 13.0 x 7.1 Å (limiting dimension underlined). LY was made up as a 3% w/v solution. The tips of the electrodes were back-filled by capillary action and the barrels were then filled with 0.1% LiCl to prevent the formation of insoluble K salts (Stewart, 1978). The fluorescence of LY was viewed with the same filter set used for CF, although not optimal for this otherwise highly fluorescent tracer (see Stewart, 1978). This was a compromise in the absence of correct filtration, since substitution of a BG38 excitation filter, although more appropriate to the excitation spectrum of LY, increased the background level as well as the emission intensity.

3.2.4 Histological Techniques

In addition to study of the living tissue by phase contrast microscopy, pieces of integument were fixed for sectioning, or were stained and examined as whole mounts.

I. For sectioning, epidermal preparations were fixed overnight in cold 5% glutaraldehyde containing 2% sucrose

and buffered with 0.05M sodium cacodylate to pH 7.0. After washing in buffer and then in water, the tissue was dehydrated with a graded series of acetone. The tissue was infiltrated over 24 hours with increasing concentrations of Araldite (Cargille), and then embedded in fresh Araldite. 2 μm sections were cut parallel to the body axis and normal to the plane of the cuticle. These were stained with 0.5% toluidine blue in 0.25% borax, and examined with phase contrast and bright field optics.

II. Cell density was studied using Hoechst 33258, a fluorescent stain for DNA. Preparations were either freshly dissected or taken from previous experiments for staining, and placed in a solution of fixative containing approximately 1 mM Hoechst 33258. After 24-48 hours, they were washed twice in culture medium, rapidly dehydrated through 2 changes of acetone and cleared in toluene. The preparations were placed on a glass slide in a drop of toluene, and cut into several pieces to minimize the effect of curvature of the now brittle cuticle. These were oriented with cells uppermost and mounted. The specific nuclear staining was viewed by epifluorescence, with the coverslip and cell surface next to the objective, using a UG1 (Reichert) excitation filter, Zeiss FT410 dicroic mirror and BG38 (Reichert) barrier filter. Under these conditions, the nuclei appear a brilliant ice-blue, against a background of varying degrees of dark blue. The intensity of the back-

ground fluorescence, due to mitochondrial DNA and non-specific staining, was variable but was minimized by careful washing before dehydration.

For some examinations of nuclear appearance and cell density, segments were fixed in Zenkers fixative for 30 minutes, and stained by the Feulgen method (Humason, 1979). Dehydration and mounting was the same as described for Hoechst stained tissue. Nuclear shape was studied with a 100x oil immersion objective.

3.2.5 Photography

Fluorescence and phase contrast images were recorded on 35 mm film with a Nikon FE° camera mounted directly on the microscope. High speed black-and-white films were used, either Ilford HP-5 developed at 400ASA in Microphen (Ilford), or Ilford XP1 developed with commercial C-41 processing. These films were preferred to Kodak Tri-X (400 ASA in HC110 - Dilution B; Kodak) for recording the low light of fluorescence, principally for their finer grain and extended sensitivity that gave more faithful reproduction of the visible detail.

Photographing the fluorescence of Hoeschst 33258 required a high contrast film to minimize the nonspecific fluorescence of the background. Kodak Technical Pan (2415) was used with long exposures, and was developed in HC110 (Dilution F) to ASA 25. The negative density of this slow

film increases unusually predictably during exposures greater than 10 seconds, making it suitable for recording this type of fluorescence, where changing light levels due to diffusion or bleaching is not a concern.

The camera's light meter determined the exposure for phase contrast and bright field images. 4 or 8 second exposures were routinely used for fluorescence work, although bracketed when feasible. During the spread of fluorescent dye in the cell sheet, these exposures were adequate to record the full range of light intensities, and brief enough to 'stop' its changing appearance. Longer exposures were little different due to reciprocity failure, and shorter exposures achieved through push-processing were unsatisfactory due to the increase in contrast and grain size of the negatives.

The slight vibration of the camera's shutter action caused motion of the microelectrodes during intracellular dye injection, preventing film exposure in the normal way. Instead, the camera was set on 'B' and the shutter was opened with a cable release. To expose the film, the sliding prism on the microscope that deflects light to the camera was inserted into the light path for the required time.

3.3. Results

In the abdomen of stage IV nymphs, the dorsal body wall is formed by a shallow convex sheet of cuticle. Transverse lines of slight indentation mark the intersegmental region, and spiracle placement and the pigmentation pattern are repeated in each segment. Toward the posterior of the animal, the segments decrease in width and breadth, and have increased curvature (Fig. 16A). Dissection of the preparation and examination under the light microscope shows the extent of the repeating elements (Fig. 16B).

In an epidermal preparation, there are roughly 21,000 cells, forming a continuous monolayer 8.1 +/- 0.7 μm thick. It is free of muscle insertion sites, and the only visible elements are small bristles that point backwards and can be used for orientation.

In the posterior of each segment, a white pigment, the only one present in the IV instar, increases in concentration, tending to darken the cells and obscure their margins. At the segment border, these cells meet the clear ones at the anterior of the next segment. The slighly convex curvature of the cuticle in each segment reverses its direction here, and begins to bulge outwards.

Cell shape is roughly hexagonal and uniform within the segment, but undergoes a characteristic change at the intersegmental zone (Fig. 17A). At the posterior of the segment, the cells are still roughly isodiametric, but at the

Figure 16

A cell preparation can be dissected from the abdomen of IV Oncopeltus in which the junctional properties of the cells at the intersegmental region can be examined.

Scale bars: A, 300 μm; B, 150 μm.

A. On the surface of the dorsal abdomen, the intersegmental regions appear as shallow lateral grooves. Small bristles point backwards. A square of integument was dissected free, containing the two segment borders anterior of the black spot.

B. Placed in medium and viewed under phase contrast, the intersegmental borders are identified by the change in cell shape and pigmentation. Corresponding segment borders in A and B are marked by an arrow. In the centre of the preparation, epidermal cells can be discerned, but curvature prevents a uniform focus. Clamps, seen as the black margins at top and bottom, hold down the lateral edges of the tissue.


A

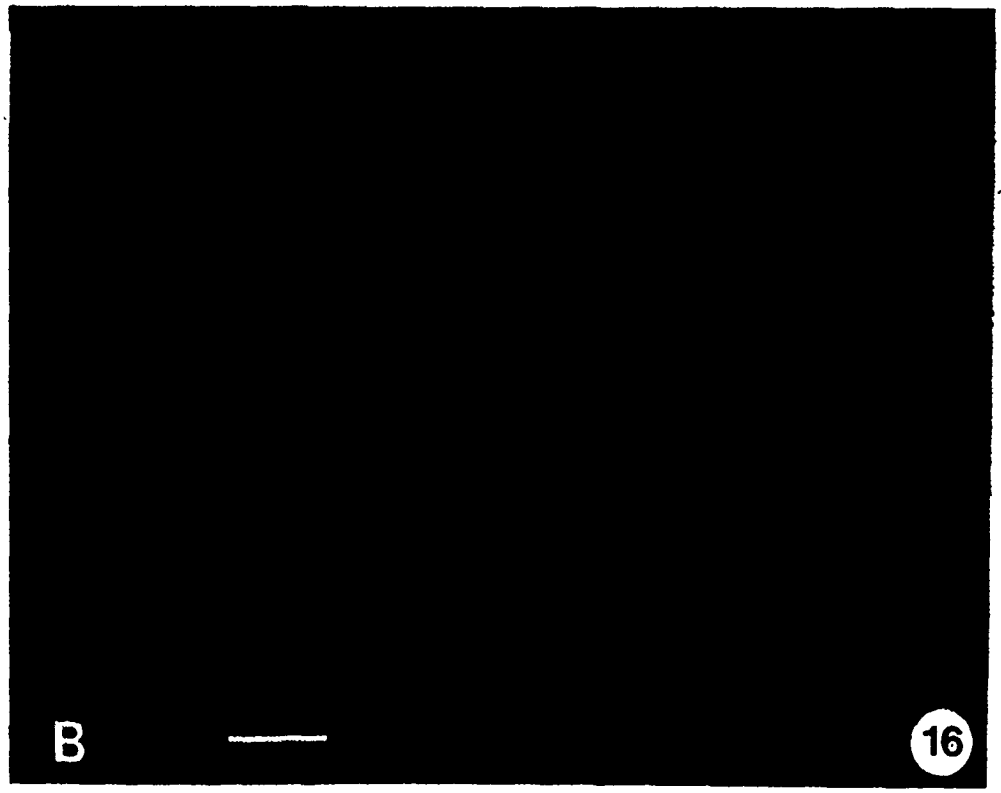
B
16

Figure 17

In the continuous sheet of epidermis, the segment border is identified by the change in cell clarity and shape to either side. The usually obvious demarcation of the segment border in phase contrast is not due to a particular structure, but rather to the lack of intermingling of the cells there, that causes the alignment of their margins along a line in space. Scale bars: A, 20 μm; B, 50 μm; C, 10 μm.

A. Phase contrast view of the segment border in a preparation in tissue culture. To the anterior (to the left, by convention in these and subsequent figures), cell detail is relatively obscured by intracellular pigment granules. This changes abruptly at the segment border, and are elongated laterally close to the border. Again, curvature throws part of the field out of focus.

B. A cross section through the segment border, parallel to the midline, shows that the epidermis and cuticle undergo a reversal in curvature at the segment border, but there is no other obvious structural change.

C. Examination at higher magnification of the segment border in B shows a continuous, uniformly thick epidermis. The arrow marks the approximate position of the segment border. Here, a slight change in the cuticle (not obvious in most sections) may indicate a more pliable region that effectively hinges the segment.

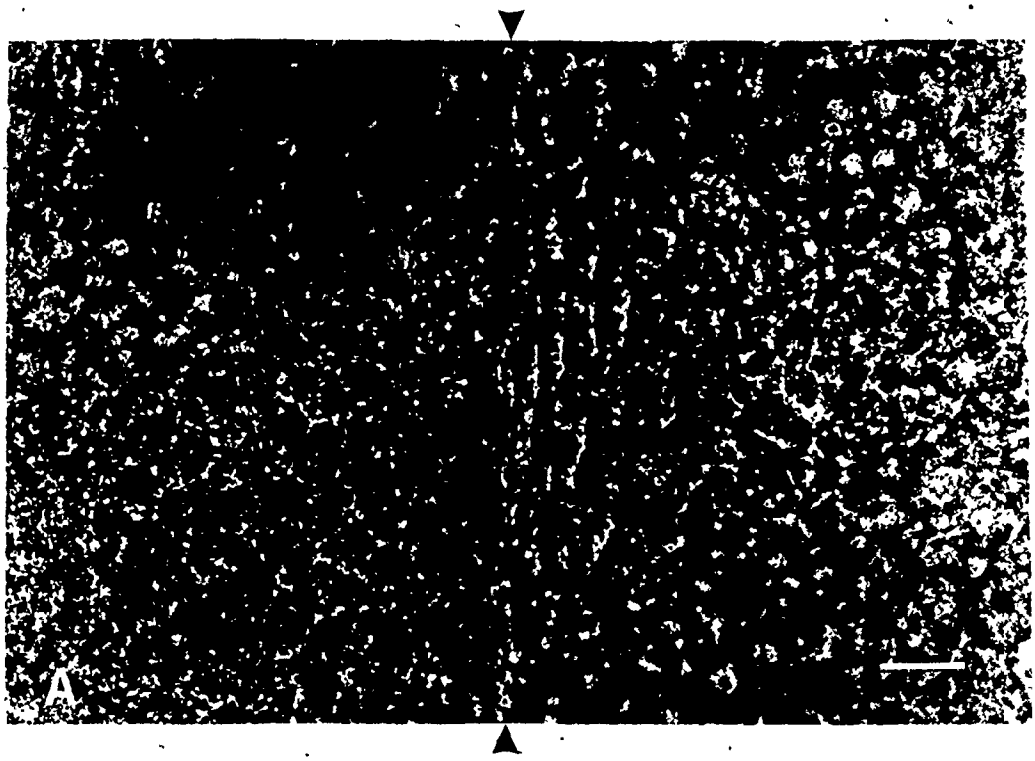
A


B


C

boundary with the next segment, these cells line up along the interface. The posterior margins of the last cells of the segment are aligned along the interface of contact with the clear cells of the next segment. They are not elongated along that interface, and neither is there any change in the size or nature of the intercellular spaces there. A slight ridge in the cuticle sometimes coincides with this interface, and may be equivalent to the pliable intersegmental cuticle of other insects.

Just posterior to the segment border, the most anterior cells of the next segment are distinctly different in appearance from their immediate neighbours. Several rows of laterally elongated narrow cells lie against the segment border. Posterior to these, the cells quickly revert to the normal appearance of cells in the middle of the segment. The degree of change in cell shape at the border can vary considerably between animals of equivalent development, and even along the segment border itself. Typically, elongation is least at the midline of the segment, and increases toward the sides and in the more posterior segment borders. A role in expansion of the cuticle is not likely since this appearance is constant throughout the stadium, including apolysis.

A typical cross section of a segment border (Fig. 17B) shows that it involves no discernible change in cell height or appearance. The cells tend to overlap each other at the

apical interface. The cuticle is uniform in thickness with a slight irregularity just posterior to the apparent segment border that may represent the more pliable intersegmental cuticle (Fig. 17C).

3.3.1 Spread of intercellular tracers at the segment boundary

Three fluorescent dyes were used to investigate the junctional permeability of Oncopeltus epidermal cells. Injection of any of these dyes into a cell in the middle of the segment produced symmetrical intercellular spread of dye away from the cell into the sheet (Fig. 18). The rates of spread of CF and LY were similar, and both moved between cells faster than LRB.

However, injection of dye into cells lying close to the segment border produced a completely different pattern of dye spread. When dye was injected into a normally shaped cell one or two cells distant from the border, Fig. 19 shows that cell-to-cell spread of all the dyes was radially asymmetrical, with normal spread into the segment, but retarded passage across the segment border. The rate of dye movement near the border was the same as seen during injection into cells in the centre of the segment. In spread across the border, these rates were decreased, so that LRB was the slowest tracer to pass into the cells of the next segment.

The events of a typical CF spread are shown in Fig.20.

Figure 18

CF and LRB spread symmetrically within the epidermis when injected into a cell near the centre of the segment. Left, photographs of the fluorescence at equivalent times of injection; right, the appearance with phase contrast. Anterior is to the left.

A. CF injected into a cell for 20 s spreads to the surrounding cells, without the mottled appearance seen in Tenebrio epidermis.

B. Phase contrast appearance of the cells in A, an area at the centre of the segment. The injected cell (+) uncoupled during injection, and is enlarged.

C. LRB has spread more slowly, entering 3 orders of cells at 25 s of injection.

D. In the phase contrast appearance of C, cell margins are obscured, and the slight lateral elongation suggested by the fluorescence appearance is not visible.

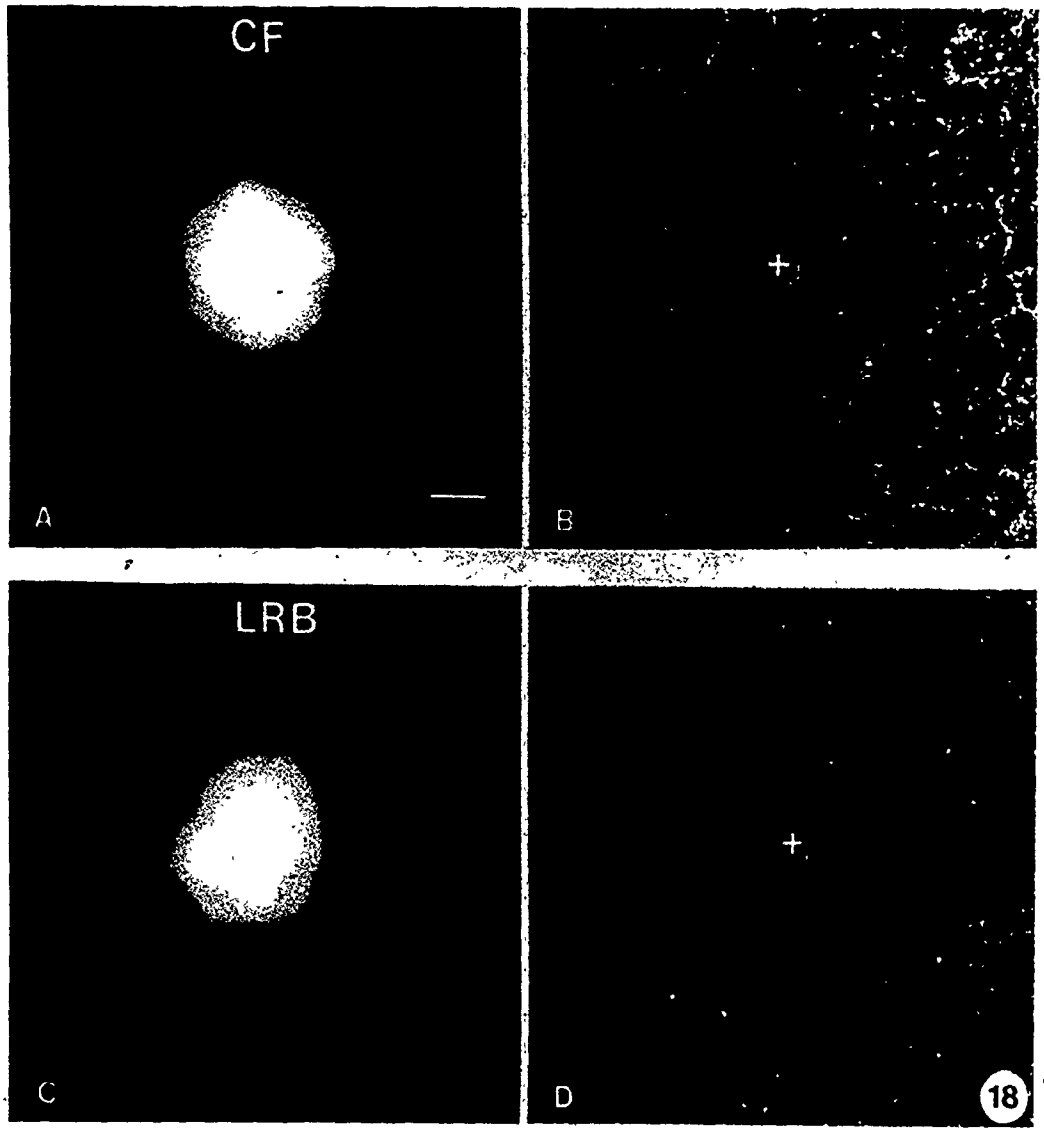
CF
A
B
LRB
C
D
18

Figure 19

Fluorescent tracers microinjected into epidermal cells near the segment border pass across it, although a drop in fluorescence occurs in this region. Left: record of three different tracers spreading across the segment border. Right: the same preparations shown in phase contrast. Membrane potentials were between 26 and 35 mV, stable during the injection period. The position of the segment border is marked by the arrowheads above and beneath the micrographs. A, anterior segment; P, posterior segment. Scale bar, 25 μm.

A. Lucifer Yellow (LY) was injected into a cell (+) anterior to the segment border for 30 s, the electrode removed, and the extent of dye photographed (60 s exposure). The spread of dye is impeded by the border. The appearance of the cells, imaged by dye localized in their nuclear regions, suggests that cells at the border were not particularly elongated. The source cell was damaged during electrode removal and failed to retain dye. The dark area just across the border from the injection site is a dead cell imaged by the dye that diffused around it.

B. Phase contrast appearance of A. In some cells of preparations such as this one, the presence of small vesicles that exclude dye (diagonal arrow in A and B) allow the micrograph pairs to be matched up independently of the cell margins which are often obscure.

C. Carboxyfluorescein (CF) injected for 20 s into a cell (+) posterior to the segment border, and the extent of its spread photographed (7 s exposure). CF was impeded in passage across the segment border. This dye fills the individual cells more uniformly than does LY (A). The tip of the electrode (e) was left in the source cell after the period of dye injection was over.

D. Phase contrast appearance of C. The position of the segment boundary is marked by a thin intercellular space (horizontal arrow). Cell margins, though difficult to discern here, are seen as step-like drops in fluorescencce in C.

E. Lissamine rhodamine B (LRB) injected continuously for 120 s into a cell (+) in the anterior compartment and the extent of spread photographed (12 s exposure) with the electrode (e) inside the source cell. This dye was the slowest to image cell detail across the border.

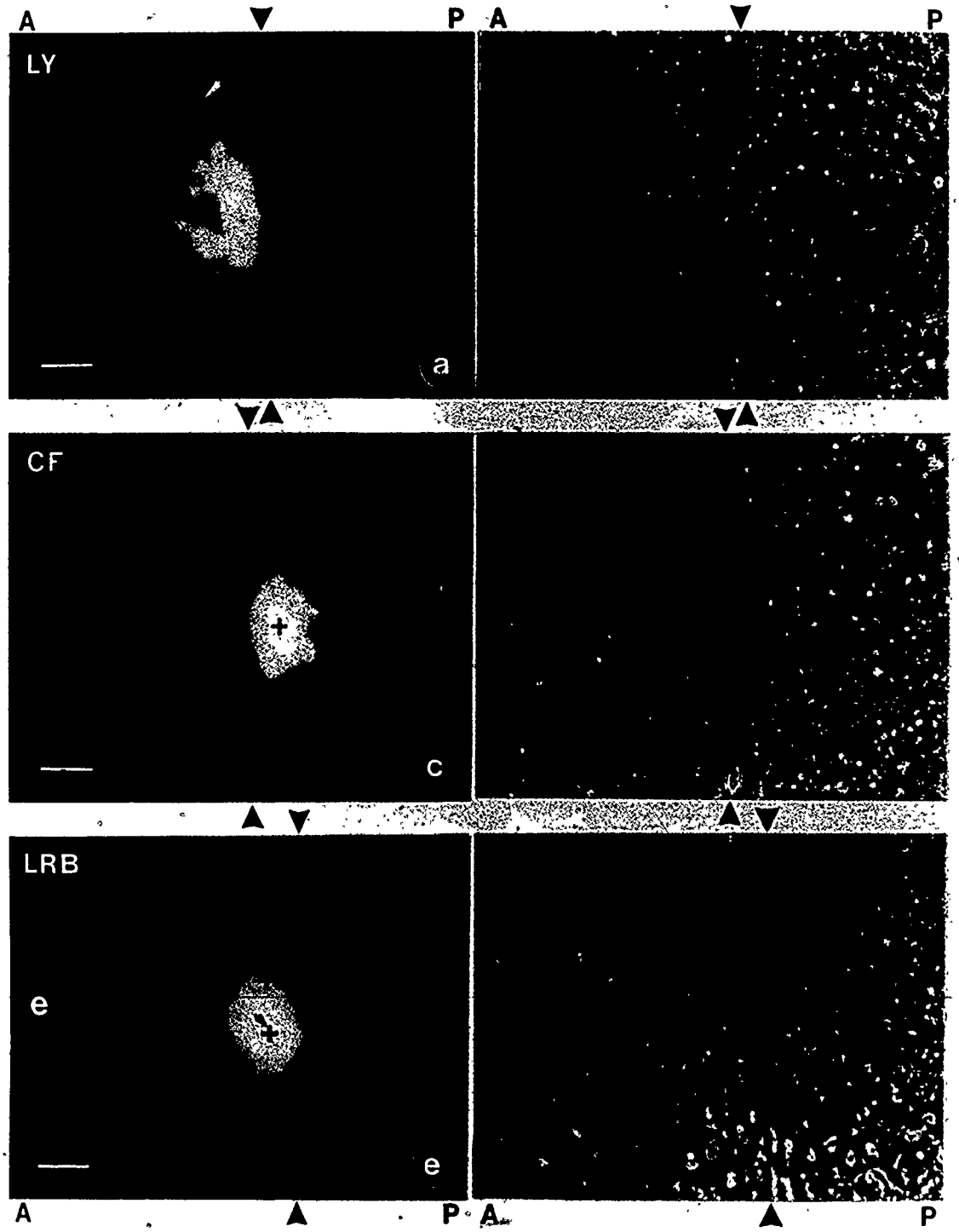

19

Figure 20

A series of photographs of the spread of fluorescence during the injection of CF into a cell near the segment border shows that a partial barrier to dye spread causes a step in intensity to develop at the segment border. The impedance to dye movement was maintained during the 1.5 minute injection period and caused asymmetric spread of dye: dye spread laterally 7 cell orders and 6 orders within the segment, but banked up against the segment border and entered only 3 cell orders in the next segment. In these circumstances, the segment border acts as a partial barrier to inter-segmental dye passage, slowing but not preventing its movement. Scale bar, 20 μm.

A-G. A series of 4 s exposures (processed and printed identically) recorded the changing appearance of the asymmetric spread of CF, starting at 14 s of injection when dye was detectable in adjacent cells (A). Dye spreads within the segment, but banks up against a partial barrier at the segment border. Relatively slower passage into the next segment is visible by 40 s (C), but the extent of passage remains less throughout injection period. The medium was M4, in which inter-segmental dye passage is relatively rapid.

H. A phase contrast view of the cell field shows that the barrier to dye spread coincides with the segment border (dashed line). Source cell, (+).

I. The chart recording of the injection shows the membrane potential of the injected cell, which stabilized after the electrode entered the cell, and was constant until the electrode was removed. Negative-going current pulses run off scale at the bottom. Deflections in the trace of the event marker (upper line) indicate the times of film exposure. Scale bars: horizontal, 10s; vertical, 10 mV.

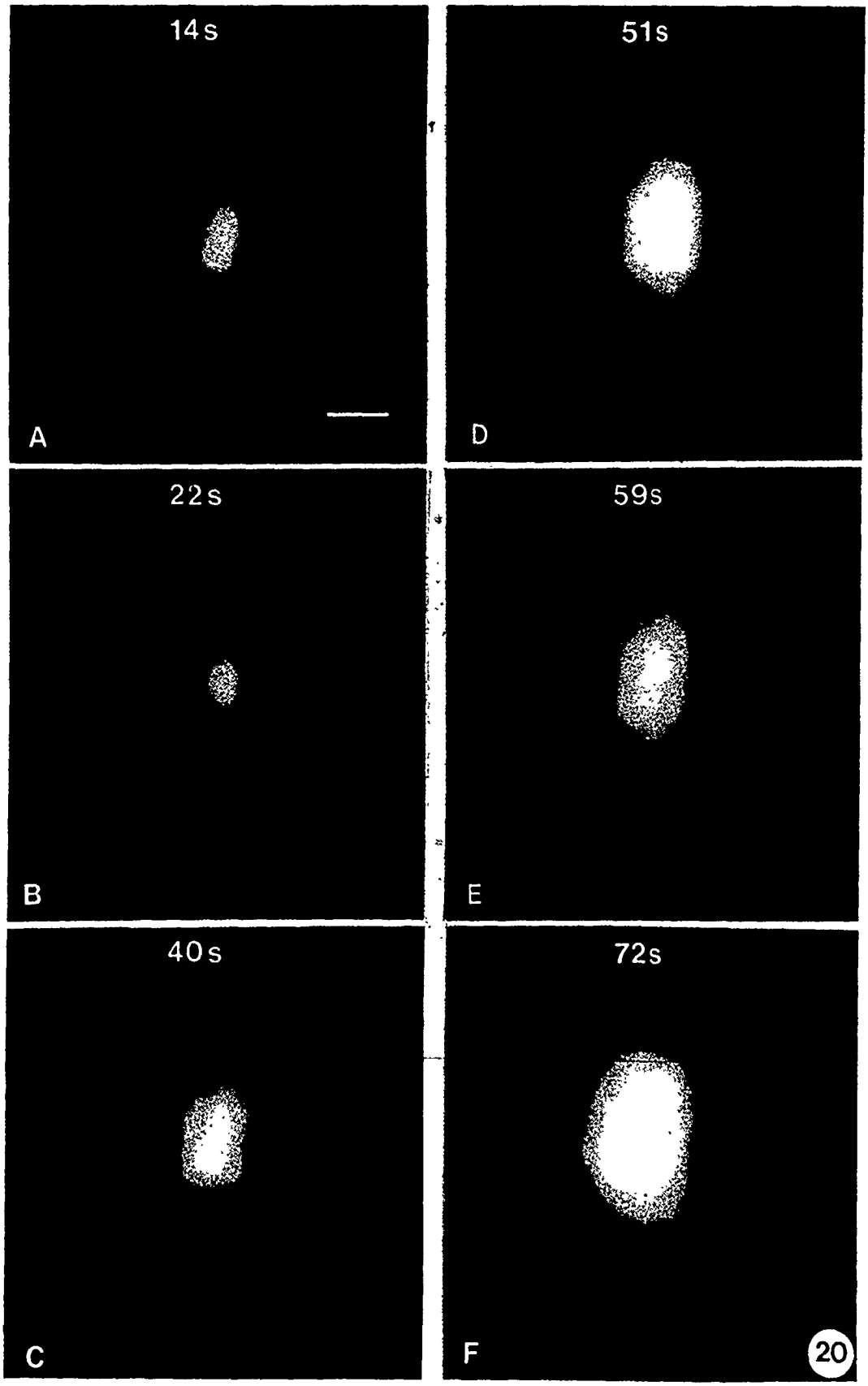
14s
A
51s
D
22s
B
59s
E
40s
C
72s
F
20

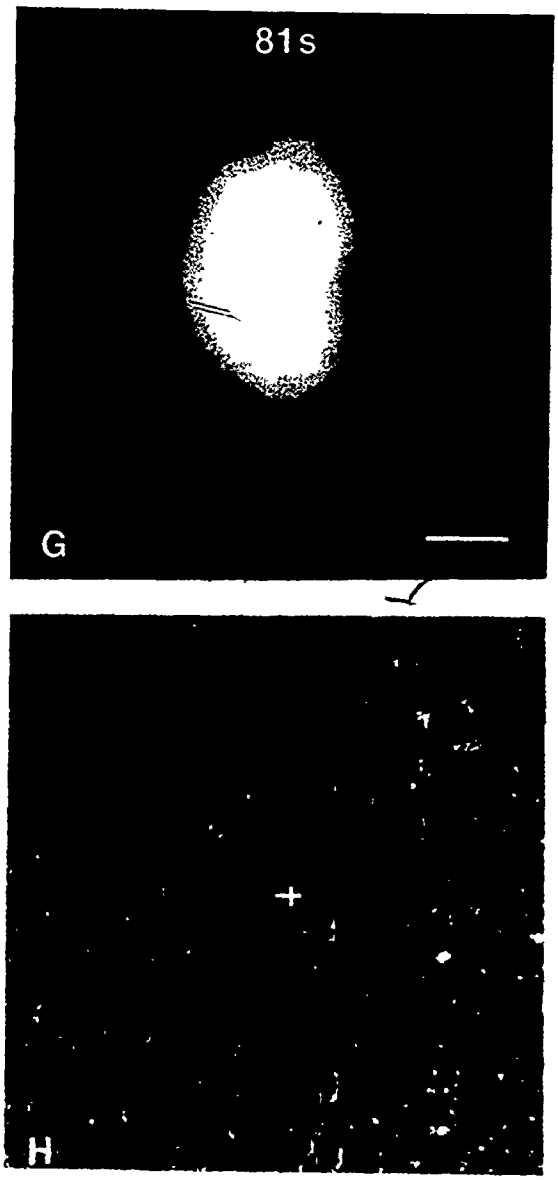
81s
G
H
I
20

The culture medium used was M4, which may best resemble the natural condition - the effect of culture media on inter-segmental dye spread is described later. Within 14 s of injection, an appreciable amount of dye has passed into the cells next to the source cell, and spreading uniformly, has reached the segment border. During the next 15 s, it continued to spread within the segment, but the increasing intensity of fluorescence between the source cells and the segment border suggests that dye was prevented from passing easily over into the cells of the next segment. By 22 s, dye is detectable within the border cells, and by 40 s, within the normally shaped cells of the next segment. However, dye had spread further, and reached a greater concentration within the segment during this time, so that a step in the intensity of fluorescence developed along the segment border. This step was maintained during the rest of the 100 s of injection, and the spread of dye parallel to the border appeared to have been emphasized by the banking-up of dye along the segment border.

A standard set of conditions was used for testing dye passage across the segment border in preparations between 10 and 50 minutes after dissection. Initially, there had to be a flat and undamaged field of cells with no previous dye spreads in view. The dye electrode was inserted into normally shaped cells one or two cells distant from the segment border. This prevented the electrode tip from

crossing the border inadvertently, either during insertion into the source cell or due to any slight electrode drift during injection, while allowing dye to bank up between the border and the source cell. The dye spread had to image cell margins, while extending within the segment at least 5 orders of cells radially to the source cell.

The appearance of the dye movement to the adjacent segment was then scored as either absent (and remaining so, with observation for at least 5 minutes), present but impeded in passage over the border, or present and minimally retarded by the segment border.

Within the segment, LRB passed between cells noticeably more slowly than either CF or LY. At the segment border, this dye also suffered a greater impedance to its inter-segmental passage: it was the slowest to image cell detail in the adjacent segment, producing the strongest step in fluorescence intensity at the segment border.

The spread of dye in preparations tested immediately (<10 min) after dissection into any of the culture media had roughly the same appearance: dye always passed to the adjacent segment at a distinctly reduced rate, estimated to be half the rate of movement within the segment. The subsequent rates of dye movement and appearance of dye spread were typical of the culture media used and the particular tracer injected. Fig. 21A shows the typical initial appearance of the spread of CF over the segment border at 5

Figure 21

The rate of intersegmental dye spread seen immediately after dissection becomes reduced in medium M1, but is maintained indefinitely in M4. Left, fluorescence micrographs of dye spread. Right, phase contrast appearance, with arrowheads above and beneath marking the segment border. (+), source cell. Scale bar, 20 μm.

A. CF injected for 30 s in a preparation 5 minutes after dissection into M1. Dye spreads over the segment border with little retardation, which is typical in preparations in any medium for 5-10 minutes after dissection.

B. Phase contrast appearance of A.

C. By 27 minutes in M1, the same preparation in (A) has developed a strong barrier to dye passage. Dye has banked up within the segment and its presence in only the first row of elongated cells beyond the border shows that passage to the next segment is strongly retarded, but not prevented.

D. Phase contrast appearance of C.

E. After 24 hours in culture in M4, the asymmetry of dye spread from an injected cell near the segment border is similar to that seen in A. The overall extent of spread is slightly less due to a shorter injection period of 20 s.

F. Phase contrast appearance of E. The cells are dead by this time in culture in the other media, but here appear normal, resembling epidermis seen immediately after dissection (B) or after adjustment to M1 (D).

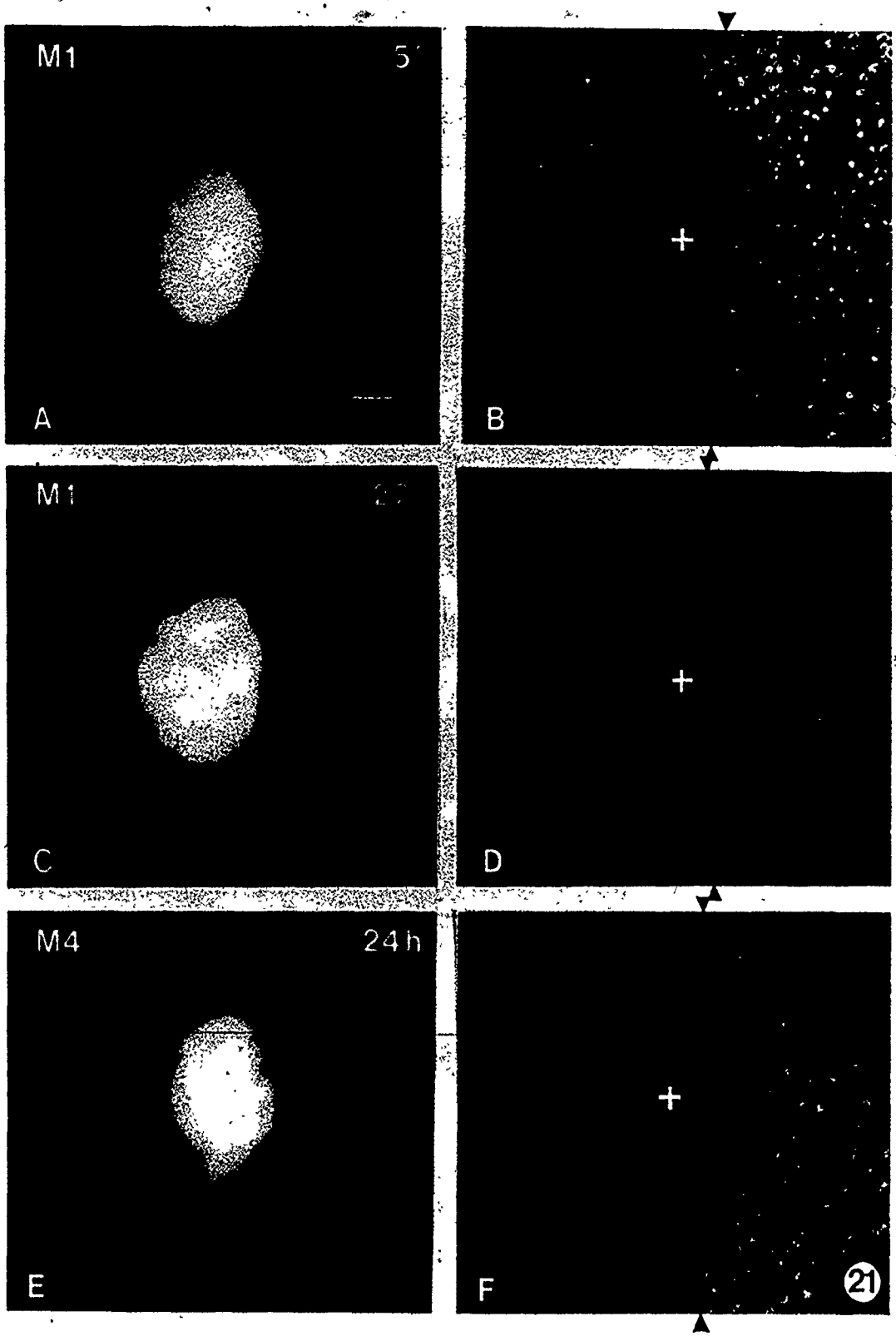
M1
5'
A
B
M1
C
D
M4
24h
E
F
21

minutes in M1. The characteristic appearance of the dye spread in this medium is seen in Fig. 21C, where CF is slower to pass over the border at 27 minutes in M1. In general, dye injections performed at greater than 50 minutes after dissection of the preparation tended to result in slower appearance of the dye in the next segment. Hence, CF and LY became further retarded while the passage of LRB became barely detectable or was lost.

The spread of the three fluorescent dyes across the segment border when injected into preparations immersed in either of media 1-3 is summarized in Table 4. The majority of results in all cases (130/166) fell into the middle category of impeded spread over the border.

Failure of dye spread across the border occurred in 23 of 166 of the trials, and was associated with M1. The intersegmental passage of CF and LY was impeded more than in the other media (compare Fig. 21B to Fig. 20 or 19C), and under these conditions, LRB commonly failed to pass over the border. In such cases, the apparent rate of dye spread within the segment was unchanged. The other extreme of minimal impedance of intersegmental dye spread was seen infrequently and occurred randomly, only 13 times in 166 trials. In those instances, the medium was usually M3. This suggests that <u>in vitro</u>, some aspect of the culture medium influences segment-to-segment dye spread.

Use of M4 was begun after the other 3 media, and is

TABLE IV: The extent of the cell-to-cell spread of 3 fluorescent tracers across the segment border.*

Tracer	No. of Preparations tested	Appearance of individual dye spreads		
		Dye spread restricted to within one segment by border cells	Dye spreads into adjacent segment but impeded by border	Dye spread minimally retarded by border
Carboxyfluorescein	29	13[1]	69[1-3]	3[2]
Lucifer yellow	10	0	25[1-3]	8[2,3]
Lissamine Rhodamine B	19	10[1]	36[1-3]	2[2]

* About equal numbers of spreads were done in which the source cell lay anterior or posterior to the border. No differences in dye spread were noted.

1,2,3 Superscripts indicate the medium in which results are obtained.
1, M1; 2, M2; 3, M3.

considered separately because of its different properties. First, it alone could support prolonged survival of the epidermal cells in culture. After 24 hours in the other media, the cells were opaque, detached from the cuticle, and had no detectable membrane potential, whereas the appearance of preparations kept in M4 was little changed, and the membrane potential was 32 +/- 6 mV (n = 24 from 4 animals). Second, dye injections into preparations at 30 minutes or 24 hours exposure to the medium showed intersegmental passage apparently equal to that seen immediately after dissection (Fig. 21C; compare to Fig. 21A). This contrasts with the effect of the other media where trans-segmental passage was reduced in M1 and M2, and actually facilitated in M3.

The properties of dye coupling seen directly after dissection probably reflect those <u>in vivo</u>. These were roughly similar in preparations in all media, but were only maintained in M4. Since M4 also supports the epidermis for 24 hours in culture with that level of coupling, it was felt that this medium best approximated natural conditions. Therefore, dye coupling between cells on either side of the segment border seems to be regulated to a level below that seen between cells within a segment. Coupling between segments is regulated, and not simply reduced, since coupling <u>in vitro</u> shows that there are conditions that can rapidly raise (M3) or lower (M1, M2) the extent of inter-segmental dye passage.

3.3.2. A row of cells at the border with reduced junctional permeability retards the intersegmental spread of dye

The intersegmental zone is characterized by increased cell packing posterior to the segment border. Since dye passes faster within a cell than between cells, that is, the junctional membrane offers greater resistance to the passage of dye than does the cytoplasm, dye moving through a region of increased cell density will appear to be impeded. Therefore, the contribution of the increased cell packing to the retardation of the intersegmental dye spread was examined. Some preparations were placed in medium 1 which depressed segment-to-segment dye coupling, a cell posterior to the segment border was injected with CF and the extent of the dye spread photographed (Fig. 22A). After the dye had mainly diffused away, a cell anterior to the border was similarly injected, and the extent of its spread photographed (Fig. 22C). In both cases, the dye has been virtually blocked from passage over the border, while spreading 4 or 5 cell orders away from the border. This could not be due to changes in cell packing alone, and since this effect occurs in dye spread from both directions, is presumably independent of it.

This procedure is one of two methods that demonstrated the true cause of retarded dye spread at the segment border: a second feature of Fig. 22A is that the line of dye restriction fell posterior to the segment border seen with

Figure 22

In a preparation in medium 1, dye injected into the anterior segment was blocked at the segment border, while that injected posterior to it was blocked at a line that did not coincide with the segment border, but was separated from it by a strip of cells. The junctional permeability of this strip of cells appears to be regulated independently, since dye moved rapidly among cells within a segment. Injected cells are labelled +. A, anterior; P, posterior segment. Scale bar, 20 μm.

A. CF injected into a cell posterior to the segment border for 9 s and the extent of dye photographed 22 s later (4 s exposure). The dye spread in a radially asymmetrical fashion and was blocked in its passage along a line passing through a marker particle (white circle, see B). Compare this with Fig. 21 A&B, to see the progressive retardation of spread of dye over the border with time in this medium.

B. Phase contrast view of the cells shown in A and C. The position of the segment border is emphasized by the dashed white line. The refractile particle lying just to the right of the border serves as reference for locating it in A and C.

C. Dye injected for 8 s and its fluorescence photographed 23 s later (4 s exposure). The asymmetrical

dye spread is strongly truncated at the segment border, just to the left of the marker particle (white circle). Residual fluorescence from the spread shown in A, done 4.5 min earlier is seen to the right of the marker particle.

D., Margins of the cells seen in B were drawn from their phase contrast and fluorescence images, and the extent of dye spread in A and C indicated by stippling. This outlines a strip of border cells whose permeability is much reduced from that of the adjacent cells within each segment.

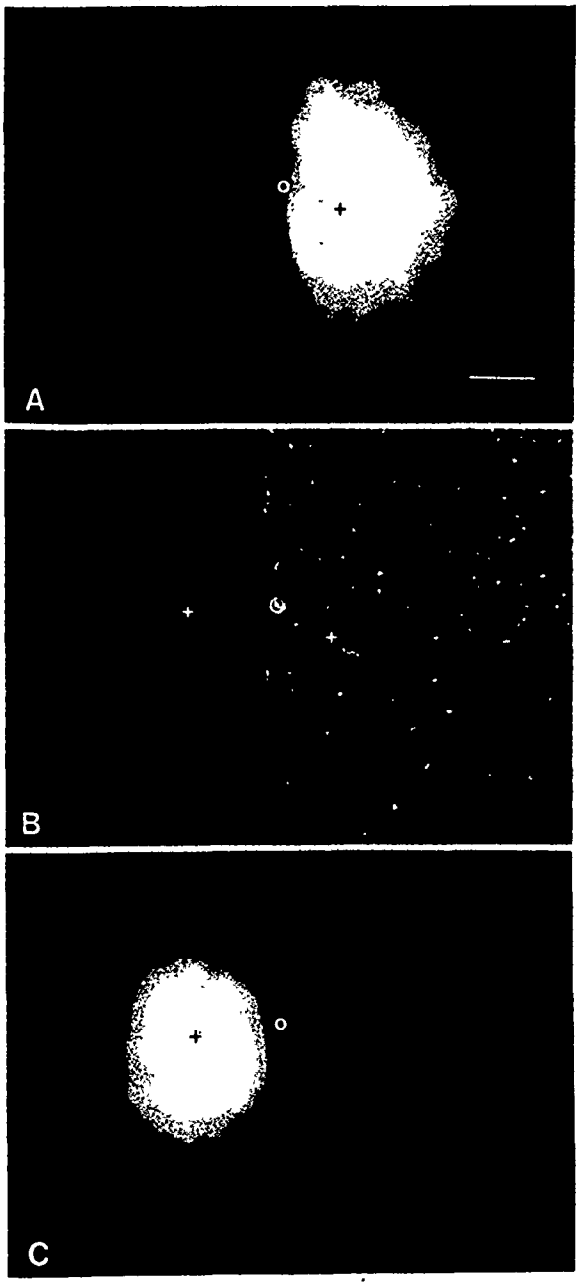

22

phase contrast in Fig. 22B, but when dye was injected immediately opposite to this spread, the line of dye restriction did coincide with the segment border. The position of the refractile lipid droplet emphasizes this, since the two dye fronts fall to either side of where it lies on the epidermis. Therefore, the cells immediately posterior to the segment border constitute the barrier to the spread of dye, and their elongated lateral margins correspond to the lines of dye restriction.

A schematic diagram of the cell outlines was made from the fluorescence and phase contrast images, and those cells containing dye were marked (Fig. 22D). This shows that there is a population of cells at the segment border, just one cell wide in this case, that on the basis of greatly reduced junctional permeability is separate from those on either side.

The presence of a cell type with reduced junctional permeability could also be demonstrated by simultaneous injection of dye into two cells, one on either side of the segment border (Fig. 23). This was done in another preparation placed in M2, with LRB injected simultaneously into cells in adjacent segments. At 20 seconds of injection, the spread of LRB revealed a narrow strip of cells lying just posterior to the segment border that were slow to receive the dye, despite the high concentrations of dye potentially able to enter from either side. Note that under these

Figure 23

The cell-to-cell spread of LRB injected into a cell on each side of the border simultaneously outlines a border strip of cells slow to receive the dye. The reduced and variable permeability of these cells may explain how molecular interactions between compartments are limited. Arrowheads mark the position of the segment border. A, anterior segment; P, posterior segment. Scale bar, 10 μm.

A. The spread of LRB was photographed between 20 and 30 s of continuous injection. This preparation is in M2, and the border strip of cells only partially restricted the segment-to-segment spread of dye. While dye spread extensively among the cells in each segment, and is in high concentration to either side of the segment border, it was retarded sufficiently to outline the border cells.

B. Outlines of the cells in A drawn from the fluorescence and phase contrast images. The extent of dye spread (stippled) from the two injection sites outlines a single row of border cells.

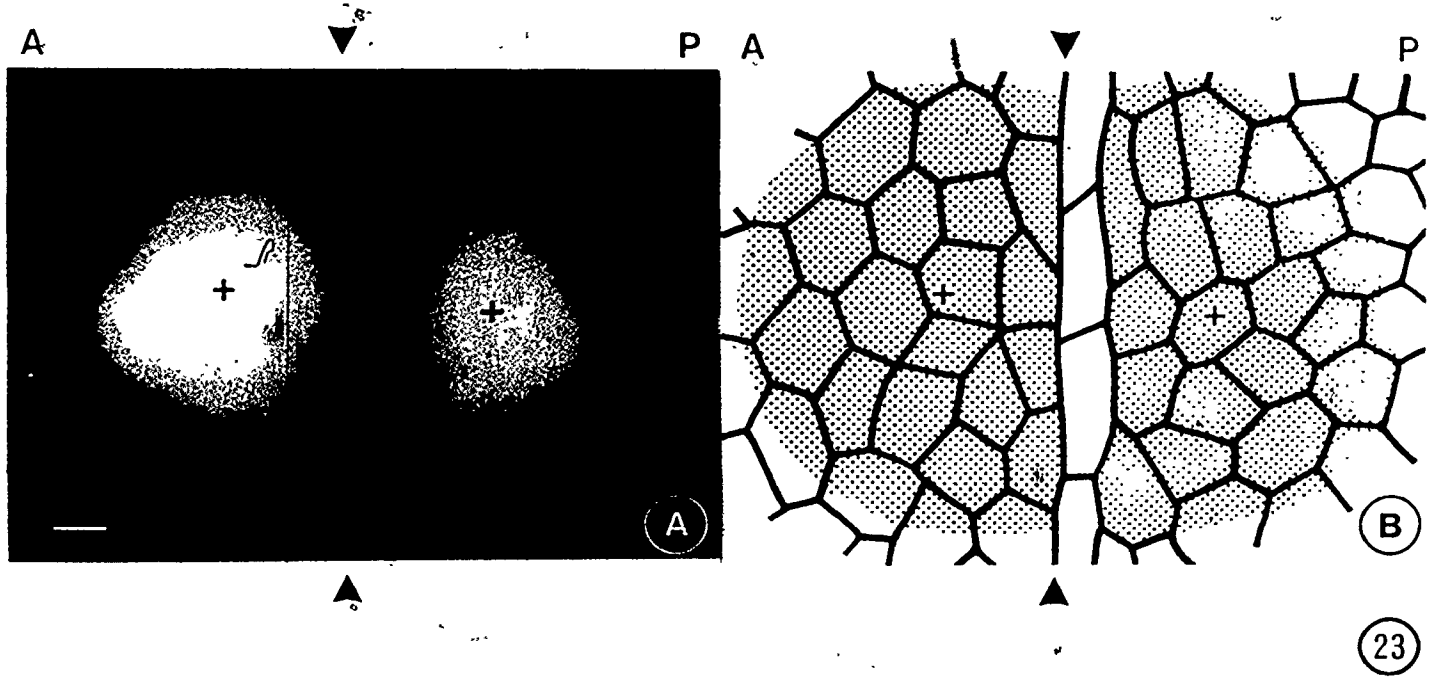

23

conditions, LRB was only partly prevented from segment-to-segment spread, being impeded here to a lesser degree than was CF (the smaller molecule) in Fig. 22. Subsequently, the continuing spread of dye 'filled in' the area of lower concentration, starting with the border cells lying between the source cells. By comparing the outlines of the cells with the initial extents of the dye spread (diagram in Fig. 23) the border strip of cells was again found to consist of a single row of cells. Dual injections of LRB or CF at different sites along the segment border, and in preparations from different animals, usually showed a single row of cells. Double rows were occasionally found at the lateral edges of the segment border.

3.3.2a Dye spreads symmetrically after injection into border cells.

Retardation of dye spreads after the injection of dye into cells on each side of the segment border served to locate the border cells. Attempts to inject dye into border cells identified in this way commonly resulted in the cells becoming uncoupled, with no dye spread. This response is very different from that seen when dye is injected into a non-border cell, and the sensitivity to dye injection suggests that these cells are poorly dye-coupled. When the cell did remain coupled long enough for detectable dye spread, the dye passed slowly and radially into the surrounding cells.

Fig. 24 shows an example of symmetrical spread of CF from a border cell into both segments, moving 2-3 cells radially. Combined phase contrast and fluorescence illumination shows the subsequently uncoupled source cell to be a single elongated cell lying along the segment border. The fluorescence of the LRB spreads that located the border cells was excluded by the CF filter set. Also, the border cell injections were performed in an area on the periphery of the LRB spreads, after most of that dye had diffused away. In some trials, the border cells were identified by position and shape alone. Those injections gave the same results, ruling out any influence of the preceding dual injections.

The slow dye spread and more usual spontaneous uncoupling suggest poorly coupled cells that, during iontophoresis, are unable to equilibrate by junctional transfer. When dye spread from a border cell, there was never preferential passage into the other border cells. There was no localization or unusual retention of dye within the border cell, and the overall appearance of the fluorescence was similar to that seen after the injection of a cell within the segment.

3.3.3 Cell and nuclear geometry alone cannot explain the asymmetry of dye spread at the segment border

Diagrams of the cell outlines in the intersegmental zone have shown that the differences in cell packing on

Figure 24

CF injected into border cell spreads symmetrically and, at best, slowly into neighbouring cells, suggesting uniform, reduced coupling of these cells with cells of the same segment as well as of the adjacent segment. Scale bar, 20 μm.

A. Fluorescence micrograph of CF spread during injection into a border cell. CF slowly passes into adjacent cells on all sides.

B. The extent of spread in A photographed 2 minutes after the 15 s injection. The extent of spread has remained symmetrical as it increased, and the intensity of fluorescence of the narrow, elongated source cell has decreased. Dye is slow to enter a cell in the posterior segment and has begun to image its outlines.

C. Combined phase contrast and fluorescence illumination of the field in A and B. Located by its fluorescence, the source cell of the dye spread is an elongated cell lying along the segment border. Comparison with B shows that dye passing from the border cell entered equally cells in both segments, as well as other border cells.

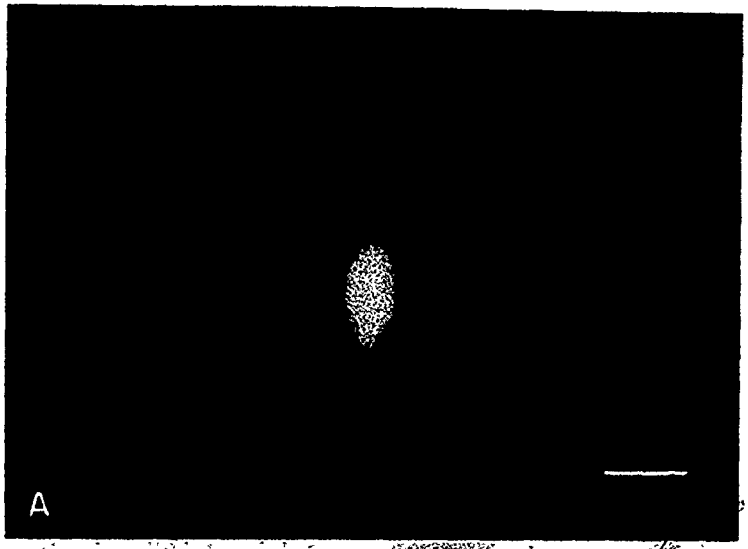
A


B

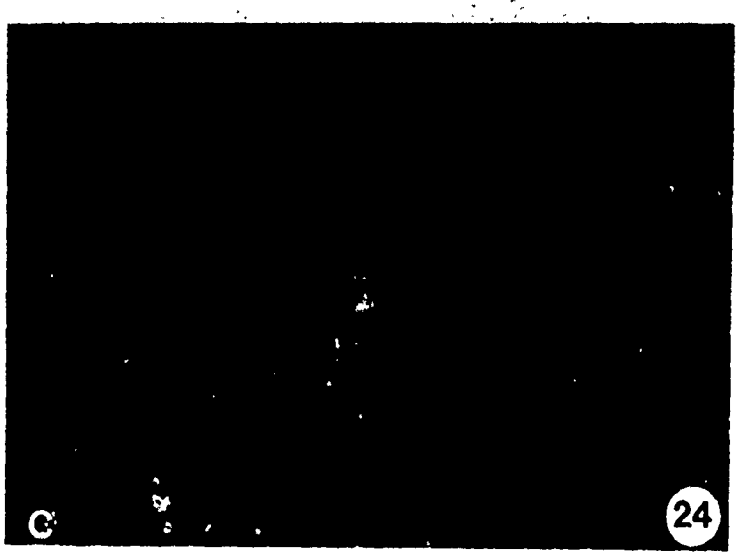
C
24

either side of the segment border were not so great as suggested by some phase contrast views, and that apparent increased cell packing posterior to the segment border was mostly due to the single row of narrow border cells. Cell packing was further investigated by nuclear staining of epidermal preparations, to compare the border cells with the regular epidermal cells on either side, and ensure that nuclear density and placement matched the interpretation of phase contrast views of cell outlines.

Epidermal preparations from 10 intermolt and 2 newly molted animals were stained with the specific nuclear fluorochrome Hoechst 33258. Examination of epifluorescence showed brighly fluorescent nuclei, with mitosis present in 3-6% of the cells in several preparations. Mitotic nuclei were more intensely fluorescent than interphase nuclei, but the overall degree of staining was variable for no identifiable reason. Fig. 25 shows the usual appearance of the nuclei. Within the segment, they are round to slightly oval, and become more uniformly oval in the vicinity of the segment border. While a degree of increased nuclear packing marked the border area, in most cases the border cells could not be specifically identified, as in Fig. 25B. In some areas, a few oval nuclei with long axes aligned formed a row among the randomly oriented nuclei that suggested the location of the border cells, and this was confirmed by phase contrast. There were no other identifying characteristics, and no mitotic activity was seen.

Figure 25

Preparations stained with the nuclear fluorochrome Hoechst 33258 show that the appearance and spacing of nuclei at the segment border are similar to that elsewhere. Arrowheads above and beneath each figure mark the segment border. Scale bar in A, 20 um; in B, 10 μm.

A. Fluorescence micrograph of Hoechst stained epidermis. In the intersegmental region, the position of the border cells cannot easily be identified. The dashed line indicates the segment border (where it could be located precisely, with the aid of phase contrast), and the nuclei of border cells immediately posterior to it appear similar to those within the segment. In some parts of other preparations, lateral alignment was slightly more distinct. Mitosis, seen here at various stages in 12 cells or cell pairs, was never seen in border cells. The variation in intensity of staining is an artefact that may result during fixation.

B. Stained nuclei in the intersegmental region of a preparation from a younger intermolt animal. Border cell nuclei are not distinguishable from those of neighbouring cells within each segment.

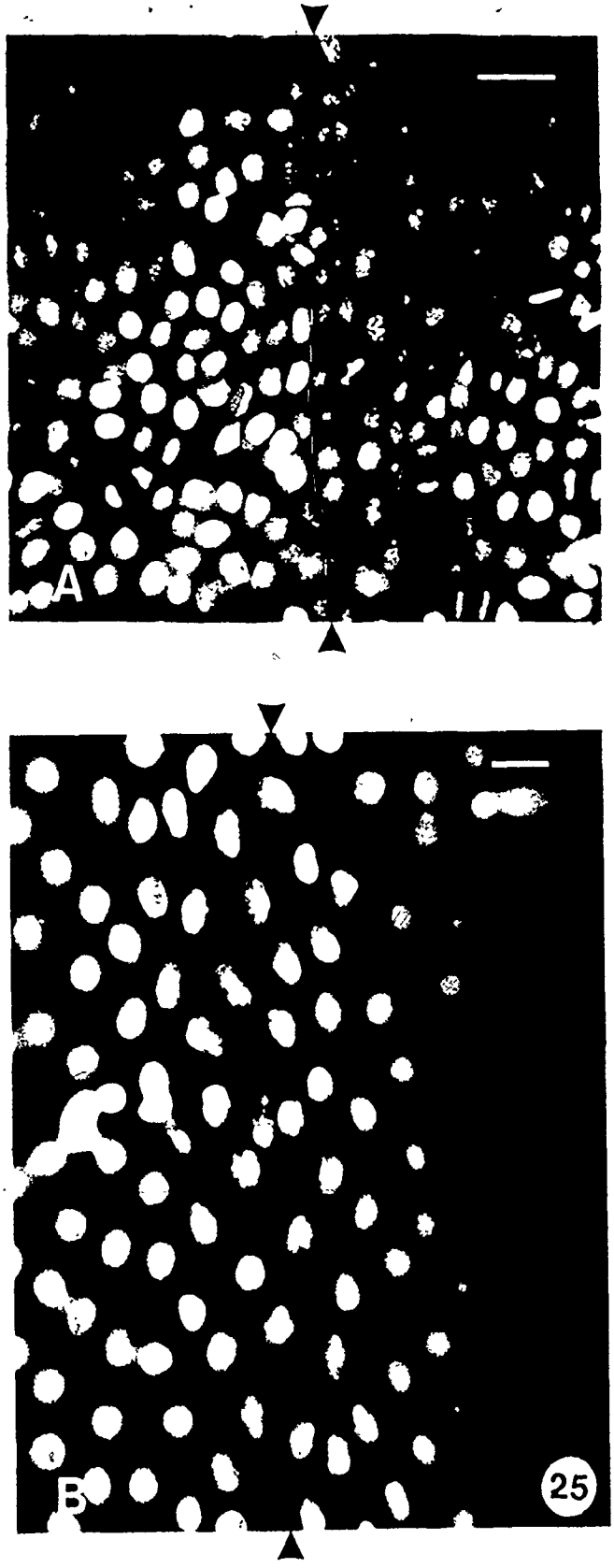
A
B
25

The appearance of epidermal nuclei was also examined on preparations stained by the Feulgen reaction (results not shown). As with Hoechst 33258 staining, there was increased packing but no other changes in the nuclei at the segment border, and border cells could sometimes be discerned as a single row of laterally aligned oval nuclei.

In typical preparations, nuclear diameters were measured with an ocular micrometer and oil immersion (100X) objective. The nuclei of identified border cells were 7.9 +/-1.0 μm by 5.0 +/- μm (n=10), with the major axis aligned laterally. In comparison, the nuclei in the centre of the segment were only slightly oval, measuring 6.5 +/- 0.8 μm by 5.4 +/- 0.7 μm (20), similarly aligned laterally. The cell density was greater posterior to the segment border: the average density there was 11,700 cells/mm^2 (6) compared to 9300 cells/mm^2 (6) anterior to the segment border. The average cell density in the middle of the segment was 9400 cells/mm^2 (5).

Therefore, changes in cell shape and density are localized to the anterior margin of the segment, and do not seem to be part of a gradual change along the segment. Complete cell outlines could be seen around each of the nuclei, matching the appearance of the border cells identified by their reduced junctional permeability. Nuclear staining does not suggest that the border cells are different from the epidermal cells, and it may that their unique appearance results from constraint of their position alone.

3.3.4 The culture medium affects intersegmental dye passage by altering border cell coupling

Epidermal preparations in different culture media showed differing degrees of segment-to-segment dye coupling. This was a characteristic of the medium, but was independent of its ability to support cell survival. The media were compared on the basis of the proportion of the major ions and osmolarity, and then contrasted with the available information on the composition of haemolymph (Table 5). Some major differences suggested a possible explanation for the variable results *in vitro*.

The concentrations in bug haemolymph of the two major monovalent cations, Na and K were matched by medium 3, in which intersegmental dye passage was the most rapid. However, the Na/K ratio and concentrations were widely different in the other media. While M3 also matched the Ca and Mg concentrations in bug haemolymph, so making it a good approximation to haemolymph in all four ions, there was no relation of either the concentration or proportion of Ca or Mg with cell coupling.

The osmolarity of bug haemolymph from 8 stage IV nymphs was 400 +/- 22 mOsm. The media unable to support the cells for 24 hours *in vitro* had osmolarities only half this, while the osmotic pressure of M4 was a good match at 423 mOsm. This suggested that cell survival in culture was contingent upon an adequate tonicity, but that intersegmental coupling

TABLE V: Comparison of composition of haemolymph of Oncopeltus and culture media.

Ion Content (mM)	Medium				Haemolymph
	M1	M2	M3	M4	
Na	137	49	44	59	35+
K	6	1	44	105	21+
Ca	1	<1	8	19	5+-7#
Mg	1	<1	23	21	26#
Osmolarity* (mOsm)	250	257	264	423	400

\+ (Mullen, 1957)
\# (Clark and Craig, 1953)
* Experimentally determined by freezing point depression

was independently controlled by the Na and K level.

To test this, two saline solutions, S3 and S4 were made that had the Na and K levels and osmolarity of media 3 and 4. They were composed only of Na, K, Ca, Mg, Cl and sucrose, in deionized distilled water with 10% foetal calf serum, and buffered to pH 6.7 with 10 mM PIPES. Ca and Mg levels appeared to have no effect on either junctional coupling or cell survival, and so were kept at the appropriate level rather than at an equal, intermediate level.

If the salines could reproduce the level of coupling seen with the corresponding media, then the number of factors in the complex media that might affect or even define the permeability would be reduced to the Na/K balance and possibly the osmolarity. Further testing could then separate these. Showing that the Na/K balance of the bathing solution could regulate the dye permeability of the segment border would allow an estimation through the haemolymph level of the extent of intersegmental coupling in vivo.

However, results of dye injections in preparations immersed in S3 and S4 were not similar to those seen with M3 and M4.

Epidermal preparations from intermolt animals were dissected directly into each of the two salines, and between 5 and 35 minutes later, dye spread between segments was tested by injecting CF into cells near the segment border.

During this time, the appearance of the epidermis in the 2 salines was similar to that seen in the media, and as in the media, gave no indication of the extent of dye coupling.

Throughout this period in saline S4, CF passed rapidly across the segment border to the adjacent segment. This was photographed at 30 minutes, and Fig. 26A shows that there is little retardation to dye passage, although dye has backed up against the segment border sufficiently to indicate its position. Fluorescence is visible within cells over the segment border at every point along it and directly opposite the source, is detectable in 3 cells beyond the single border cell. This rate of intersegmental dye spread is unlike that seen in the analogous medium M4, but is typical of the accelerated rate seen in medium 3.

However, initial injection of CF into epidermis in S2 showed distinct retardation of the dye at the segment border, with gradual intersegmental spread. This was photographed at 11 minutes after dissection (Fig. 26C). The impedance to intersegmental dye spread increased after this and dye passage to the adjacent segment was not detectable at 30 minutes (Fig. 26E).

In Fig. 26E & F, the segment border can be placed by cell shape and appearance. Just posterior to the segment border and opposite the source cell, a row of 3 narrow border cells has a small amount of dye. Only 2 cells removed from the source, they have fluorescence equal to

Figure 26

Salines that resemble media 3 and 4, and so are principally different in Na/K content (see text), nonetheless cannot duplicate their effects on intersegmental coupling. The composition of the medium, or of the haemolymph *in vivo*, may be a subtle control of intersegmental coupling. Left, fluorescence micrographs of the spread of CF; right, the phase contrast appearance. Arrowheads indicate the segment border. Scale bar, 20 μm.

A. The spread of CF in a preparation at 30 min in S4, a saline resembling M4. Dye passage across the border is relatively rapid, more so than seen in M4.

B. Phase contrast appearance of A. Elongated border cells can be distinguished from the more regular cells to either side.

C. CF injected posterior to the segment border in a preparation at 11 min in S3, a saline resembling M3. The dye has banked up against the border cells but passes over at the moderate rate typically seen after dissection into any of the media.

D. Phase contrast appearance of C.

E. A record of the spread of CF in the same preparation as C shows that intersegmental spread has become undetectable by 30 min in S3. Instead of the rapid spread between segments seen in M3, the permeability of

the border cells is reduced so much that dye has entered only the border cells closest to the source and is not visible in the adjacent cells within the next segment.

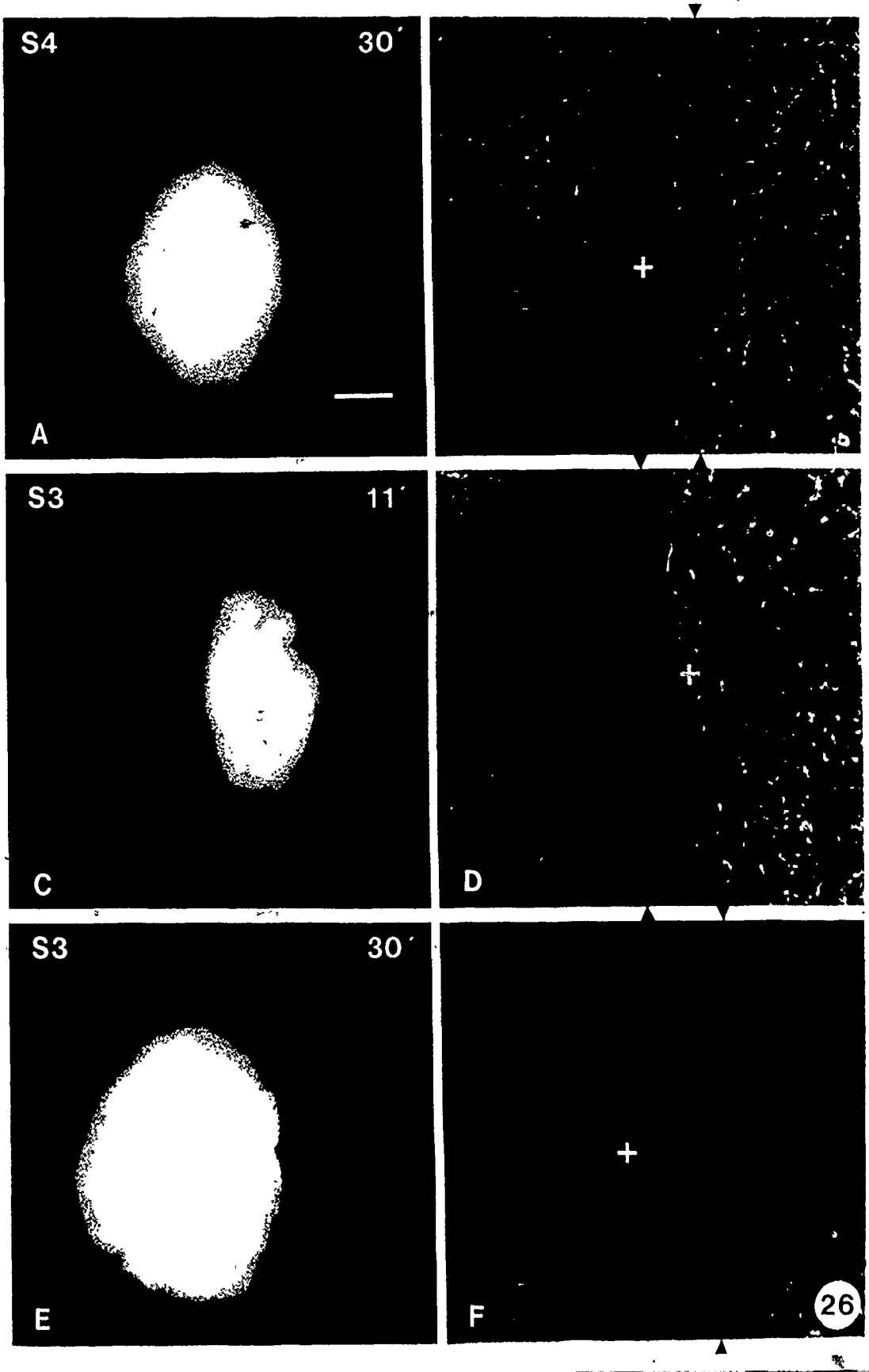
S4
30´
A
S3
11´
C
D
S3
30´
E
F
26

that seen in cells within the segment that are 4-5 cells removed. It appears that the permeability of the border cells is reduced so greatly the dye has built up to detectable levels only in those cells closest to the source. Elsewhere, the border cells are without fluorescence and appear as an absolute barrier.

Dye that enters the border cells seems to leave at the same slow rate: the distal margins of the border cells are imaged since the small amount of dye within the cells is impeded from leaving. Dual injections showed earlier that dye was slow to enter the border cells at each interface with the next segment. Here, dye leaves the border cells to the next segment, since their fluorescence increased only slightly with time. However, it is passing into cells that have normal coupling and there, can diffuse away more rapidly than the supply is entering - therefore those cells are not imaged.

At 2 minutes after the end of the injection in Fig. 26E, dye had spread over a wide area within the segment, into 8-10 cell orders from the source, but the intensity of the border cells had increased very little. However, 7 border cells were visible along the posterior face of the dye spread, and beyond them, the outlines of a single row of 3 of the first cells of the next segment were just discernible.

The analogy of a waterfall may be used to explain this

appearance. The border cells are like a pool of water between serial waterfalls. When the flow rate is reduced, water is slowed to form the pool, and on leaving is rapidly dispersed. In this way, border cells are seen when intersegmental dye spread is low, but are overwhelmed and not easily resolved when flow in and out is more rapid.

The electrical coupling of the preparations in the two different salines was meaured during the time period in which the dye injections were made. In S4, which showed the stable level of rapid dye passage between segments, intercellular resistance (r_i) was also stable for 34 minutes after dissection, at 5.6 +/- 0.5 x $10^5\Omega$ (3 animals), and the membrane potential was 42 +/- 5 mV (18) over the same period. In S3, the electrical coupling, like the dye permeability, was unstable. The average r_i over the first 20 minutes in culture was 4.2 +/- 0.2 x $10^5\Omega$ (5) but then increased to 7.2 and 12.4 x $10^5\Omega$ at 22 and 26 minutes respectively, in 2 animals. The membrane potential averaged 44 +/- 10 mV (43) but showed progressive decline.

Therefore, dye permeability between segments and electrical coupling within the segment appeared to change in parallel, either both remaining stable, or both shifting toward lower channel permeability.

The saline solutions did not reproduce the coupling levels characteristic of their parent media, preventing clear conclusions about ion balance and intersegmental

coupling. However, this experiment reinforced the conclusions that conditions in vitro can cause intersegmental coupling to vary widely, without apparent effect on dye coupling within the segment. That intersegmental coupling is related to the Na/K balance is supported by the different coupling levels seen with saline solutions that differed only in this factor and osmolarity. Since a role for osmolarity in coupling was not seen in the effects of the various media, it is still possible that the Na/K balance can modulate coupling but in an unpredictable manner.

3.3.5 Electrical coupling between segments remains strong although dye coupling is reduced

The apparent rates of dye spread within the segment were equal on either side of the border, that is, equal at the anterior and posterior margins of a given segment. The relatively slower spread of dye across the segment border was due to the reduced coupling of a strip of border cells. The rapid change in the rate of intersegmental dye spread over a wide range suggested modulation of the permeability of the channels, rather than of channel number, in the junctional membrane of border cells. Either only the border cells could perceive and react to some aspect of the culture medium, or they were especially sensitive to some general factor. In the previous chapter, work on beetle epidermis showed that change in electrical coupling and dye coupling

were related. Therefore, there should be a correlate in electrical coupling to the impedance to intersegmental movement of dye.

The initial investigation compared r_i within and between segments. This measure of electrical coupling is determined from the size of the electrotonic potentials at increasing distance from the polarizing electrode, conveniently along the diameter of the 440 μm field of view. It was expected that reduced intersegmental electrical coupling would appear as a disproportional decrease in the magnitude of the electrotonic potentials measured beyond the segment border.

In the intersegmental zone of a preparation placed in M3, r_i was determined first along a line crossing the segment border at 90°, and then within the posterior segment, giving similar values of 4.9 and 4.7 x $10^5\Omega$ respectively (Fig. 27, lines A & B). Next, r_i was determined within the anterior segment, and then along the strip of elongated cells just posterior to the segment border itself (Fig. 27, lines C&D). Again, the r_i values were similar at 4.1 and 4.2 x $10^5\Omega$, slightly less than the previous values probably due to instablility of the cells in culture causing gradual change in the coupling level. The extent of electrical coupling on either side of the segment border is identical.

In Fig. 27A, the border corresponds to an inter-electrode distance of 220 μm. Beyond the usual variation,

Figure 27

In the intersegmental region, the spatial decay of electrical coupling within and between segments appears equal. This was measured along the lines shown in the upper schematic diagram: A, r_i across the segment border was $4.9 \times 10^5 \Omega$; B and C, within the anterior ($4.7 \times 10^5 \Omega$) and posterior segment ($4.1 \times 10^5 \Omega$); D, along the elongated cells at the segment border ($4.2 \times 10^5 \Omega$). In A, the segment border is at 220 μm (arrowhead), and there is no evidence for a discontinuity.

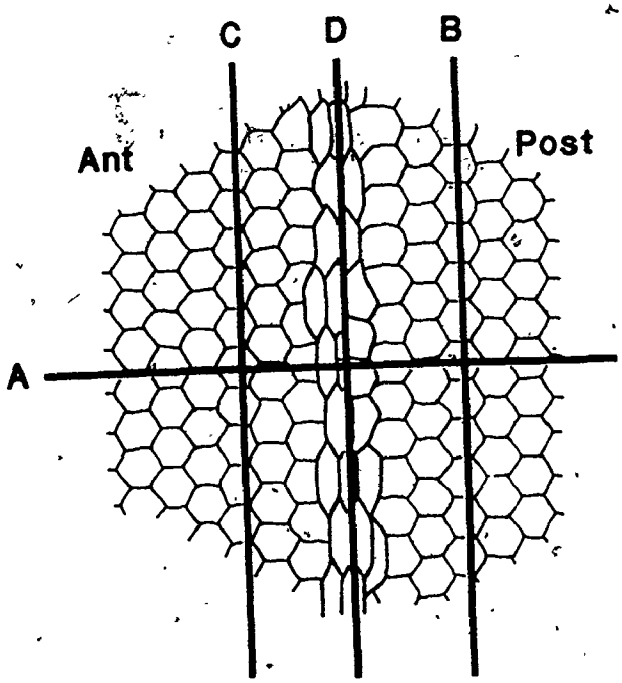
C
D
B
Ant
Post
A

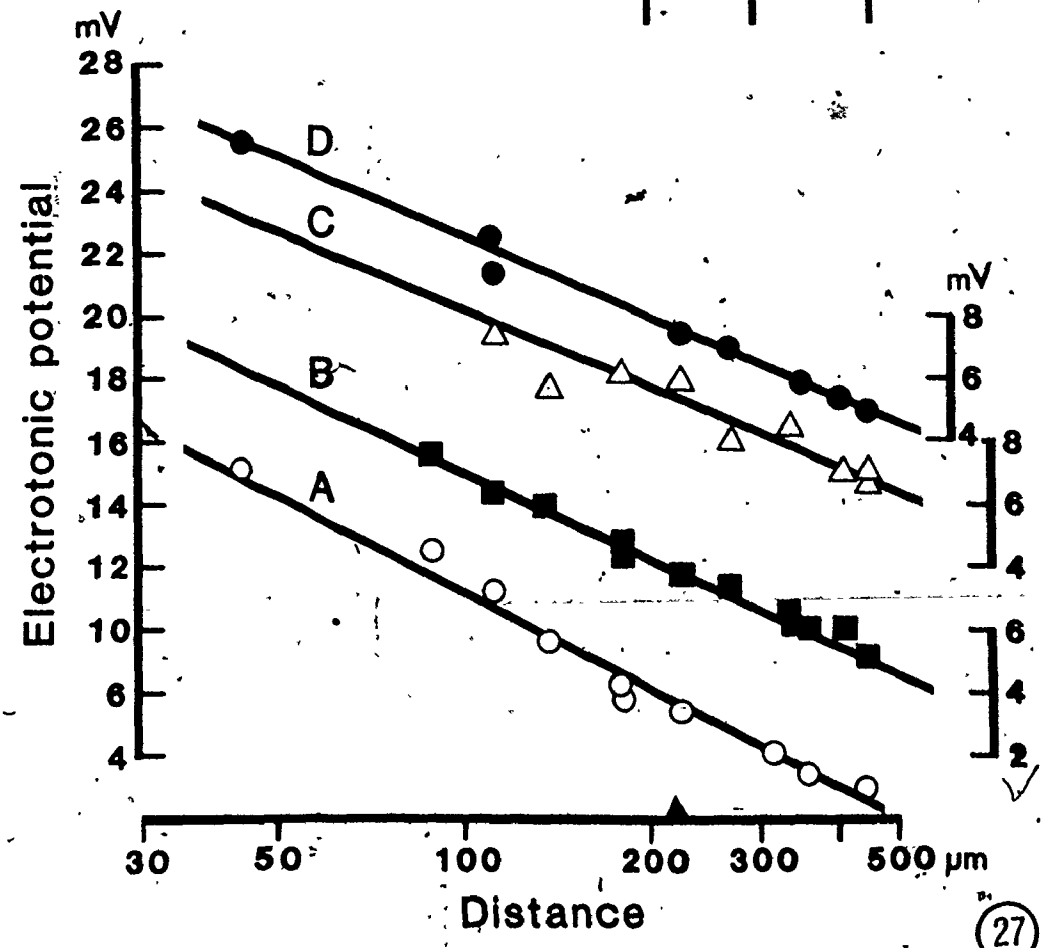
mV
28
26
24
22
20
18
16
14
12
10
6
4
Electrotonic potential
D
C
B
A
mV
8
6
4
8
6
4
6
4
2
30
50
100
200
300
500 µm
Distance

(27)

there is no step or discontinuity in the linear decay of voltage with distance to suggest that the border cells posed a greater electrical resistance to current flow than their neighbours.

In the exponential relationship of electrotonic voltage with interelectrode distance, the initially rapid drop in voltage changes to a gradual decrease as distance increases. This means that equal voltage changes occur over increasingly large distances on a linear semi-log plot. Therefore, r_i was determined along a line between segments with the border placed at a smaller interelectrode distance, 110 μm or 0.25 of the field width, which increased the sensitivity to a discontinuity although increasing the scatter of points. Since a resistance 'step' at the border might develop or become more pronounced with increased intercellular resistance, medium 4 was used in which the r_i ranged between 5 and 8 x $10^5\Omega$ for up to 50 minutes after dissection, higher than the values of 3 to 5 x $10^5\Omega$ seen with M3.

In the 12 segment borders from 6 animals examined, no discontinuities were seen. For one preparation between 26 and 31 minutes in culture, the electrotonic voltage was determined at 18 distances (Fig. 28). A line with r_i = 7.4 x $10^5\Omega$ was drawn that fit all the points reasonably well. For comparison, a line with r_i = 3.4 x $10^5\Omega$ was obtained similarly from a preparation in M3.

Figure 28

Electrical coupling may be isotropic across the border but scatter in the points determining the line of spatial decay could prevent the detection of a small resistance 'step'. The segment border was placed at 110 um, since the technique is more sensitive at shorter interelectrode distances. Measured at 16 min in M3, r_i was $3.4 \times 10^5\Omega$ (closed circles), and in another preparation in M4, was $7.4 \times 10^5\Omega$ at 31 min (open circles). There are no major steps, but variation of the points about the line at 110 um would obscure a small discontinuity. Note that an apparent step at the segment border in the lower line is countered by variation in the opposite direction in the upper line.

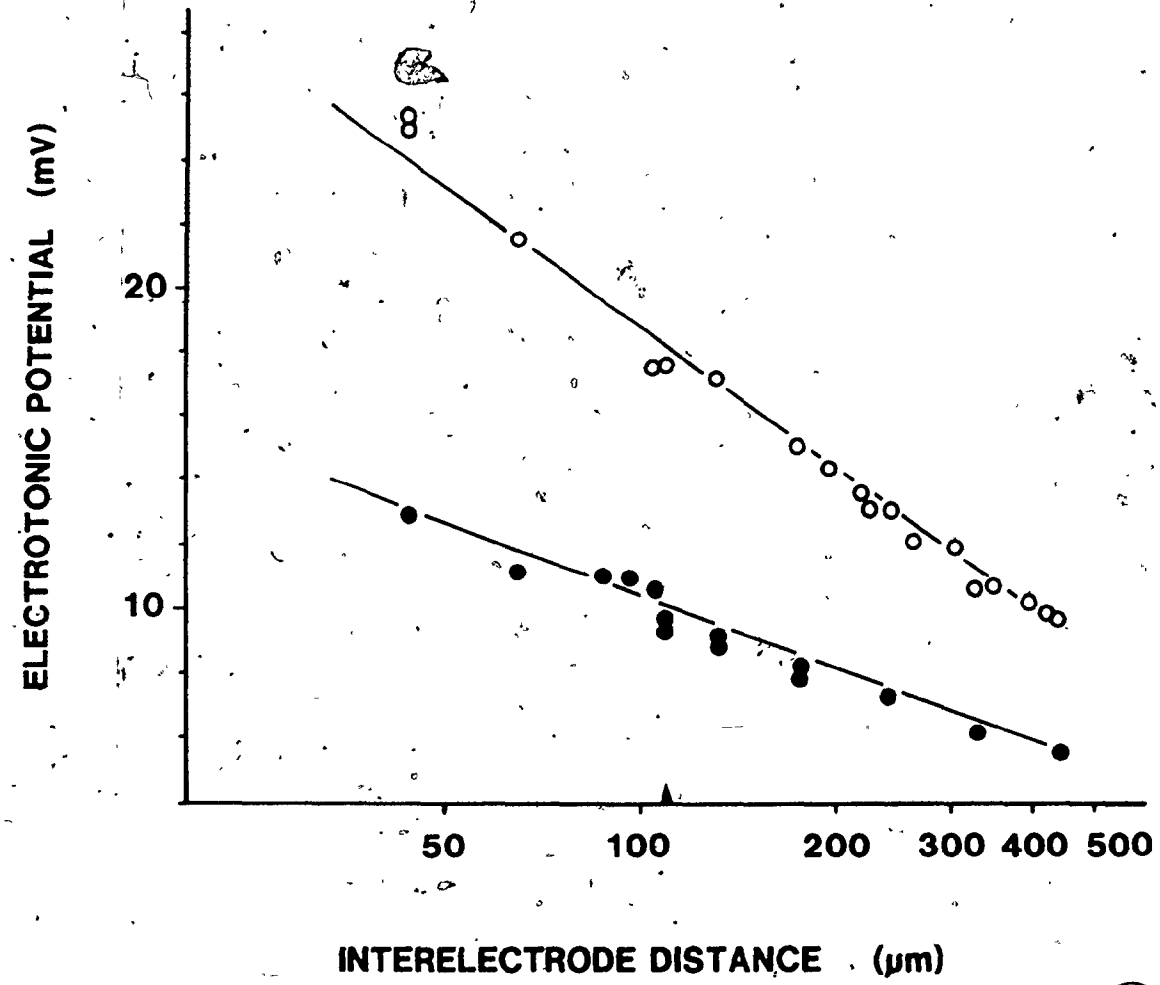
ELECTROTONIC POTENTIAL (mV)
20
10
50
100
200
300
400
500
INTERELECTRODE DISTANCE (µm)

(28)

In Fig. 28, scatter of the points measured just anterior to the segment border causes them to fall above the line in one case and below it in the other. This shows that a small discontinuity, appearing as only a slight deviation in electrotonic potential from the expected (i.e., fitting the linear plot) will be lost in the variation. One cause of variation is the increased cell density at the segment border, which would cause scatter of the points about the line in the area where precision was most needed. To compensate for this, the cell field was photographed and, from the cell outlines, the interelectrode distances were converted into numbers of cells. Sometimes, 1 mM CF was added to the polarizing electrode, which marked cell position during current injection. In the 5 experiments performed this way, the fit of some points to the line was improved in the border region.

This technique was used in Fig. 29, which shows an unusually high r_i of $18.4 \times 10^5 \Omega$ at 40 minutes in culture, that was due to an early decrease in intercellular coupling. Recordings were made from 2 border cells and 10 regular cells. Border cells were identified by shape, as well as by location, which could be verified after uncoupling during the injection had caused them to swell and stand out from their neighbours. The degree of electrical coupling of the border cells, judged by the close fit to the line of voltage decay, was equal to that of the other cells

Figure 29

Despite measures taken to compensate for variation, and to increase accuracy, the standard procedure for quantification of electrical coupling cannot detect a step in intersegmental electrical coupling that would correspond to the reduced dye permeability of border cells. The magnitude of a step might increase with raised intercellular resistance of the epidermal sheet, and in a preparation at 40 min in M4, an r_i of 18.4 x $10^5\Omega$ was measured across the segment border. There is no detectable step, despite compensation for non-uniform cell packing in the intersegmental region by measuring the cell number rather than distance between electrodes. In the diagram on the lower axis, stippled cells are anterior; the arrowhead marks the position of the segment border. Open circles are the electrotonic potentials measured within border cells.

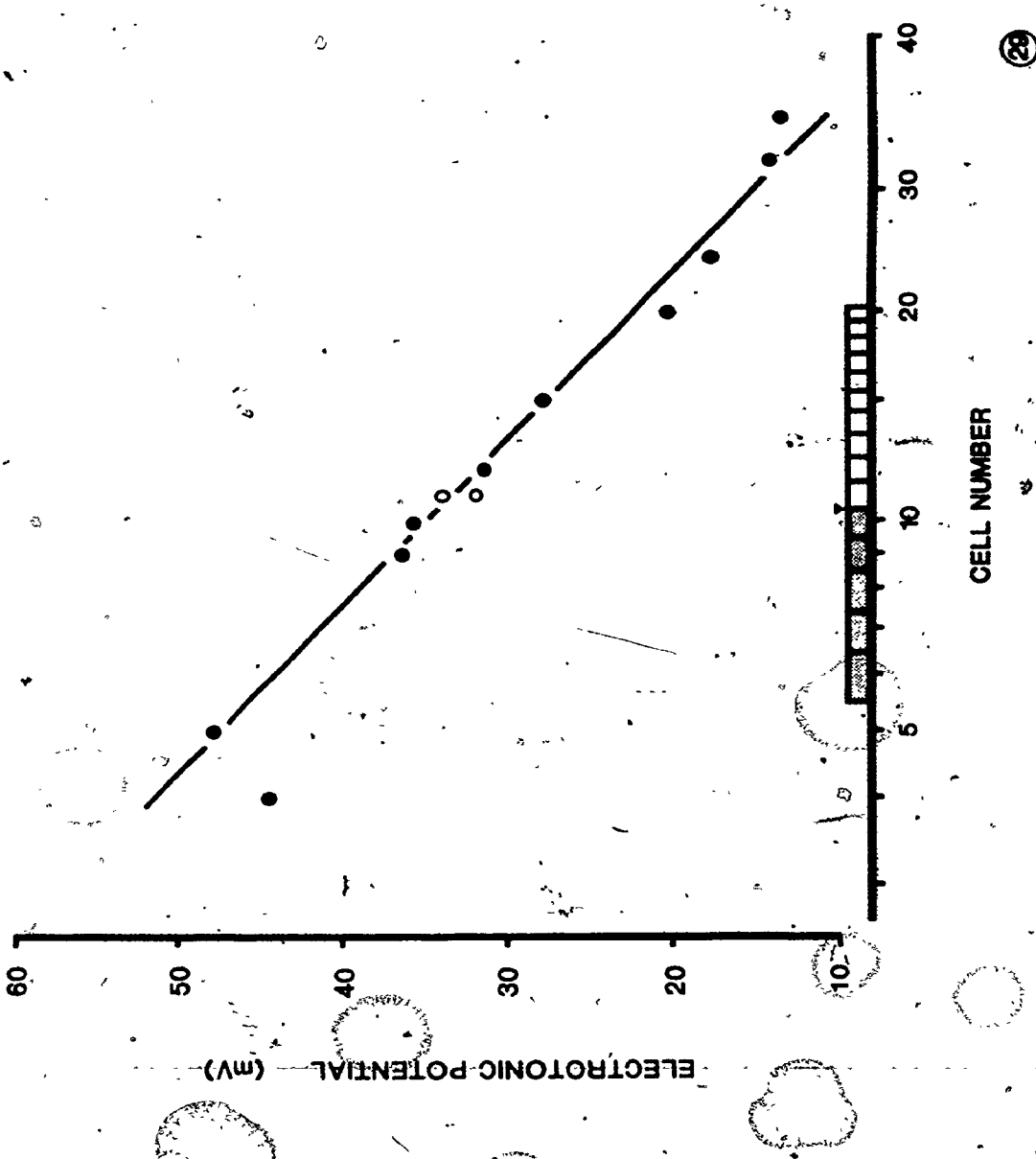
ELECTROTONIC POTENTIAL (mV)
60
50
40
30
20
10
CELL NUMBER
5
10
20
30
40
28

tested in each segment.

Obviously, there was no major discontinuity in electrical coupling between segments. Results with all points indicating a single unambiguous line on either side of the border are necessary to indicate whether the border cells formed part of a monotonic or discontinuous voltage decay. These were difficult to obtain, since the epidermis was not amenable to this type of investigation, with the thin, flexible monolayer shifting under the microelectrode and impaled cells rapidly losing their membrane potential.

3.3.5a A cell-by-cell analysis shows that border cells have an increased electrical resistance when dye permeability is minimized.

In the last modification of the technique for quantification of current spread, a cell-by-cell analysis simultaneously compared the radial spread of current over the segment border to the spread within the same segment. In preparations selected for clarity of cell outlines, an electrode was placed in a cell one cell removed from the segment border. Without relocating that electrode, the electrotonic potentials were measured in the neighbouring cells along two radii: (1) moving away from the segment border among the regular cells of the same segment, and (2)

towards the segment border, within the border cell and into the next segment. After measuring the electrotonic potentials, the degree of coupling of two cells equally far removed from the source cell could be compared. Thus, the electrical resistance of the border-cell could be compared to another cell within the segment that was also one cell distant from the source, and the first cell beyond the segment border compared to a cell two cells removed within the segment. As before, this analysis was used on preparations in either M3 or M4, for less than 60 minutes.

It was quite difficult to obtain satisfactory recordings, since the recording electrode was required to hold a stable membrane potential in a cell subject to slight motion from nearby cells being impaled by the other electrode, and all results for one experiment had to come from a single reference cell. Judging by appearance, injected cells generally remained coupled after the electrode was removed. The likelihood of this was increased by using the shortest possible penetration and careful removal of the electrode while the membrane potential was unchanged. The cells closer to the source were impaled last, so that any cells that did uncouple were not left in the area between the electrodes to alter the spread of current in subsequent measurements. The standard injection current of 60 nA was used, giving large electrotonic potentials at these small distances.

Fig. 30 shows the results from 2 preparations in M3 or M4 for 30 minutes. In these, as in other measurements of cell-to-cell current spread under these conditions, there was no disproportional drop in voltage within the border cells, or between cells separated by a border cell. In each case, the passage of current to a border cell or to a cell separated by a border cell from the source was the same as that among cells within the segment. The r_i was subsequently measured and was $3.4 \times 10^5\Omega$ (M3) and $7.0 \times 10^5\Omega$ (M4).

By 55-60 minutes in culture in any of media 1-3, the intersegmental dye coupling decreased or was lost, and subsequent electrical measurements showed increased r_i values and unstable cells. Therefore, experiments analysing the cell-by-cell spread of current using M3 could not be prolonged past 50-60 minutes. However, the cells in M4 remained coupled and reasonably stable for 60-120 minutes, although the coupling was reduced over that found in the first 60 minute period. This appeared to be mainly a reaction to the culture medium, and to a lesser extent to the duration of experimentation in room conditions, since preparations placed in the incubator after dissection and examined at 60 minutes showed similar behaviour.

Preparations from 4 animals were examined between 60 and 120 minutes after dissection into M4. During this period, the average membrane potential (E) was 39 +/- 6 mV

Figure 30

A cell-to-cell measurement of the electrotonic voltages in cells at the segment border shows that under normal conditions, the junctional resistance of border cells is not different from that of the adjacent cells. Current was injected into a cell one cell away from the segment border (see inset diagram) and the electrotonic voltage measured in the adjacent ("1" or first order), the border cell (B.C. or a 2nd order cell) and succeeding cell orders within the next segment at 30 min in M3 (open circles) or 30 min in M4 (open squares). Then, measurements were made in cells of equivalent order within the segment (closed circles; closed squares). Since these measurements coincide, the resistance of a border cell to current spread is not different from that of a cell within the segment, and intersegmental current spread appears isotropic. Note that, for simplicity, lines connect the points and do not show a realistic voltage profile, where voltage is constant within a cell and drops at the junctional interface.

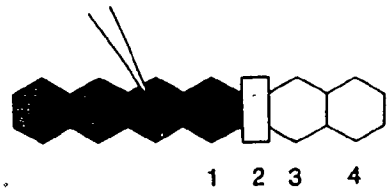
1 2 3 4

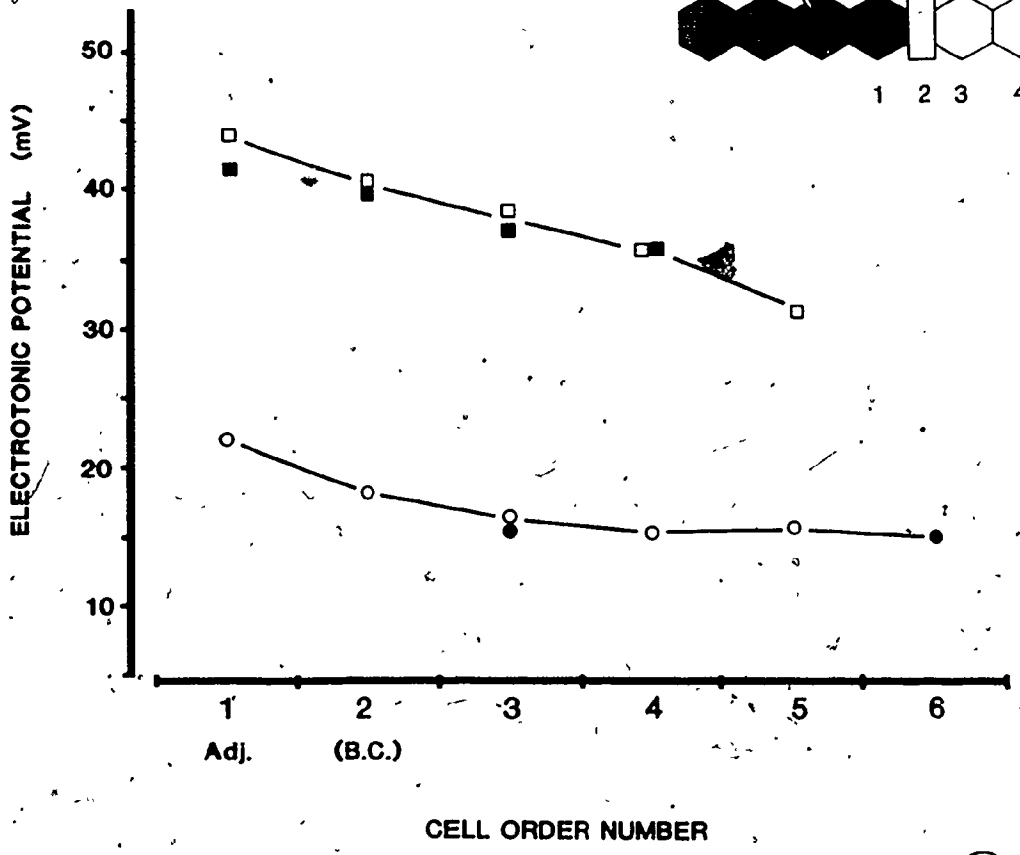
ELECTROTONIC POTENTIAL (mV)
50
40
30
20
10
1
Adj.
2
(B.C.)
3
4
5
6
CELL ORDER NUMBER

(30)

(20). Comparison of the spread of current across the border with the control spread within the segment showed that the electrotonic potentials within the border cells were reduced compared with those in equivalent cells within the segment and caused a drop in the current passage over the segment border that was not seen in the spread within the segment (Fig. 31). The border cells constituted a greater resistance to current entry into the next segment than would a normal cell. In the next segment, the now-lower voltage decreased in a fashion parallel to that seen in the control segment. After the measurements within the segment were made for the control spread, recordings were made from another border cell and the cell beyond it that confirmed those initial values. Considered alone, the electrotonic potentials measured in cells across the border show a step decrease that was not seen earlier in Fig. 30. Comparison of this with the control spread away from the border confirms that the spread is not isotropic.

Previous results had shown that dye spread into and out of the border cell strip was equally retarded, and suggested that uniform coupling properties existed around the perimeter of the border cells. The nature of the resistance step also suggests that a border cell has reduced electrical coupling with both the adjacent cells in each segment, since the electrotonic voltage dropped more sharply between the adjacent cell and the border cell, and between the border

Figure 31

There is an electrical correlate to the reduced dye permeability of border cells: under circumstances that minimize intersegmental dye passage, a border cell also constitutes a greater resistance to current passage than neighbouring cells within the segment. At 100 min in M4, a cell-by-cell analysis (inset diagram) was used to measure the electrotonic voltage in adjacent (first order) cells, border cells (second order) and succeeding cell orders in the adjoining segment (▲). This shows a greater drop in voltage between the adjacent and border cell, and between the border cell and third order cell, (dashed lines) than between successive cells within the segment (solid lines). Subsequent measurements of the electrotonic voltage in the equivalent order cells within the segment (△) showed no such drop. Finally, another measurement across the segment border confirmed the lower electrotonic potential in border cells and in the cell beyond it (▼). The r_i was $10 \times 10^5 \Omega$, a higher value than in Fig. 30. It seems that a sensitive analysis, with reduced electrical coupling, is necessary to show that border cells have a disproportionately higher junctional resistance and cause a discontinuity in electrical spread.

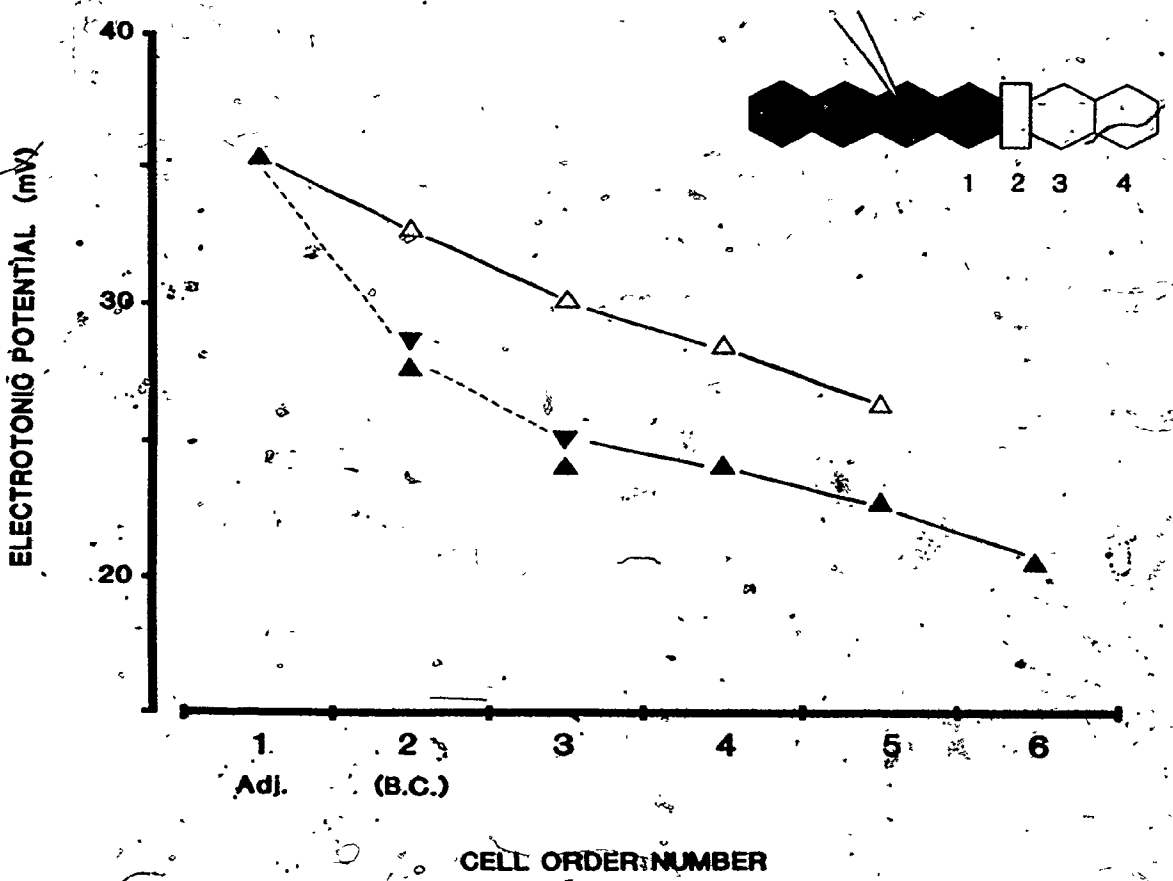
40
30
20
ELECTROTONIC POTENTIAL (mV)
1
2
3
4
5
6
Adj.
(B.C.)
CELL ORDER NUMBER
1 2 3 4

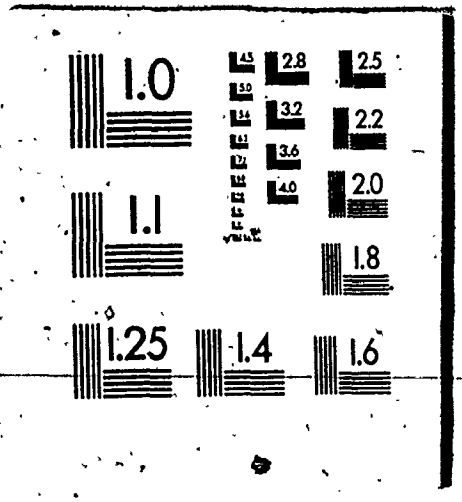

cell and the first segmental cell, than between two segmental cells (Fig. 31). That is, the step occurred between the cells on either side of the border cell, with the border cell occupying an intermediate position.

The magnitude of the resistance step was not great - in these preparations, the electrotonic potentials recorded from border cells ranged between 79 and 86% (average of 5 experiments was 83%) of that found in the equivalent cell within the segment.

Under these conditions, r_i could not be determined easily, but in two preparations, values of 8.5 and $8.8 \times 10^5 \Omega$ were found, which are likely minimum values for this period in culture. The r_i of the preparation in Fig. 31, which showed a detectable step, was roughly $10 \times 10^5 \Omega$ whereas the r_i of the preparation in Fig. 30 (with no step by the same technique) was $7.0 \times 10^5 \Omega$. For step detection, it appeared necesary (1) to generate large electrotonic potentials (2) in a region where maximum change in the electrotonic voltage occurred over each additional cell order and (3) under conditions of reduced electrical coupling.

3.3.6 Reduced intersegmental coupling can be reversed with molting hormone in vitro

The few cases where dye injection showed no retardation of dye spread across the segment border in epidermis freshly

dissected into any of the media occurred randomly and were never satisfactorily photographed. This was one extreme of the range of rates of intersegmental spread seen, but unlike the opposite extreme of absent coupling, this was not a response to experimental conditions, and appeared independent of them.

Possibly, animals at certain stages of development contain haemolymph that modified the extent of intersegmental coupling. However, dye injections into newly molted epidermis (<60 minutes after ecdysis) and into the epidermis of pharate V nymphs tested the level of intersegmental coupling at each end of the molt cycle but gave results appropriate to the medium used. In these cases, the dissection and subsequent manipulation of the flimsy cuticle tended to damage the underlying epidermis, but dye injections were always made in intact areas.

The insect developmental hormone 20-hydroxyecdysone (20-HE) increased electrical coupling in Tenebrio epidermis in vitro (Caveney and Blennerhassett, 1980). Since border cells appeared to be part of the epidermis, although characteristically different in some properties, this suggested that 20-HE might affect the coupling level between segments as well. Therefore, the effect of 20-HE on modulation of intersegmental coupling was tested by incubating trimmed epidermal preparations in M4 containing 10 µg/ml 20-HE and determining the spread of CF injected.

Preparations exposed to hormone responded to it with apolysis (the separation of the epidermis from its cuticle), which became noticeable by 12-15 hours and nearly complete by the end of 24 hour incubation period. This in itself made electrical measurement difficult, but in addition, the nature of the basal cell surface changed, and consistently caused irreversible blockage of the electrodes after penetration of a cell. Therefore, it is not known whether electrical coupling increased in response to hormone.

Initial tests showed that the dye spread in preparations incubated in M4 + 20-HE and examined in fresh M4 was similar to that seen in freshly dissected preparations. (4 trials in 2 animals; E = 38 +/- 3 mV; 12). This was also true for preparations incubated for the same time in M4 alone and tested in M4 (16 trials in 4 animals, E = 32 +/- 6 mV; 24).

One remaining question was explored: since freshly dissected preparations showed faster rates of intersegmental dye spread in M3 than in M4, was this difference maintained after this period in culture? Since preparations could not have been cultured in M3 for this long, some of those in M4 or M4 + 20-HE were placed in M3 and then tested. In preparations from 4 animals that had been switched from M4 to M3, 6 trials with CF and 8 trials with LRB resulted in impeded intersegmental dye spread resembling that seen in preparations freshly dissected into M3 (E = 30 +/- 5 mV; 10). However, switching preparations from M4 + 20-HE to M3

resulted in dye spread across the border with no apparent retardation.

Fig. 32 shows an example of unimpeded dye spread across the segment border from 2 different animals; in one preparation at 5 minutes in M3 after 15 hours in M4 + 20-HE and another after 16 hours exposure to hormone. In each case, there was radial symmetry of the extent and intensity of fluorescence. Individual border cells can be identified from phase contrast micrographs of the cell fields, and are as intensely fluorescent as regular cells that are an equal distance from the source.

In all, 29 trials of CF spread in 7 animals, and 9 trials of LRB in 3 of those, showed no detectable impedance to dye spread (14 segment borders from 7 animals; the average E was 24 +/- 6 mV; 49). Therefore, the state of minimal or absent retardation of dye seen naturally as a rare event can be duplicated <u>in vitro</u>, but only by the combination of these two treatments.

Figure 32

The functional permeability of border cells can be experimentally raised to the level of the surrounding cells. Preparations cultured in M4 with 10 ug/ml 20-hydroxyecdysone (20-HE) and tested in M3 showed no barrier to the intersegmental spread of CF. This duplicates the transient natural absence of a barrier to dye spread at the border, and suggests that intersegmental coupling may be regulated to permit the free exchange of molecules at certain times during development. Left, record of the fluorescence of CF; right, the phase contrast appearance. +, source cell. Scale bar, 20 μm.

A. CF injected anterior to the segment border in a preparation at 8 min in M3 after exposure to M4 + 20-HE for 15 hours. No asymmetry of spread can be seen, and unlike the rare natural occurrence, this appearance was stable in vitro.

B. Phase contrast appearance of A.

C. CF injected posterior to the segment border in a preparation at 6t min in M3 after exposure to M4 + 20-HE for 16 hours. Spreading symmetrically from the source, the appearance of the dye does not suggest the presence of a barrier in this preparation. Note that the fluorescence towards the edge of the spread appears uneven and slightly mottled. This was characteristic

of epidermis exposed to hormone for this time, as it began to loosen on the cuticle, but is not yet noticeable in A, a preparation from a different animal.

D. Phase contrast view of the cells in C.

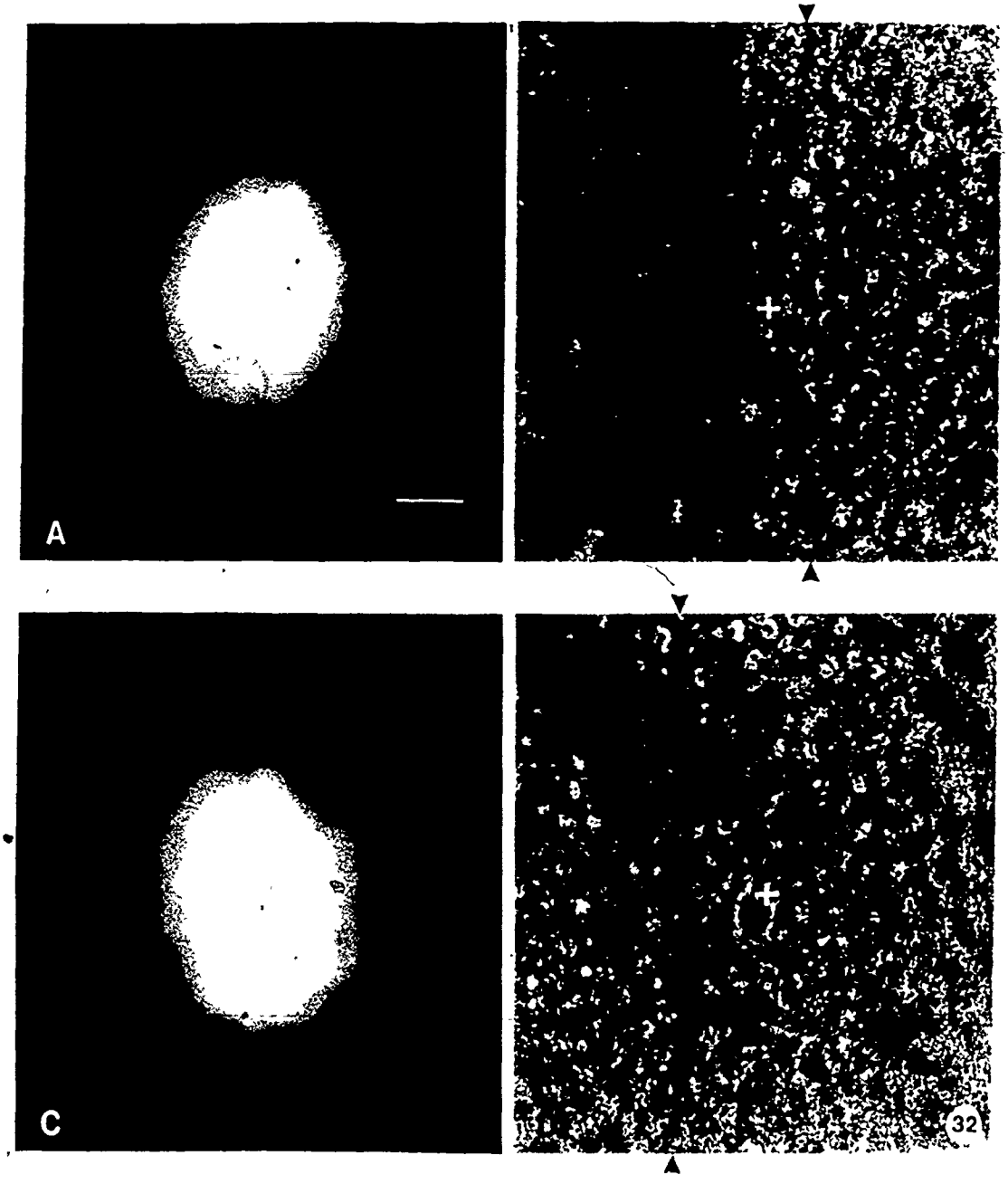
A
C
32

3.4 Discussion

3.4.1 Introduction

When segments are delineated, adjacent cells can become members of different cell groups, that will to a large extent, develop independently. This might result from the loss of intercellular communication between those neighbouring cells, and the restriction of transfer of developmentally relevant information. However, cells in adjacent segments are electrically coupled to each other across the segment border in Rhodnius (Warner and Lawrence, 1973) and in Tenebrio (Caveney, 1974).

It was therefore surprising that Warner and Lawrence (1982) reported an absence of dye coupling across the segment border in Oncopeltus - once electrical coupling was demonstrated, dye coupling would be expected to occur as well. In those experiments, dorsal abdominal integument of Oncopeltus was dissected into an unspecified medium, and Lucifer Yellow injected into cells near the segment border. In 27 of 30 cases, the dye failed to pass over the segment border, while spreading among cells of the same segment. This suggested that a cell at the border was normally coupled with the cells of its own segment, but had reduced or absent coupling with adjacent cells of the next segment (which were also normally coupled amongst themselves). Therefore, some intercellular junctions formed by a cell at the border must be different, or regulated to a different

level, than others in the same cell. This too was surprising since factors which regulate cell coupling, such as ions or electrical potential are assumed to be uniform within the cell.

Instead, results presented in this thesis have shown that there is a separate population of cells at the anterior margin of each segment that communicate less among themselves as well as with the cells of adjacent segments. Spatial selectivity in communication makes the segment a communication compartment: cells within the segment can communicate freely, but reduced coupling with border cells allows only limited interaction with cells of the adjacent segments. This may allow each segment to keep to its own developmental programme. Since modulation of the degree of selectivity can occur in vitro, it may do so naturally to permit the synchronization of developmental events that affect the whole animal.

3.4.2 Junctional permeability is asymmetrically regulated at the segment border

Spatial selectivity of coupling in the epidermis distinguished border cells from cells within the segment. Assuming that the anterior and posterior epidermal cells within the segment are equivalent, at least in coupling level, dye injection has tested the permeability of 3 different types of junctional interfaces formed by segmen-

tal and border cells - epidermal cell:epidermal cell, epidermal cell:border cell and border cell:border cell junctional interfaces. The results of dye injection into both cell types showed that both homotypic and heterotypic border cell junctions had equal permeability; that is, in the three combinations, any cell interface involving a border cell has the permeability of the border cell type.

Since all the junctions made by border cells had reduced permeability, the coupling level appears to be uniform around the perimeter of each of these cells. While slight differences in rate could not be ruled out, dye appeared to enter and leave border cells at equal rates, giving the appearance of symmetrically permeable junctions. However, the reduced permeability of the heterotypic junctions at one cell face of an epidermal cell, relative to the homotypic junctions of that same cell, suggests different coupling levels around the perimeter of those cells. Instead, I propose that there is asymmetrical regulation of junctional permeability at such cell interfaces - when two cells in contact regulate their coupling to different levels, a channel between them has the lower of the two conducance levels. The principle for this was described by Obaid et al. (1983), who showed that the intercellular channel of an insect has two gates, one in each hemichannel, and that these can respond independently to controlling agents. In the situation above, conditions in each of the two different cells regulate the permeability of their hemi-

channels to a uniform but characteristically different level. In this way, coupling can be uniform around the perimeter of cells that form heterotypic junctions.

An alternate explanation to asymmetric regulation of permeability, whether by graded closure or not, would be that border cells have fewer intercellular channels, so that fewer functional channels are formed between border cells or in heterotypic junctions. However, Lawrence and Green (1975) found that gap junctions occurred as frequently between cells of different segments as between cells within the segment. Here, some freshly dissected preparations briefly showed no retardation of dye passage at the segment border, which is physiological evidence showing that border cells can have the same degree of coupling as cells within the segment, but suggesting that regulation of permeability normally prevents this. The rapid re-setting of the permeability level, also seen in the loss of intersegmental coupling that could occur during the course of an experiment, is more likely to occur by change in the state of existing channels than by variation in channel number.

The interpretation of results in Tenebrio epidermis was that intercellular channels close in a graded fashion. In part, electrical coupling detected in the absence of dye coupling suggested the reduction of the average channel diameter, which occluded the dye but continued to permit the passage of small ions. In Oncopeltus, graded closure of

border cell junctions may explain how electrical coupling between segments is maintained under conditions that minimize dye passage.

After culturing with hormone, intermolt preparations showed no retardation of dye spread across the border, suggesting that the depressed coupling levels of the border cells had been reset to a higher, stable level in response to the hormone. A selective increase in channel number between border cells could have explained this, but is unlikely since increased coupling in response to this hormone in Tenebrio epidermis did not involve a measurable change in junctional area (Caveney et al., 1981).

Changes in the junctional permeability of the border cells appeared able to occur independently of the coupling level within the segment. This was particularly evident when the dye coupling of the border cells was reduced below detectable levels (Fig. 22) while dye continued to pass within the segment. The apparent rate of dye spread within the segment does not appear different between this and Fig. 19, in which intersegmental spread was relatively rapid. However, the rate of spread within the segment may have increased in preparations exposed to hormone and tested in M3, which showed that dye passage across the border cells could be as rapid as within the segment. This is subjective, and based on the appearance of the dye spread in those preparations. In Tenebrio, 20-HE increased coupling within

the segment, so that a parallel response in Oncopeltus would be expected. If true, border cell coupling might be modulated disproportionately, and not independently, of coupling in the segment. Factors that affected coupling within the segment slightly, either here or in general, might cause border cell coupling to increase to a maximum, or drop to a minimum. The greater effect in the border cells might be due to the counteraction of a larger degree of coupling depression.

3.4.3 Intersegmental coupling is probably reduced in vivo

Cell culture in vitro is only an approximation of conditions in vivo, and can be more the adaptation of the cells to the proffered medium than of the medium to the cells' requirements. To draw conclusions about coupling in vivo, an experimental medium should be a close match to known physiological conditions and should allow continued cell survival. Among the media used, the cation levels of M3 were the most closely matched to those in the blood of Oncopeltus (Mullen, 1957), and of plant-eating hemiptera in general. However, cells could not survive for long in M3, and so it is possible that the results of coupling are not representative of those in vivo.

M4 satisfied the requirement of cell survival, but its ion levels are not as closely matched to haemolymph as those of M3. The rates of intersegmental dye-spread were differ-

ent among the other 3 media, none of which allowed cell survival, and so it seems that the quality of the medium determining the degree of border cell coupling may be independent of that required for survival alone.

There is additional evidence to suggest that the intersegmental coupling seen in M4 does resemble the level *in vivo*. In freshly dissected preparations, the initial rates of dye transfer between segments were similar in all 4 media, subsequently becoming characteristic of the particular medium. Border cell coupling decreased in M1 and M2, increased in M3 and remained stable in M4. Evidence in *Tenebrio* suggests that the coupling level seen immediately after dissection is a reflection of the condition *in vivo* (Chapter 2). When either newly molted or intermolt beetle epidermis was first placed in culture, the level of electrical coupling in medium was characteristic of the developmental state, and was retained briefly after transfer to Li-saline. Therefore, intercellular coupling can be a sensitive measure of reaction to the environment, but the coupling levels found immediately following transfer *in vitro* probably reflect *in vivo* levels. Subsequently, the cells may adapt to those conditions. Therefore, on this basis, and on its ability to permit survival, M4 appears to approximate natural conditions. The results found with its use suggest that hydrophilic molecules of the size of CF and LRB are able to pass freely among cells within the segment,

but are considerably impeded from passing into adjacent segments.

3.4.4 Intersegmental coupling may be regulated during development

Spatial selectivity of intercellular coupling arises from local control of coupling at the segment border, and *in vitro* is influenced both by the culture medium and by molting hormone, and rarely, by some naturally occurring circumstances. This suggests that regulation of intersegmental coupling might occur during development as well. Changes in haemolymph composition or some other general (but perhaps locally perceived) factor might also affect border cell coupling, and so control the size range of molecules able to pass from segment to segment.

Experiments to duplicate the rare natural absence of dye retardation at the border succeeded with a combination of two factors, exposure to molting hormone and to M3. This appeared to be a synergistic effect, rather than additive, and prevents an easy explanation of a common principle. Perhaps M4 inhibits the expression of a hormone induced coupling increase, or M3 elicits it. In any event, it seems that if certain conditions, possibly of ionic balance, are present in the haemolymph at the time of the molt (or whenever 20-HE is present) the barrier to intersegmental molecular passage will be removed.

Warner and Lawrence (1982) reported that LY could initially pass over the segment border in 10% of their experiments and they too found a subsequent reappearance of the barrier to dye spread. While those preparations were from stage V nymphs, and in medium of unknown composition, the similarity of the pattern to results described here is striking and suggests that the level of intersegmental coupling of developing bugs may be temporarily increased in apparently intermolt insects. The reprogramming or commitment peak, a transient surge of ecdysteriod that occurs before the molt (Riddiford, 1977), might have this effect. The blood concentration would likely be less than the peak of 4.3 mg/ul 20-HE found in V nymphs at the molt (Redfern et al., 1982) and certainly of shorter duration, and so might have an effect on coupling less enduring *in vitro* than that seen here in epidermis exposed to 10 µg/ml 20-HE.

3.4.5 The segment border is repaired by border cells, and both can be regenerated

The segment border is the edge of the major metameric unit as well as the edge of a developmental compartment. Also, the discontinuity in the repeating axial gradient of positional information occurs at the segment border. How does this relate to the presence of the border cells? Are they a separate cell type, that perhaps created discontinuities in a universal gradient and so effectively pre-date the

segments, or are they an example of differentiated cells within the segment, like gland cells? Results from earlier experiments favour the latter, that border cells are derived from epidermal cells within the segment, but acquire a degree of independence.

Locke (1960) showed in Rhodnius that excision of a small piece of the intersegmental margin was followed by complete regeneration. However, it could be that the border was repaired instead by the remaining cells of the border and their descendants. Wright and Lawrence (1981a) showed that this was indeed the case, and that cautery of part of the segment border resulted in its replacement by the preferential migration and proliferation of cells from the intact intersegmental edge. Lawrence (1966) had found that the intersegmental membrane has "extraordinary" powers of this apparent regeneration: after extirpation of even large parts of the intersegmental membrane, a stream of elongated cells migrated out from each cut end, and rapidly reconstructed it. Presumably, these were true border cells, and it is interesting that their behaviour fits the theory of Loewenstein (1979) relating growth control with the degree of cell communication, such as the rapid growth of some neoplastic cells that is associated with reduced or absent cell-to-cell coupling.

Wright and Lawrence (1981a) also showed that the segment border could be regenerated by non-border cells, after

cautery of its entire width. Moreover, they demonstrated that ectopic borders could be formed, but not from the confrontation of cells of different segmental origin alone. The confrontation had to be between cells of sufficiently disparate positions in the antero-posterior axis, from the same or any segment. This difference had to be more than one half the length of the segment, and so appears to follow the principle of intercalation of missing positional values by the shortest possible route (French et al., 1976).

In either regenerated or ectopic borders, the normal appearance of laterally elongated cells was seen (Wright and Lawrence, 1981a). This suggests the establishment of a new border cell population. Since pigmentation and clonal origin of the elongated cells at the border indicated that they were part of the more posterior segment (Lawrence, 1973), it seems that they can differentiate from the regular cells of each segment under an appropriate stimulus.

Because cells with sufficiently dissimilar positional values can regenerate the border, it is possible that border cells originated from such an interaction during the primary organisation of the epidermis. Interacting across the newly formed segment border, cells posterior to the border might differentiate either directly or by an aligned mitosis to form a line of border cells. These cells appear quiescent, since Feulgen and Hoechst staining of epidermis from IV and V nymphs showed no mitoses, although prevalent and randomly

oriented elsewhere within the segment*. Conceivably, they need to increase their number only as the girth of the body wall increases during development, and Lawrence (1973) did see mitosis in cells at the anterior segment margin that was characterised by its medio-lateral orientation.

3.4.6 Are developmental compartments also communication compartments?

Since the segment border is also a compartment border, spatial selectivity of junctional coupling might be a characteristic of the compartment border. It could be involved in the spatial organization of structures within the segment. The alternative is that reduced junctional communication of the border cells is unique to segmentation.

Clonal analysis in the Oncopeltus segment suggested that the dorsal and ventral hemi-segments were further divided to form a short posterior compartment and larger anterior one, and also along the midline into right and left quadrants (Lawrence, 1981; 1973). In the preparations examined here, there were no apparent markings for these secondary compartments. Lawrence (1973) suggested that the

---

* P. Bryant (pers. comm.) also finds a zone of non-proliferating cells at the D/V boundary in the imaginal disc of Drosophila.

pigmentation is different between the anterior and short posterior compartments, which might not be evident here. However, the sites of dye injections ranged the width of the segment along the border, and along the midline, but no cryptic alteration of coupling forming lateral or antero-posterior subunits was detected.

Evidence from the Drosophila wing imaginal disc supports the idea that compartment boundaries within the segment can be communication boundaries: Weir and Lo (1982; 1984) injected fluorescent dyes into cells of wing discs and showed that zones of dye retardation subdivide the disc into communication compartments, whose boundaries coincide in space with compartment borders identified by clonal analysis.

It is also true that most of these lines of impedance occur along folds in the epidermis that involve considerable change in its thickness. The difference in the vertical measurements (the path length) would inevitably cause a decrease in fluorescence intensity, and this may be an alternate explanation for some of the lines of apparent dye retardation. Further complicating the matter, the distribution of gap junctions is non-random in the imaginal disc, being reduced in the folds that coincide with compartment boundaries (Ryerse, 1982). This too may contribute to the reduced dye transfer in the folded regions.

On the evidence presented, judgement should be reserved

for those lines that are accompanied by such thickness changes. I accept that dye spread is altered at the anteroposterior (A/P) and dorsoventral (D/V) boundaries within the disc, where the sheet thickness is more regular.

Weir and Lo (1982) described a band of cells across which the dye was slow to pass that is analogous to the border cells in Oncopeltus. It lay on only part of the A/P boundary in the wing pouch, and intercompartmental dye spread seemed to circumvent this band, since they found that:

> "most of the dye transfer between both sides appeared to occur through cells to the left of this band."

Elsewhere in the disc, they saw or could resolve, no such band of cells. The fluorescence pictures show no cell margins or other detail and fluorescence images of LY distribution in discs sectioned after injection did not show clear boundaries.

This band of cells was independently identified by Kuhn et al. (1983), who combined enzyme localization and clonal analysis to study compartment formation in the disc. They found a narrow band of cells just posterior to the A/P border that had a characteristic enzyme distribution* and by clonal analysis belonged to the posterior compartment.

---

* aldehyde oxidase (+) in a (-) disc; isocitrate dehydrogenase (-) and G6PDH (-) in a (+) disc.

Similar to the dye passage within the disc, clones transgressing the A/P boundary did so peripherally to this area and never through it.

This suggests that compartmentation of the wing disc is accompanied by the development of communication compartments. This may be associated with a discrete population of cells at the anterior margin of the posterior compartment. The nature, extent and possible lability of the reduction in junctional permeability is still uncertain.**

3.4.7 The segment border may organize the segment

A regenerating segment border is initially a convoluted frontier between the two masses of migrating cells, but it soon straightens (Wright and Lawrence, 1981b). Differences in cell adhesion may be responsible for this, and could also explain the straight edges formed by clones where they respect a compartment border. However, it may not be adequate to interpret the segment border as an expression of Steinberg's (1964) rule of selective adhesion.

If intercellular adhesion were the major organizing factor in the segment and in particular at its margins,

---

** Fraser and Bryant (1984) were not able to duplicate these results, achieving only limited spread of LY within the disc, but extensive, homogeneous spread of fluorescein complexon (Fluorexon; MW 623).

there might be no need of altered intercellular communication there, as Nubler-Jung (1979) observed. But, there is altered communication, and it is due to a population of cells that prevents direct contact between adjacent segments. Adhesion forces seem to be different between the anterior and posterior of one segment and, since Nardi and Kafatos (1976) have shown graded adhesion in the wing epidermis, are possibly graded within this compartment as well. It seems possible that intercellular adhesion is a result of the axial gradient, and separate from the mechanism that maintains the segment edge and its positional values.

Although Piepho's (1955) experiments suggested that intersegmental membrane had an active part in polarity of the segment, Locke (1960) showed that the cells in a piece of reversed cuticle can retain an orientation inappropriate to the position of the segment border, and that in fact the border region seems to be neutral in gradient value. This suggests that the border cells, by virtue of their reduced cell-to-cell communication, are part of neither one of the adjacent segmental gradients. Acting as a no-man's-land, the border cells allow the gradient discontinuity to exist. They maintain the gradient for the other cells that are inside the segment, which then respond to it by expression of cuticle contours, adhesion differences or properties that other tissues can perceive (such as migrating muscle cells:

Williams et al., 1984; or sensory neurons: Walthall and Murphey, 1984).

Therefore, border cells by their presence may allow the organization of the segment. It is also possible that the intersegmental zone has the ability to control the cells in its vicinity: when central areas of the segment are reoriented, there is gradual regulation back to normal (Lawrence et al., 1972), but the segment margin is very stable after transplantation, maintaining its pattern as if in isolation, and dominating cells in its vicinity (Locke, 1960; Nubler-Jung, 1979). Wright and Lawrence (1981a) found that regeneration of a segment border could cause the reversal of polarity of the cells anterior to the border, that had migrated into the cauterized region. Also, they found that an ectopic segment border, which formed after grafting, would affect the polarity and pattern of host tissue far more greatly than a similar graft that formed no segment border. In the wax moth Galleria mellonella, Bhaskaran and Roller (1980) have shown that the posterior margin of the segment acts at certain times in development as if it were a source of a diffusible morphogen which influences the pattern and polarity of surrounding cells.

This suggests that cells in the intersegmental zone, possibly the border cells, but maybe the adjacent cells of extreme positional value that can cause their regeneration, are able to organize some aspects of the segmental plan.

3.4.8 Spatial selectivity and regulatory signals

The route of cell-to-cell transmission allows the specific action of molecules in low concentrations, since there is insulation from loss to the much larger external volume. Since embryonic fields are small when first established, in general less than 100 cells wide, Crick (1970) felt that gradients of diffusible morphogens could establish the limits of such fields or carry developmental information within them. The time limits for the events of pattern specification required a reasonably rapid movement of such molecules, and so it is important that recent measurement of the rates of diffusion of molecules in an epidermis shows that their passage among cells is just one order of magnitude slower than that in water alone (Safranyos and Caveney, 1985).

The Oncopeltus segment is a model system for the study of diffusible morphogens in gradient action, since there is an antero-posterior gradient of positional information (Lawrence et al., 1972), it permits the passage of small molecules among its cells, and contains boundary cells that restrict their passage into the next segment. The spread of fluorescent tracers showed that a morphogen of comparable size would not be completely blocked at the segment border, but could pass slowly to the next segment. There is a considerable size range of molecules that could pass within the segment, but that would be effectively blocked from

passing between segments. Making the assumptions about intersegmental coupling in vivo discussed above, these would be larger than 14Å but less than the maximum channel diameter of 20-30Å (Schwarzmann et al., 1981).

Conceivably, the action of morphogens could range from regulation of cell division to more complex activities such as the establishment of the antero-posterior axis in a primary field. Intercellular substances with morphogenetic activity have been found in Hydra (Schaller, 1981), where they appear to specify the pattern. They are hydrophilic molecules between 500 and 1100 MW (Schaller and Bodenmuller, 1981) and could conceivably pass between cells via gap junctions.

Morphogens and compartment boundaries are combined in a theoretical work by Meinhardt (1983). He proposes that the region of intersection of boundaries resulting from primary embryonic organisation acts as an organising centre in subsequent development. He used existing evidence on patterning in the wing imaginal disc and the cockroach leg to show that treating the intersection of compartment borders as a source of a gradient of positional information (which could be a diffusible molecule) could first, explain the separate locations of leg and wing structures on the same segment and, second, accommodate the existing results, in predicting the regeneration of the structure. One advantage of his theory is that it provides a feasible molecular

basis for the polar coordinate model of French et al. (1976).

A contrasting point of view is emphasized by Nardi and Stocum (1983) who feel that the cell surface carries much of the molecular basis of morphogensis, in the form of adhesion gradients. They showed this in the urodele limb and earlier, in the lepidopteran wing epidermis (Nardi and Kafatos, 1976). The existence of Nardi's 'biochemical basis of positional non-equivalence' is supported by the existence of region-specific molecules in the imaginal disc (Greenberg and Adler, 1982) and a gradient of a cell surface molecule in the avian retina that appears to control neuronal position (Trisler et al., 1981).

The major difference between these classes of models is that one requires direct communication between cell interiors, and in the other, the cell membrane itself is involved instead. This emphasizes our ignorance of the interplay between the basic mechanisms in pattern formation, and suggests that the little we know and even what we suspect to occur, may not be easily applied to the more complex later stages.

CHAPTER 4

General Discussion

The concept of developmental gradients was formulated by Child and set forth as a general problem in biology in 1941. While elaborated as being based on metabolic activity or an indefinable 'morphogenetic potential', this failed to connect satisfactorily a quantitative cellular property with cellular pattern. It was the idea of positional information of Wolpert (1969), along with his realisation that primary embryonic fields are uniformly small, that allowed Crick (1970) to demonstrate that intercellular diffusion of a morphogen would rapidly produce a gradient of positional information. This linked cells to cellular pattern by an acceptable, though still theoretical, graded mechanism. Subsequently, intercellular diffusion, as the biology of cell coupling and the gap junction, has become a separate field of study. My contributions show how regulation of intercellular communication can affect the nature of substances able to pass betweeen cells and describe a possible link between the 'private pathway' and the control of cell development.

In insects, there are two distinct phases of development in which diffusion might determine the outcome. After

fertilization, there is an acellular period with a number of synchronous nuclear divisions without formation of cell membranes, followed by more usual development after enclosure of the nuclei with cell membranes. For example, in Drosophila there are 13 rounds of nuclear division before cell membranes form to make a blastoderm of roughly 6000 cells (Turner and Mahowald, 1976).

The blastoderm becomes divided circumferentially into segments, and a dorsal-ventral compartment boundary is drawn longitudinally around the whole. Pattern formation that occurs in the acellular embryo is primarily under the influence of maternal and not zygotic genes. Diffusion among the nuclei is relatively unimpeded, and it may be in this way that maternal gene products determine the polarity of the embryo in the three major axes: anterior-posterior, dorsal-ventral and left-right. In particular, the dorsal-ventral axis is determined from maternal mRNA stored in the egg (Anderson and Nusslein-Vollhard, 1984). Experimentally, the level of ventral development is proportional to the amount of such mRNA in the egg, and so its product is a true physiological morphogen.

A biochemical model involving molecules undergoing diffusion and reaction for the spontaneous formation of pattern (Turing, 1953) was applied to Drosophila by Kauffman et al. (1978). They showed that the nodal lines of successive patterns correctly predicted the sequence and position

in which the compartment boundaries appear both in the embryo and in the imaginal discs. The formation of cell membranes was a critical event that, by reducing the effective diffusion constant, decreased wavelengths initially too long to 'fit' onto the egg. As the wavelength continued to decrease, successive patterns arose as the boundary conditions were met.

The reaction/diffusion model can also describe compartment formation in the wing disc. Here, as in embryonic segmentation, compartmentation seems to involve a genetic change, possibly of a limited number of binary genetic switches (Kauffman, 1973). Indeed, a compartment can be defined as the spatial domain of a (homeotic) gene (Morata and Lawrence, 1975).

The gene 'fushi-tarazu' (FTZ) shows part of the extent of genetic involvement in segmentation. Mutations in this gene disturb the periodicity of segmentation and its spatial distribution tends to support the concept of segmental determination used in the model above. By hybridization of cloned FTZ^+ DNA, Hafen et al. (1984) showed that a uniform band forms across the acellular syncytial blastoderm by the 9^{th} nuclear division, which breaks down by the 11^{th} division into a pattern of stripes, with each stripe equal in length to one prospective segment. Because FTZ is a pair-rule mutation that halves the number of segments, this indicates that a prepattern, in which the repeating unit is twice as

large, precedes the ultimate segmental repeating pattern, and is itself derived from a continuous distribution. This fits well with the reaction/diffusion model.

A compartment boundary at the segment edge marks groups of cells which have been committed to their destiny before cellularity was complete. The imaginal discs, however, are definite monolayers of cells when they are compartmented (Eichenberger-Glinz, 1979). It is probable that one mechanism specifies position in both cases, which responds to physical parameters such as diffusion constants and field size, and is similar, at least in effect, to the reaction/diffusion scheme. Therefore, the reduced junctional communication at the compartment boundaries in both cases seems to be a consequence of the specification of the boundary, that presumably stabilizes and maintains the pattern. Once established, regional differences in intercellular diffusion would cause the unstable wavelength to decrease and form the next stable pattern.

The correlation between regional differentiation and the formation of communication compartments in the post implantation mouse embryo (Lo and Gilula, 1979) suggests that here, too, reduced junctional communication at the intersection between contiguous cell fields is involved in the maintenance of pattern.

Graded channel closure is the sine qua non of true selectivity in junctional communication. Initial inspection

shows that the intercellular channel is a selective filter for exchange of the cytoplasmic constituents, in that it allows only the smaller hydrophilic molecules to pass through, but it is the effect upon the individual channel when intercellular coupling is regulated to a new level that determines whether selectivity changes as well. The simplest interpretation of the changing electrical conductance and dye permeability during uncoupling of Tenebrio epidermal cells was that the channels close in a graded fashion, so that different coupling levels are selective among the permeant molecules.

The nature of channel closure is basic to the understanding of channel function. Principally, the results have shown that the modulation of coupling level in a stable population of channels has a different effect on intercellular coupling than the regulation of channel number. When hormones increase gap junction number in their target cells, there is simple amplification of the properties of a single channel, and new or more rapid metabolic processes matched with more rapid equilibration of non-homogeneity. Instead, an altered coupling level changes the nature of molecules passing among cells, so that one cell receives different molecules instead of a greater or lesser number of the previous ones.

A graded channel bore permits a uniform field of cells to create a discontinuous spatial distribution of mole-

cules. This suggests that autonomous, yet interconnected cell fields can retain developmentally active molecules while cooperating in essential functions that involve passage of common metabolites.

Originally, selectivity of junctional communication in time and space was proposed to 'purposefully' control the distribution of molecules. The means for selectivity are shown to exist, with an example of spatial control of coupling, but without the molecules in question, the purpose must remain theoretical. The insect segment may be still the best place to find the molecules, perhaps by showing that uncoupling or loss of regulation of their passage alters the course of development. The long awaited 'magic bullet' or specific channel blocker that might help in this may have been found: Warner et al. (1984) have injected an antibody to the gap junction into frog blastomeres that appeared to block junctional communication without causing cell death and resulted in specific developmental effects. Pursuit of this line of research may establish the role of junction coupling in routine cellular activity as well as in development of the organism.

Appendix I

Carboxyfluorescein

(MW 376)

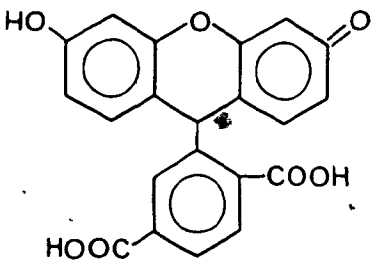

Lissamine Rhodamine B

(MW 559)

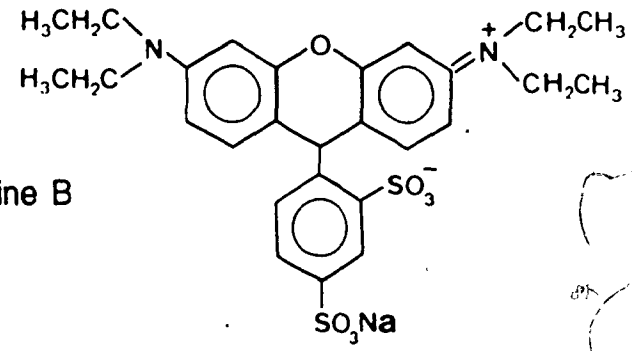

Lucifer yellow CH

(MW 457)

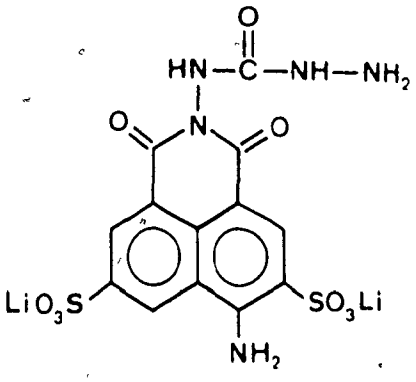

References

Aboulafia, J., Sanioto, S.M.L. and Lacaz-Viera, F. (1983). Cellular Li opens paracellular path in toad skin: amiloride blockable effect. J. Membrane Biol. 74, 59-65.

Akerman, K.E.O. (1978). Effect of pH and Ca on the retention of Ca by rat liver mitochondria. Arch. Biochem. Biophys. 189, 256-262.

Alberty, R.A. (1979). "Physical Chemistry". 5th Edition, Wiley, New York.

Anderson, K.V. and Nusslein-Volhard, C. (1984). Information for the dorsal-ventral pattern of the Drosophila embryo is stored as maternal RNA. Nature 311, 223-227.

Azarnia, R., Dahl, G. and Loewenstein, W.R. (1981). Cell junctions and cyclic AMP. III. Promotion of the junctional membrane permeability and junctional membrane particles in a junction deficient cell type. J. Membr. Biol. 63, 133-146.

Baerwald, R.J. (1975). Inverted gap and other cell junctions in cockroach haemocyte capsules: a thin section and freeze fracture study. Tissue Cell 7, 575-585.

Bassot, J.-M., Bilbaut, H., Mackie, G.O., Passano, L.M. and Pavans de Ceccatty, M. (1978). Bioluminescence and other responses spreads by epithelial conduction in the siphonophore Hippopodius. Biol. Bull. 55, 473-479.

Bennett, M.V.L. and Goodenough, D.A. (1978). Gap junctions, electrotonic coupling and intercellular communication. Neurosciences Research Prog. Bull. 16, 377-488.

Bennett, M.V.L., Spira, M.E. and Pappas, G.D. (1972). Properties of electrotonic junctions between embryonic cells of Fundulus. Dev. Biol. 29, 419-435.

Bennett, M.V.L., Spira, M. and Spray, D.C. (1978). Permeability of gap junctions between embryonic cells of Fundulus: a reevaluation. Dev. Biol. 65, 114-125.

Bhaskaran, G. and Roller, H. (1980). Segmental gradients specifying polarity and pattern in the wax moth, Galleria mellonella. The posterior margin as a source of a diffusible morphogen. Dev. Biol. 74, 65-85.

Brink, P.R. (1983). Effect of deuterium oxide on junctional membrane channel permeability. J. Membr. Biol. 71, 79-87.

Brink, P.R. and Dewey, M.M. (1980). Evidence for fixed charge in the nexus. Nature 285, 101-102.

Browne, C.L. and Wiley, H.S. (1979). Oocyte-follicle cell gap junctions in Xenopus laevis and the effects of gonadotropin on their polarity. Science 203, 182-183.

Burghardt, R.C. and Anderson, E. (1979). Hormonal modulation of ovarian interstitial cells with particular reference to gap junctions. J. Cell Biol. 81, 104-114.

Caveney, S. (1973). Stability of polarity in the epidermis of a beetle, Tenebrio molitor L. Dev. Biol. 30, 321-335.

Caveney, S. (1974). Intercellular communication in a positional field: movement of small ions between insect epithelial cells. Dev. Biol. 40, 311-322.

Caveney, S. (1976). The insect epidermis: a functional syncytium. In "The Insect Integument" (ed., Hepburn, H.R.) pp. 259-274. Elsevier, Amsterdam.

Caveney, S. (1978). Intercellular communication in insect development is hormonally controlled. Science 199, 192-195.

Caveney, S. and Berdan, R. (1982). Selectivity in junctional coupling between cells of insect tissues. In "Insect Ultrastructure" Vol. I. (eds. King and Akai), pp. 434-465 Plenum: New York.

Caveney, S., Berdan, R. and McLean, S. (1981). Cell-to-cell ionic communication stimulated by 20-hydroxyecdysone occurs in the absence of protein synthesis and gap junction growth. J. Insect Physiol. 26, 557-567.

Caveney, S. and Blennerhassett, M.G. (1980). Elevation of ionic conductance between insect epithelial cells by B-ecdysone in vitro. J. Insect Physiol. 26, 13-25.

Caveney, S. and Podgorski, C. (1975). Intercellular communication in a positional field: Ultrastructural correlates and tracer analysis of communication between insect epidermal cells. Tissue Cell 7, 559-574.

Cereijido, M., Meza, I., and Martinez-Palomo, A. (1981). Occluding junctions in cultured epithelial monolayers. Am. J. Physiol. C96-C102.

Chance, B., Pye K., and Higgins, J. (1965). Energy linked reactions of calcium with mitochondria. J. Biol. Chem. 240, 2729-2732.

Child, C.M. (1941). "Patterns and Problems of Development", University of Chicago Press: Chicago.

Clark, E.W. and Craig, R. (1953). Calcium and magnesium in insects. Physiol. Zool. 26, 101-107.

Cole, W.C., Garfield, R.E. and Kirkaldy, J.S. (1983). Increased gap junction area improves cell-to-cell diffusion of H-3 labelled 2-deoxyglucose between uterine smooth muscle cells. Biophys. J. 41, A84.

Crick, F.H.C. (1970). Diffusion in embryogenesis. Nature 225, 420-422.

Dahl, G., Azarnia, R. and Werner, R. (1981). Initiation of cell-cell channel formation by mRNA. Nature 289, 683-685.

Decker, R.S. (1976). Hormonal regulation of gap junction differentiation. J. Cell Biol. 69, 669-685.

Delachambre, J., Besson, M.T., Connat, J.-L. and Delbecque, J.-P. (1980). Ecdysteroid titres and integumental events during the metamorphosis of Tenebrio molitor. In "Progress in Ecdysone Research", pp. 211-222, (ed. J.A. Hollman), Elsevier/New Holland Biomedical Press.

Delbecque, J.-P., Hirn, M., Delachambre, J., and DeReggi, M. (1978). Cuticular cycle and molting hormone levels during the metamorphosis of Tenebrio molitor (Insecta, Coleoptera). Dev. Biol. 64, 11-30.

DeMello, W.C. (1975). Effect of intracellular injection of calcium and strontium on cell communication in heart. J. Physiol. 250, 231-245.

Eichenberger-Glinz, S. (1979). Intercellular junctions during development and in tissue cultures of Drosophila melanogaster: an electron microscopic study. Roux's Arch. Dev. Biol. 186, 333-349.

Eisenberg, R.S. and Johnson, E.A. (1970). Three dimensional electric field problems in physiology. In: "Progress in Biophysics and Molecular Biology", pp. 1-65, (eds. A.V. Bitter and D. Noble), Oxford: Pergamon.

Epstein, M.L. and Gilula, N.B. (1977). A study of communication specificity between cells in culture. J. Cell Biol. 75, 769-787.

Feir, D. (1974). Oncopeltus fasciatus: a research animal. Ann. Rev. Ent. 19, 81-96.

Fentiman, I.S., Taylor-Papadimitriou, J. and Stoker, M. (1976). Selective contact-dependent cell communication. Nature 264, 760-762.

Finbow, M.E. (1982). A review of junctional mediated intercellular communication. In "The Functional Integration of Cells in Animal Tissues", pp. 1-54, (eds. Pitts, J.D. and Finbow, M.E.) Cambridge University Press, New York.

Flagg-Newton, J.L., Dahl, G. and Loewenstein, W.R. (1981). Cell junctions and cyclic AMP: I. Upregulation of junctional membrane permeability and junctional membrane particles by administration of cyclic nucleotides or phosphodiesterase inhibitor. J. Membr. Biol. 63, 105-121.

Flagg-Newton, J.L. and Loewenstein, W.R. (1979). Experimental depression of junctional membrane permeability in mammalian cell culture. A study with tracer molecules in the 300 to 800 dalton range. J. Membr. Biol. 50, 65-100.

Fraser, S.E. and Bryant, P.J. (1984). Dye coupling in the Drosophila imaginal wing disc. J. Cell Biol. 99, 344A.

French, V., Bryant, P.J. and Bryant, S.V. (1976). Pattern regulation in epimorphic fields. Science 193, 969-981.

Furshpan, E.J. and Potter, D.D. (1968). Low resistance junctions between cells in embryos and tissue culture. Curr. Top. Dev. Biol. 3, 95-127.

Garfield, R.E., Merrett, D., and Grover, A.K. (1980). Gap junction formation and regulation in myometrium. Am. J. Physiol. 239, C217-C234.

Gilula, N.B., Epstein, M. and Beers, W.H. (1978). Cell-to-cell communication and ovulation. A study of the cumulus-oocyte complex. J. Cell Biol. 78, 58-75.

Greenberg, R.M. and Adler, P.N. (1982). Protein synthesis and accumulation in Drosophila melanogaster imaginal discs. Detection of a protein with a nonrandom spatial distribution. Dev. Biol. 29, 273-286.

Gross, J.D., Bradbury, J., Kay, R.R. and Peacey, M.J. (1983). Intracellular pH and the control of cell differentiation in Dictyostelium discoidei. Nature 303, 244-245.

Hafen, E., Kuroiwa, A. and Gehring, W.J. (1984). Spatial distribution of transcripts from the segmentation gene fushi tarazu during Drosophila embryonic development. Cell 37, 833-841,

Harris, A.L., Spray, D.C. and Bennett, M.V.L. (1981). Kinetic properties of a voltage dependent junctional conductance. J. Gen. Physiol. 77, 95-117.

Harris, A.L., Spray, D.C. and Bennett, M.V.L. (1983). Control of intercellular communication by voltage dependence of gap junctional conductance. J. Neuroscience 3, 79-100.

Hax, W.M.A., Van Venrooij, G.E.P.M. and Bossenberg, J.B.J. (1974). Cell communication: a cyclic AMP mediated phenomenon. J. Membr. Biol. 19, 253-266.

Humason, G.L. (1979). "Animal Tissue Techniques", 4th ed., W.H. Freeman & Co.: San Francisco.

Hunter, G.K. and Pitts, J.D. (1981). Non-selective junctional communication between some different mammalian cell types in primary culture. J. Cell Science 49, 163-175.

Jahnke, E., and Emde, F. (1960). "Tables of Higher Functions" 6th ed., McGraw-Hill, New York.

Kannan, M.S. and Daniel, E.E. (1978). Formation of gap junctions by treatment in vitro with potassium conductance blockers. J. Cell Biol. 78, 338-348.

Kauffman, S.A. (1973). Control circuits for determination and transdetermination. Science 181, 310-318.

Kauffman, S., Shymko, R.M. and Trabert, K. (1978). Control of segmental compartment formation in Drosophila. Science 199, 259-270.

Kimmel, C.B., Spray, D.C. and Bennett, M.V.L. (1984). Developmental uncoupling between blastomere and yolk cell in the embryo of the teleost Fundulus. Dev. Biol. 102, 483-487.

Kuhn, D.T., Fogerty, S.C., Eskens, A.A.C. and Spray, T.H.E. (1983). Developmental compartments in the Drosophila melanogaster wing disc. Dev. Biol. 95, 399-413.

Lane, N.J. and Skaer, H.L. (1980). Intercellular junctions in insect tissues. Adv. Insect Physiol. 15, 35-213.

Lane, N.J. and Swales, L.S. (1980). Dispersal of junctional particles, not internalization, during in vivo disappearance of gap junctions. Cell 19, 579-589.

Larsen, W.J. (1983). Biological implications of gap junction structure distribution and composition: a review. Tissue Cell 15, 645-672.

Larson, D.M. and Sheridan, J.D. (1982). Intercellular junctions and transfer of small molecules in primary vascular endothelial cultures. J. Cell. Biol. 92, 183-192.

Lawrence, P.A. (1966). Gradients in the insect segment: Reorientation of hairs in the milkweed bug Oncopeltus fasciatus. J. Exp. Biol. 44, 607-620.

Lawrence, P.A. (1970). Some new mutants of the milkweed bug, Oncopeltus fasciatus Dall. Genet. Res. 15, 347-350.

Lawrence, P.A. (1973). A clonal analysis of segmental development in Oncopeltus (Hemiptera). J. Embryol. Exp. Morph. 30(3), 681-699.

Lawrence, P.A. (1981). The cellular basis of segmentation in insects. Cell 26, 3-10.

Lawrence, P.A., Crick, F.H.C. and Munro, M. (1972). A gradient of positional information in an insect, Rhodnius. J. Cell Sci. 11, 815-853.

Lawrence, P.A., and Green, S.M. (1975). The anatomy of a compartment border, the intersegmental boundary of Oncopeltus. J. Cell Biol. 65, 373-382.

Lawrence, T.S., Beers, W.H. and Gilula, N.B. (1978). Transmission of hormonal stimulation by cell-to-cell communication. Nature 272, 501-506.

Lawrence, P.A., Crick, F.H.C., and Munro, M. (1972). A gradient of positional information in an insect, Rhodnius. J. Cell Science 11, 815-853.

Lawrence, P.A., and Green, S.M. (1975). The anatomy of a compartment border, the intersegmental boundary of Oncopeltus. J. Cell Biol. 65, 373-382.

Lees-Miller, J.P. and Caveney, S. (1982). Drugs that block calmodulin activity inhibit cell-to-cell coupling in the epidermis of Tenebrio molitor. J. Membr. Biol. 69, 233-245.

Lehninger, A.L. (1975). "Biochemistry", 2nd Edition. Worth, New York.

Lo, C.W. and Gilula, N.B. (1979). Gap junction communication in the post-implantation mouse embryo. Cell 18, 411-422.

Locke, M. (1959). The cuticular pattern of an insect, Rhodnius prolixus. J. Exp. Biol. 36, 459-477.

Locke, M. (1960). The cuticular pattern in an insect - the intersegmental membranes. J. Exp. Biol. 37, 398-407.

Loewenstein, W.R. (1966). Permeability of membrane junctions. Ann. N.Y. Acad. Sci: 137, 441-472.

Loewenstein, W.R. (1979). Junctional intercellular communication and the centre of growth. Biochem. Biophys. Acta Cancer Rev. 560, 1-65.

Loewenstein, W.R. (1981). Junctional intercellular communication: the cell-to-cell membrane channel. Physiol. Rev. 61, 829-913.

Makowski, I., Caspar, D., Philips, W. and Baker, T. (1984). Gap junction structures. VI. Variation and conservation in connexon conformation and packing. Biophys. J. 45, 208-218.

Margiotta, J.F. and Walcott, B. (1983). Conductance and dye permeability of a rectifying electrical synapse. Nature 305, 52-55.

Meda, P., Perrelet, A. and Orci, L. (1979). Increase of gap junctions between pancreatic B-cells during stimulation of insulin secretion. J. Cell Biol. 82, 441-448.

Meech, R.W. and Thomas, R.C. (1977). The effect of calcium injection on the intracellular sodium and pH of snail neurons. J. Physiol. 265, 267-283.

Meinhardt, H. (1983). Cell determination boundaries as organizing regions for secondary embryonic fields. Dev. Biol. 96, 375-385.

Mellerup, E.T., and Rafaelsen, O.J. (1975). Lithium and carbohydrate metabolism. In "Basic Mechanisms in the Action of Lithium", pp. 381-389, (eds., H. Emrich, J. Aldenhoff and H. Lux), Academic Press, London.

Merck, F.B., Botticelli, C.R. and Albright, J.J. (1972). An intercellular response to estrogen by granulosa cells of the rat ovary. Endocrinol. 90, 992-1007.

Mitsuhashi, J. (1965). In vitro cultivation of the embryonic tissues of the green rice leafhopper, Nephrotettix cincteps (Uhler). Jap. J. appl. Ent. Zool. 9, 107-114.

Moor, R.M., Smith, M.W. and Dawson, R.M.C. (1980). Measurement of intercellular coupling between oocyte and cumulus cells using intracellular markers. Exp. Cell Res. 126, 15-29.

Morata, G. and Lawrence, P.A. (1977). Homeotic genes, compartments and cell determination in Drosophila. Nature 265, 211-216.

Mullen, J.A. (1957). Sodium, potassium and calcium ions in the haemolymph of Oncopeltus fasciatus (Dallas). Nature 180, 813-814.

Nairn, R.C. (1976). "Fluorescent Protein Tracing", 4th ed., Churchill Livingstone, New York.

Nardi, J.B. and Kafatos, F.C. (1976). Polarity and gradients in lepidopteran wing epidermis. II. The differential adhesiveness model: a gradient of a non-diffusible cell surface parameter. J. Embryol. Exp. Morphol. 36, 489-512.

Nardi, J.B. and Stocum, D.L. (1983). Surface properties of regenerating limb cells: Evidence for gradation along the proximo-distal axis. Differentiation 25, 27-31.

Nubler-Jung, K. (1979). Pattern stability in the insect segment. II. The intersegmental region. William Roux's Archives 186, 211-233.

Obaid, A.L., Socolar, S.S. and Rose, B. (1983). Cell-to-cell channels with two independently regulated gates in series: analysis of junctional conductance modulation by membrane potential, calcium and pH. J. Membr. Biol. 73, 69-90.

Peracchia, C. (1980). Structural correlates of gap junction permeation. Int. Rev. Cytol. 66, 81-146.

Popowich, J. (1975). An electrophysiological study of epidermal cell membranes in larval Tenebrio molitor L. M.Sc. Thesis, University of Western Ontario, London, Ontario, Canada.

Popowich, J. and Caveney, S. (1976). An electrophysiological study of the junctional membrane of epidermal cells in Tenebrio molitor. J. Insect Phys. 22, 1617-1622.

Piepho, H. (1955). Uber die polare Orientierung der Balge and Schutzen auf dem Schmetterlingsrumpf. Biol. Zbl. 74, 467-474.

Pitts, J.D. (1971). "Molecular exchange and growth control in tissue culture. In: "Ciba Foundation Symposium on Growth Control" (eds. G.E.W. Wolstenholme and J. Knight). pp. 89-105, London: Churchill-Livingston.

Pitts, J.D. and Finbow, M.E. (1977). Junctional permeability and its consequences. In "Intercellular Communication" (ed. W. DeMello). pp. 61-86, Plenum, New York.

Radu, A., Dahl, G., and Loewenstein, W.R. (1982). Hormonal regulation of cell junction permeability: upregulation by catecholamine and prostaglandin E1. J. Membr. Biol. 70, 239-251.

Reber, W.R. and Weingart, R. (1982). Ungulate cardiac Purkinje fibres - the influence of intracellular pH on the electrical cell-to-cell coupling. J. Physiol. 328, 87-104.

Redfern, R.E., Kelly, T.J., Borkovec, A.B. and Hayes, D.K. (1982). Ecdysteroid titres and molting aberrations in last stage Oncopeltus nymphs treated with insect growth regulators. Pesticide Biochemistry and Physiol. 18, 351-356.

Revel, J.-P. and Karnovsky, M.J. (1967). Hexagonal array of subunits in intercellular junctions of the mouse heart and liver. J. Cell Biol. 33, C7-C18.

Riddiford, L.M. (1979). Ecdysone-induced change in cellular commitment of the epidermis of the tobacco horn worm, Manduca sexta, at the initiation of metamorphosis. Gen. Comp. Endocrinol. 34, 438-446.

Rink, T.J., Tsien, R.Y. and Warner, A.E. (1980). Free calcium in Xenopus embryos measured with ion-selective microelectrodes. Nature 283, 658-660.

Rose, B. and Loewenstein, W.R. (1971). Junctional membrane permeability. Depression by substitution of Li for extracellular Na, and by long term lack of Ca and Mg; restoration by cell depolarization. J. Membr. Biol. 5, 20-50.

Rose, B. and Loewenstein, W.R. (1976). Permeability of a cell junction and the local cytoplasmic free ionized calcium concentration: a study with aequorin. J. Membr. Biol. 28, 87.

Rose, B. and Rick, R. (1978). Intracellular pH, intracellular free Ca and junctional cell-cell coupling. J. Membr. Biol. 44, 377-415.

Rose, B., Simpson, I. and Loewenstein, W.R. (1977). Calcium ion produces graded changes in permeability of membrane channels in cell junction. Nature 267, 625-627.

Ryerse, J.S. (1982). Gap junctions are non-randomly distributed in Drosophila wing discs. William Roux's Arch. Dev. Biol. 191, 335-339.

Safranyos, R.G.A. and Caveney, S. (1985). Rates of diffusion of fluorescent molecules via cell-to-cell membrane channels in a developing tissue. J. Cell Biol. (in press).

Santos-Sacchi, J. and Dallos, P. (1983). Intercellular communication in the supporting cells of the organ of Corti. Hearing Research 9, 317-326.

Schaller, H.C. (1981). Morphogenetic substances in Hydra. Fortschr. Zool. 26, 153-162.

Schaller, H.C. and Bodenmuller, H. (1981). Isolation and amino acid sequence of a morphogenetic peptide from hydra. Proc. Nat. Acad. Sci. 78, 7000-7004.

Schwarzmann, G., Weigandt, H., Rose, B., Zimmerman, A., Ben-Haim, D. and Loewenstein, W.R. (1981). Diameter of the cell-to-cell junctional membrane channels as probed with neutral molecules. Science 213, 551-553.

Shields, G. and Sang, J.H. (1970). Characteristics of five cell types appearing during in vitro culture of embryonic material from Drosophila melanogaster. J. Embryol. Exp. Morph. 23, 53.

Shiba, H. (1971). Heavisides' "Bessel Cable" as an electric model for flat epithelial cells with low resistive junctional membranes. J. Theor Biol. 30, 59-68.

Siegenbeek Van Heukelom, J., Denier Van Der Gon, J.J., and Prop, F.J.A. (1972). Model approaches for evaluation of cell coupling in monolayers. J. Membr. Biol. 7, 88-102.

Socolar, S.J. and Politoff, A.L. (1971). Uncoupling cell junctions of a glandular epithelium by depolarizing current. Science 172, 492-494.

Spray, D.C., Harris, A.L., and Bennett, M.V.L. (1979). Voltage dependence of junctional conductance in early amphibian embryos. Science 204, 432-434.

Spray, D.C., Harris, A.L. and Bennett, M.V.L. (1981). Gap junctional conductance is a simple and sensitive function of intracellular pH. Science 211, 712-715.

Spray, D.C., Stern, J.H., Harris, A.L. and Bennett, M.V.L. (1982). Gap junctional conductance: comparison of sensitivities to H and Ca ions. Proc. Nat. Acad. Sci. 79, 441-445.

Spray, D.C., White, R.L., de Carvalho, A.C., Harris, A.L., and M.V.L. Bennett. (1984). Gating of gap junction channels. Biophys. J. 45, 219-230.

Stewart, W.W. (1978). Functional connections between cells as revealed by dye-coupling with a highly fluorescent napthalimide tracer. Cell 4, 741-759.

Steinberg, M.S. (1964). The problem of adhesion selectivity in cellular interactions. In: "Cellular Membranes in Development", (ed. M. Locke), pp. 321-366. Academic Press.

Szollosi, A. and Marcaillou, C. (1980). Gap junctions between germ and somatic cells in the tests of the moth, Anagasta kuhniella. Cell Tissue Res. 213, 137-147.

Trisler, G.D., Schneider, M.D. and Nirenberg, M. (1981). A topographic gradient of molecules in retina can be used to identity neuron position. Proc. Nat. Acad. Sci. 78, 2145-2149.

Turing, A.M. (1952). The chemical basis of morphogenesis. Proc. Roy. Soc. B 237, 37-54.

Turner, F.R. and Mahowald, A. (1966). Scanning electron microscopy of Drosophila melanogaster embryogenesis. I. The structure of the egg envelopes and the formation of the cellular blastomeres. Dev. Biol. 50, 95-108.

Unwin, P.N.T. and Ennis, P.D. (1983). Calcium-mediated changes in gap junction structure: evidence from the low angle X-ray pattern. J. Cell Biol. 97, 1459-1466.

Unwin, P.N.T. and Ennis, P.D. (1984). Two configurations of a channel-forming membrane protein. Nature 307, 609-613.

Unwin, P.N.T. and Zampighi, G. (1980). Structure of the junction between communicating cells. Nature, 283, 545-549.

Vaughan-Jones, R.D., Lederer, W.J. and Eisner, D.A. (1983). Ca ions can affect intracellular pH in mammalian cardiac muscle. Nature 301, 522-524.

Walthall, W.W. and Murphey, R.K. (1984). Rules for neural development revealed by chimaeric sensory systems in crickets. Nature 311, 57-59.

Warner, A.E. and Lawrence, P.A. (1973). Electrical coupling across developmental boundaries in insect epidermis. Nature 245, 47-48.

Warner, A.E., Gutherie, S.C. and Gilula, N.B. (1984). Antibodies to gap-junctional protein selectively disrupt junctional communication in the early amphibian embryo. Nature 311, 127-131.

Warner, A.E., and Lawrence, P.A. (1982). Permeability of gap junctions at the segmental border in insect epidermis. Cell 28, 243-252.

Weidmann, S. (1952). The electrical constants of Purkinje fibres. J. Physiol. 118, 348-360.

Weir, M.P. and Lo, C.W. (1982). Gap junctional communication compartments in the Drosophila wing disk. Proc. Nat. Acad. Sci. 79, 3232-3235.

Weir, M.P. and Lo, C.W. (1984). Gap junctional communication compartments in the Drosophila wing imaginal disk. Dev. Biol. 102, 130-146.

Williams, G.J.A., Shivers, R.R., and Caveney, S. (1984). Active muscle migration during insect metamorphosis. Tissue Cell 16, 411-432.

White, R.L., Spray, D.C., Carvalho, A., and Bennett, M.V.L. (1982). Voltage-dependent gap junctional conductance between fish embryonic cells. Soc. Neurosci. 8, 944A.

White, R.L., Carvalho, A.C., Spray, D.C., Wittenberg, B.A., and Bennett, M.V.L. (1983). Gap junctional conductance between pairs of ventricular myocytes from rat. Biophys. J. 41, 217A.

Wolpert, L. (1969). Positional information and the spatial pattern of cellular differentiation. J. Theor. Biol. 25, 1-47.

Wright, D.A. and Lawrence, P.A. (1981a). Regeneration of the segment boundary in Oncopeltus. Dev. Biol. 85, 317-327.

Wright, D.A. and Lawrence, P.A. (1981b). Regeneration of segment boundaries in Oncopeltus: cell lineage. Dev. Biol. 85, 328-333.

Yancey, S.B.D., Easter, D. and Revel, J.-P. (1979). Cytological changes in gap junctions during liver regeneration. J. Ultrastructural Res. 67, 229-242.

Yancey, S.B., Nicholson, B.J. and Revel, J.-P. (1981). The dynamic state of liver gap junctions. J. Supramolecular Structure and Cellular Biochemistry 16, 221-232.

Yee, A.G. and Revel, J.-P. (1978). Loss and reappearance of gap junctions in regenerating liver. J. Cell Biol. 78, 554-564.

Zackson, S.L. (1982). Cell clones and segmentation in leech development. Cell 31, 761-770.

Zimmerman, A.L., and Rose, B. (1983). Analysis of cell-to-cell diffusion kinetics: changes in junctional permeability without accompanying changes in selectivity. Biophys. J. 41, 216A.

END

14-11-85

FIN